Department of Precision and Microsystems Engineering

Failure criteria for evaluating Strength of Adhesive joints

Sainath Kadam

Report no : EM 2014.020
Coach : Dr. Matthijs Langelaar
Professor : Prof. Fred van Keulen
Specialisation : Structural Optimisation and Computational Mechanics
Type of report : Master thesis
Date : 28 September 2014

Failure criteria for evaluating Strength of Adhesive joints.

Sainath Kadam
s.kadam@student.tudelft.nl

Thesis Report submitted to

Technische Universiteit Delft

in partial fulfilment for the award of the degree of

Master of Science
Solid and Fluid Mechanics

Mechanical Analysis Group
Veldhoven, THE NETHERLANDS
September 2014

Contents

Abstract

Adhesives are increasingly used in ASML machines as they provide some distinct advantages over conventional mechanical joining techniques. At the same time with these adhesive joints being exposed to environments like vacuum in the future, it is imperative to design these joints efficiently. So that effects like shrinkage or swelling which depend on the thickness of the adhesive joint do no effect the purpose of these joints adversely.

For an efficient adhesive joint the adhesive used should be optimum, which brings us to the factor of safety that is used while designing these joints. With a large uncertainty regarding the failure criteria to be used for adhesives the factor of safety during design has to be large to account for an uncertainty. This large factor of safety is undesired.

An attempt is made to evaluate all possible stress based failure criteria that have been otherwise traditionally used for ductile metals and also some other criteria popularly used for polymers. In additional some other intuitive criteria were also derived.

The project consisted of the following methodology,

1. Selecting and developing test setups for testing of adhesives.
2. Testing of standard adhesive bulk and test joints.
3. Analysis of test data to remove outlier data.
4. Development of elasto-plastic and equivalent Drucker-Prager material models.
5. FEM modeling and analysis of test cases using various material models.
6. Study the standard deviation for various failure criteria considering all possible test types.

At the end a Way of working was established for Design and Analysis engineers to be able to calculate allowable stress for a given adhesive taking into consideration the mode of failure, the respective failure criteria for the mode of failure and the factor of safety for that design.

The design factor of safety before conducting this research was based on the Von Mises failure criterion which resulted in a higher FOS. Post the results from this research it is shown that Von Mises is not the best criterion to evaluate failure in adhesives. Other criteria like the Drucker-Prager and Fracture criterion give 2-3 times more accurate results.

Acknowledgements

The results documented in this Thesis Report are a product of an year long cooperation between various people involved from **ASML** and **TU Delft**.

First and foremost I would like to thank my mentor, **Ilja Malakhovsky**. His unrelenting and dedicated help with every small aspect of my project over this extensive period of time was one of the main reasons for me to be able to finally achieve the desired results. Because he had a clear idea of what was possible and what needed to be done, especially at times when I was struggling to find the right direction to move forward, meant that I could rely on his knowledge and expertise to keep my work progressing.

I would like to thank my supervisor **Prof. Matthijs Langelaar** for his continuous support throughout the project. His focus on the fundamentals of any failure criteria helped me make sure that the criteria under investigation was not just mathematically accurate but also made sense from a physical point of view. Discussions about the project at regular time intervals with him helped me stay focussed and on track.

I would also like to thank **Marcel Snel**, **Piet de Vries** and **Ton Arends** for helping me out during the testing phase of the project and also for the training I received regarding working with adhesives which helped me build some confidence working with adhesives at the onset of the project. I would also like to mention **Sebastiaan in 't Hout** for his expert advice with the reliability and statistical calculations with the test data.

Finally I would like to thank my Group Leader **Fred Huizinga** and **Prof. Fred van Keulen** my Head of Department for providing me facilities and the opportunity to conduct this project.

Part I

Introduction & Literature Study

Chapter 1

Introduction

1.1 What is an adhesive?

Kinloch defined adhesives as, “A material which when applied to surfaces of materials can join them together to resist separation"[36]. We are primarily concerned about structural adhesives which are mostly polymers that are hard and flexible at room temperatures (below glass transition temperatures, T_g). Above this T_g they tend to get soft and flexible. This rubbery state is at higher temperatures as the polymeric chains are free to move about.

Adhesives usually have polymers as the principal component or if they are monomers then they are mixed with other compounds to form a polymer. In the application phase, it is important that is adhesive is in a liquid phase, as it is important for the joint that the adhesive makes intimate contact with the adherends, the property which is known as wetting.

From this liquid state during application of adhesive the adhesive needs to be hardened to produce an effect adhesive joint. This process is known as curing. Curing is the process when the hardening of the bulk adhesive takes place and adhesion occurs at the adherend adhesive interface. This adhesion is a result of Van der Waals forces which are inter-molecular forces of attraction. This hardening can be achieved various ways, either by heating the adhesive joint to lose the solvent or water or in other words to induce polymerization. Sometimes if the adhesive is heated to get to its liquid state during application then the curing is done by cooling. In this study we are using High-temperature adhesives. These normally cure by chemical reaction at high temperature and under pressure. Once hardening is done we have either a linear or a cross-linked polymer. Cross-linking makes the adhesive insoluble and infusible and reduces the creep for the material. All structural adhesives are cross-linked.

1.2 History of Adhesives

Adhesives have been used for several centuries by mankind. However, only in the last 80 years the science and technology of adhesion and adhesives has progressed significantly, the major advances which were made during the 1940s. The most significant reason has been the use of synthetic polymers. These materials possess the balance of properties that enable them to adhere readily to other materials and to have adequate strength to be able to transmit applied loads and forces from one substrate to the other.

1.3 Advantages of Adhesives

Advantages that adhesives relative to other joining techniques:

1. Ability to join dissimilar materials; e.g. metals, plastics, rubbers, fiber-composites, wood, paper products, etc.
2. Compared with metals, adhesives do not possess large tensile strength, but they have the ability to join this sheets or metal or non-metals with adequate strength.
3. Improved stress distribution in the joint.
4. Convenient and cost effective joining method.
5. Can be automated, right from mixing of the component of the adhesive to repeatability of application at a particular location by robotic assembly techniques.
6. Flexibility with choice of materials, gives the designer more freedom to design.
7. The appearance of the joint in comparison with say the spot welding technique is blemish free and thus more appealing.
8. Improved corrosion resistance in comparison again with say the spot-welded component.

However some disadvantages are:

1. Surface pre-treatment is an additional step especially if the adhesive joint is to be designed for long service life.
2. Adhesives have problems withstanding high service temperatures.
3. Adhesive have lower strength in tension and shear than compression. They perform well for joining thin sheets, but in case of joints thick adherents, the surface area needs to be large and the adhesive needs to be kept in compression.
4. Non-destructive testing (NDT) for adhesives is limited.
5. Adhesives have outgassing characteristics. Outgassing is the property of the material to release the trapped gas when the adhesive joint is in use. This is especially a drawback with adhesives are used in vacuum.
6. Shrinkage is another problem that adhesive joints suffer. Again in conditions such as vacuum, because the relative humidity is very low, the adhesive starts to lose moisture and the joint shrinks which results in compressive stresses in the joint.
7. In the reverse conditions, when the adhesive joint is exposed to an atmosphere with high relative humidity, the adhesive has the tendency of soaking up the moisture and swell in volume. This change in volume can not only affect the strength of the joint but also affects the stability of the joint. This can be a drawback for adhesive joints where a lot of precision for the joint is a requirement.
8. The adhesive is also known to age with time. This deterioration is the loss of strength of the joint or deformations in the joint with respect to time.

9. Most adhesives are also sensitive to UV light. This again is a direct drawback for the use of adhesives in the ASML NXE machines, as these machines use EUV light for performing photolithography.

Chapter 2

Literature study

2.1 Introduction

2.1.1 Challenging areas

There are various challenging areas in the adhesive field dealing with the understanding of the mechanics of failure. Some of them are listed below.

- Reliable adhesive tests.
- Failure criteria.
- Surface preparation for durability.
- Joint strength optimization.

Our focus in this research is going to be on designing more reliable joints which will primarily involve identifying a appropriate failure criteria for adhesives.

2.1.2 Steps to identify failure criterion

As we focus on identifying or developing an appropriate failure criteria for adhesives we envisage dividing the process in the following steps.

1. Measuring the force needed to initiate a crack in different geometries.
2. Using FEA to predict stress and strain components in regions of maximum stress and strain where crack initiation is expected.
3. Exploring various expressions of stress and/or strain that have a critical value at failure common to all joint geometries.

2.2 Types of loads

Adhesive joints in practice are loaded by a combination of different types of loads. Although in our research we shall focus on individual load types to try and understand their affect on the joint.

Also to be able to apply the various types of load we have different geometries which allow us to suitably apply those forces. Hence we can have different joint geometries for different loads.

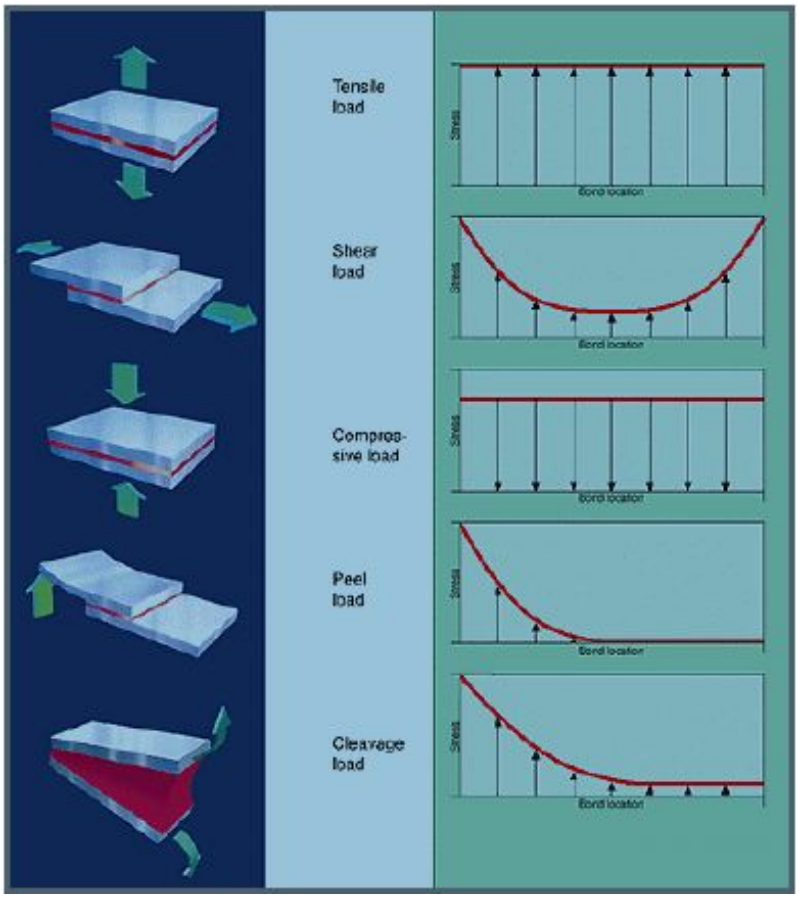

Figure 2.1: Stress distribution for various load types — Tensile, shear, compressive, peel and cleavage loads.

1. Tensile load.
   The joint is loaded perpendicular to the surface of the adhesive with force acting away from the adhesive surface resulting in a pulling or tensile force on the adhesive.

2. Shear load.
   The joint is loaded in the direction parallel to the adhesive surface. Shear stresses are developed in the adhesive. Shear tests are very common for adhesives as adhesive joints are often designed to resist shear loads. The list below has some common joints that are used for shear testing.

   - Single lap joint.

- Double lap joint.
- Scarf joint.
- Step joint.

3. Compressive load.
   Similar to the tensile load. The only difference being the loads are directed into the plane of the adhesive surface resulting in compressive stresses inside the adhesive.

4. Peel load.
   These are tensile loads with the loading concentrated on a edge of the adhesive joint and varying across the adhesive joint.

5. Cleavage load (Boeing wedge test).
   These loads are used to study the behavior of crack propagation through the adhesive joint.

   - Fracture mechanics.

2.3 Testing

In this section we would like to discuss the different types of tests that can be conducted and the test equipment that is needed to conduct these tests.

2.3.1 Types of tests

Adhesives are materials which exhibit complex behavior under different types of tests.

- Quasi-Static Strength Tests
- Quasi-Static Fracture Tests
- Higher Rate and Impact Tests
- Durability Tests

The adhesives are very sensitive to type of loading. As such it is very important to state under what tests we plan to obtain our results and derive our conclusions from. Our focus in this research is primarily on Static or Quasi-static strength tests. To a certain extent we will try and study the sensitivity of our results to inclusion of cracks or change in the rate of loading. Impact tests which have a much higher rate of loading will be outside the scope of the research. Also durability tests which include creep or fatigue loading have life based failure criteria as such they would not be a part of our research.

2.3.2 Bulk specimen testing

Apart from the joint test which is conducted on various joint geometries, we will also conduct bulk specimen tests to obtain bulk properties of the material. Bulk properties of adhesives tells us about the behavior of the material when its is not restricted within the joint boundary conditions. The most popular sample for conducting these tests is the dog-bone sample.
Typically we have uniaxial tensile tests conducted on the dog-bone sample which give us force displacement measurements which are further converted to stress strain curves. Alternatively we can also conduct uniaxial compression tests on similar samples, but in this case the sample has to be supported at the sides to avoid bulking of the sample. To be able to study the development of hydrostatic stresses in the material a test can be arranged where in a cube shaped adhesive bulk material can be tested under the action of hydrostatic compression from surrounding liquid. There are no standards yet for this type of test.

2.3.3 Testing of Butt joints in tension

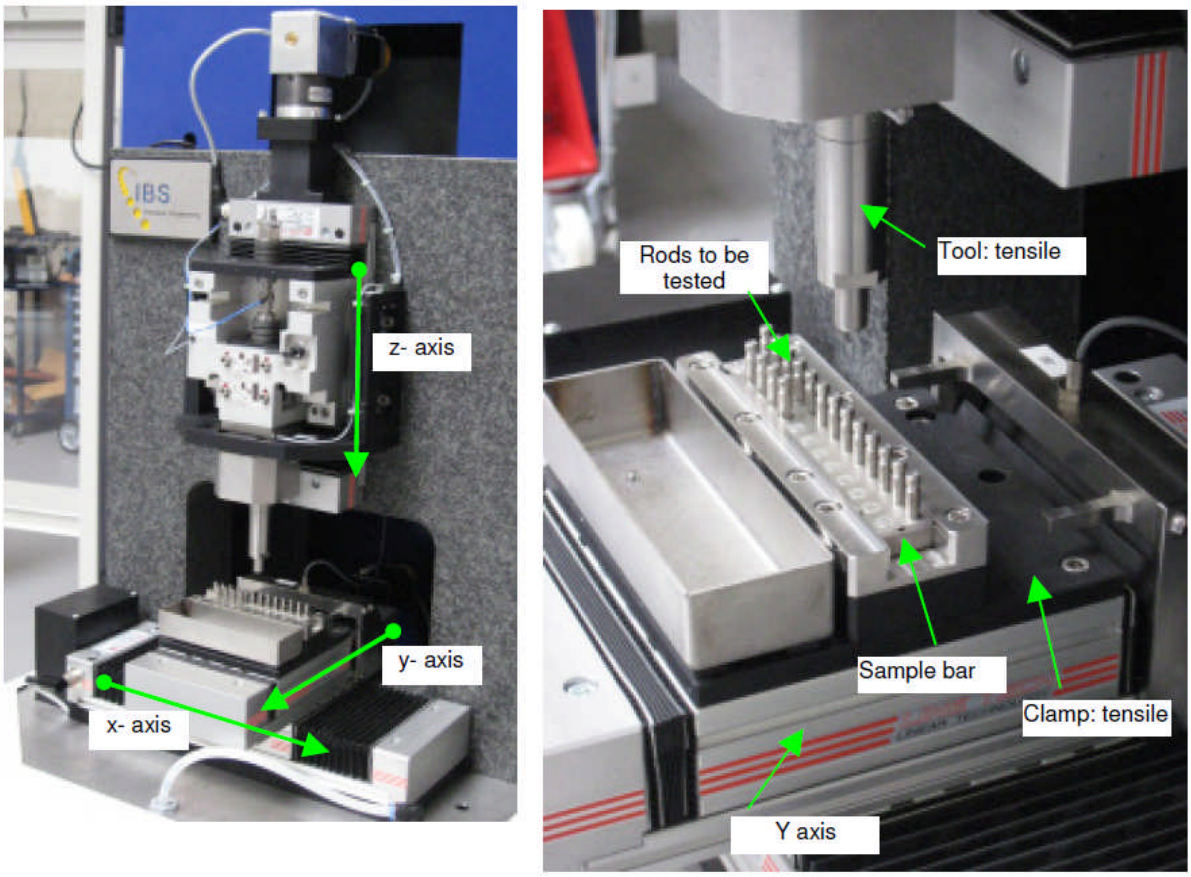

Figure 2.2: IBS 1 test setup

This is the most standard testing arrangement at ASML. 26 Stainless steel pins are glued to a stainless steel bar as seen in the figure. The setup is built by IBS Precision Engineering and henceforth referred to as the IBS1 or IBS Stein test machine. The contraption is such that the tool clamps on top of the test pins and pulls the pins in the vertical z-direction. This test is used to determine the tensile strength of the bond.

1. Requirements
    - Adhesive layer should not have voids.
    - Loading must be axisymmetrical.

2.3.4 Solid Butt joints in Torsion

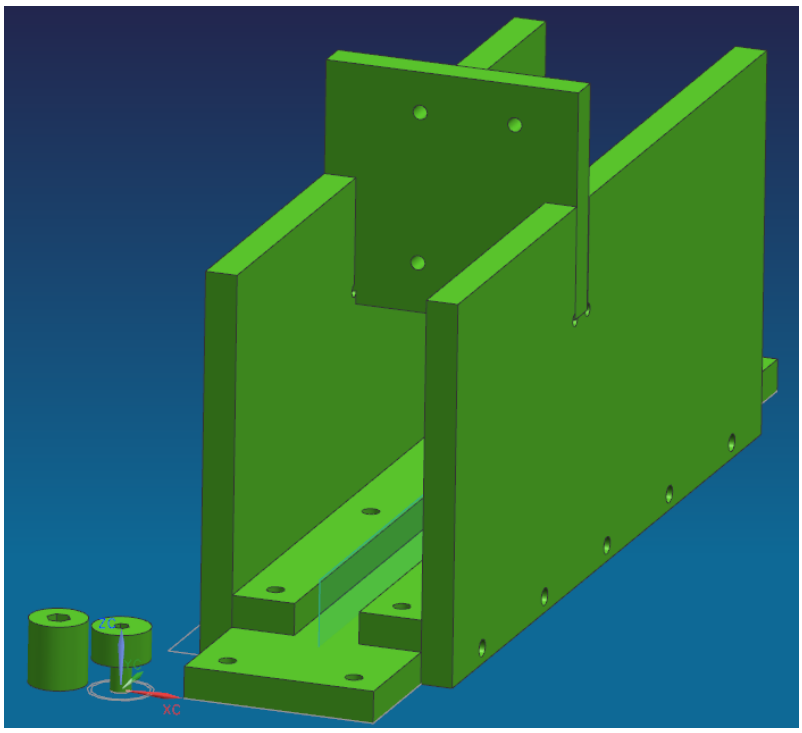

Figure 2.3: Shear testing setup

This is a setup which was designed internally especially for the purpose of this research. Its a simple yet effective contraption which uses the same specimen joint as that used in the tensile butt joint tests. The difference is in the type of loading. A pure shear or torsion load is applied to the butt joint manually using a two-handed torque wrench. The torque is applied manually keeping the strain rate as uniform as possible during the testing. The torque in transferred to the test pins through a digital torque sensor which measures the speed, angular measurements and the torque applied. The torque sensor has single couplings on either ends which provide angular and radial allignment so that only uniaxial torque is transmitted to the sample. No bending forces or compressive forces are transmitted.

This test is a simpler and more economical alternative to the Napkin ring test [8]. These tests are used to determine the shear strength of the bond.

1. Advantages over Napkin ring test.
    - If $r_o \approx r_i$ then difficult to manufacture.
    - Errors in alignment in samples.
    - Adhesive of low viscosity can be tested.
2. Disadvantage over Napkin ring test.
    - Shear strain varies linearly with radius of the pins.

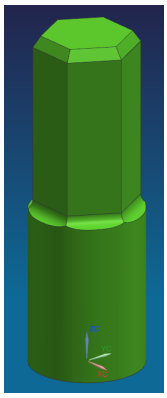

Figure 2.4: Test pin geometry

Figure shows a closeup of the steel pin that is used for the torsion tests. The head of the pin is modified for the torsion tests to accommodate the head of the torque wrench. Also a chamfer at the transition from the hex head to the cylinder of the pin is lowered to avoid any transfer of axial compressive loads on the adhesive joint.

2.3.5 TAST testing

TAST stands for the Thick Adherend Shear Test.

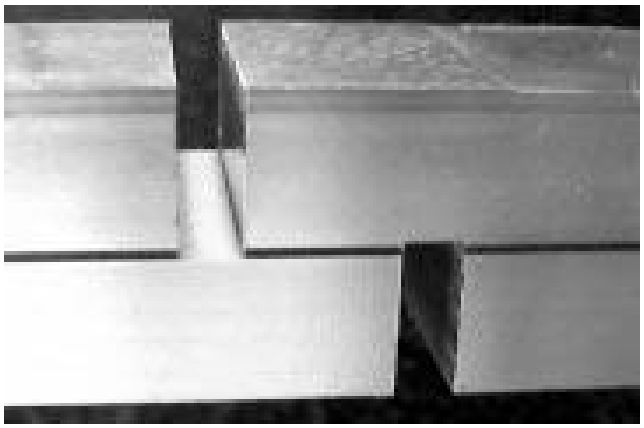

Figure 2.5: TAST specimen

The testing on the TAST specimen can be conducted on the Instron machine. The Instron machine applies a tensile load at one end of the specimen. The advantage of the geometry of the TAST specimen over a lap shear specimen is that we can avoid the bending moments hence the peeling stresses in the TAST specimen. A more homogenous deformation of the adhesive is obtained.

2.3.6 Lap shear testing

The lap shear test is the most popular test for adhesive joints. This can be attributed to various reasons. The most important being ease to manufacture the joint specimen and also the joint depicting the practical application of most adhesive joints.

This joint is a part of our research and is discuss in depth later in the document. Here is appropriate we enumerate some key characteristics of the test.

1. Very common test method in industry.
2. Single lap joint (SLJ) or Double lap joint (DLJ).
3. Testing with thin adherends similar to the aeronautics industry.
4. There are many standards and variations for this test.

2.3.7 Modified Arcan test

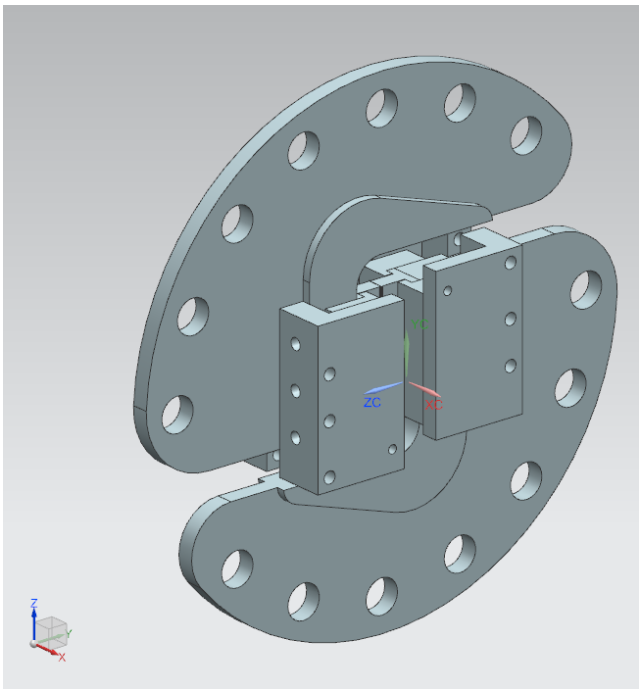

Figure 2.6: Arcan setup

The Arcan test setup has many unique advantages.

1. Proportional tensile/compression - shear loading.
2. Results are useful to model the non-linear adhesive behavior.
3. Instron can be used to load the setup.

This setup was designed by me during my research based on designs that were found during the literature study. Simulation results showed that the setup was indeed reliable for testing. The applied loads were effectively transferred to the adhesive specimen as desired in the test type.

2.4 Failure in Adhesives

Failure in adhesives can be a result of many effects or even a combination of these effects.

2.4.1 Mechanical Effects

1. Static Loads
2. Cyclic Loads
3. Sustained Loads
4. Impact/Dynamic Loads

2.4.2 Chemical Effects

1. Effect of humidity and water condensation
2. Effect of atmospheric oxygen
3. Concentration of gases, solvents and salts in environment

2.4.3 Physical Effects

1. Temperature
2. Ultraviolet radiation

2.5 Types of adhesives

2.5.1 Flexible adhesives

Flexible adhesives as the name suggests are more flexible. A hyper-elastic material model is more suitable to define the behavior of this material.

2.5.2 Tough adhesives

Tough or toughened adhesives are more widely used. In our research we use non-toughened epoxies. The epoxies and acrylics which are classified as tough adhesives can be accurately modeled using the Drucker-Prager material model. Also literature suggest a critical strain based failure criteria is suitable. The strain is dominated by the volumetric component of strain and the contribution from the shear component.

2.6 Material Models

2.6.1 Linear visco-elastic models

1. Simple spring and dash-pot analogies.
2. Can be solved as either one of creep or relaxation models.
3. Power law representation of creep, has constant terms that cannot be derived from one form of loading and used to predict behavior in another.

2.6.2 Non-linear visco-elastic models

1. Excellent correlation with experimental data.
2. Not the easiest to implement.

2.6.3 Visco-plasticity

1. Non-linear visco-plastic models depend on strains and over-stress. Over-stress is difference between actual stress and equilibrium stress.
2. Most promising is the visco-plasticity based on over-stress (vbo) model.
3. Easier to implement than non-linear viscoelasticity, but still requires reasonable amount of material data.

2.7 Parameters affecting adhesive performance

Some of the parameters that can heavily effect the performance of an adhesive joint are temperature variation and time scale over which the loading is applied. We do not intend to study the effects but would like to ensure that the effects due to time and temperature do not play a role in variation in test results.

2.7.1 Glass transition temperature — glass to rubber transition

1. Flexible Adhesives — For adhesives with T_g around room temperature, the bond strength and E is substantially reduced.

2. Tough Adhesives (Structural adhesives) — Generally adhesives with T_g much higher than room temperature.

2.7.2 Time-temperature superposition

- The material properties of polymers are very temperature dependent around T_g.

- Time also plays an important role in polymer properties. Not chemical but a purely physical phenomenon.

2.8 FEA limitations

This chapter would be incomplete without addressing some of the aspects of FEA calculations that can affect the results from our research. Also refer Chapter 8.

2.8.1 Limitations

A major limitation with FEA is the inability to account for points of stress singularity, such as those present at the ends of bonded joints. The FEA results depend on the element size with the value of the stresses increasing as the element size near the singularity is reduced. If stresses become infinite, then the predicted load at failure is zero [7].

2.8.2 Solution

Following are standard solutions for the usual suspects with respect to FEA. We will see some these solutions implemented in the FEM modeling chapter.

1. Remove singularities.

2. Imposing radius on all edges.

3. Using a suitably fine mesh. It has been suggested that the element size in regions of high stress gradients be equal to 1/3 of the adhesive thickness [7].

4. Accurately represent joint geometry near the bond.

5. Stiffness softening effect in non-linear material properties takes care of stress concentration at edges. [40] [39].

Chapter 3

Literature study - Failure Criteria

The crux of the research is the applicable failure criteria for adhesives. It is therefore essential to understand the different criteria that can be explored. Upfront is it perhaps wise to express that we would be focusing on the criteria based on strength and yield. Hence the focus of the literature study also primarily includes these criteria.

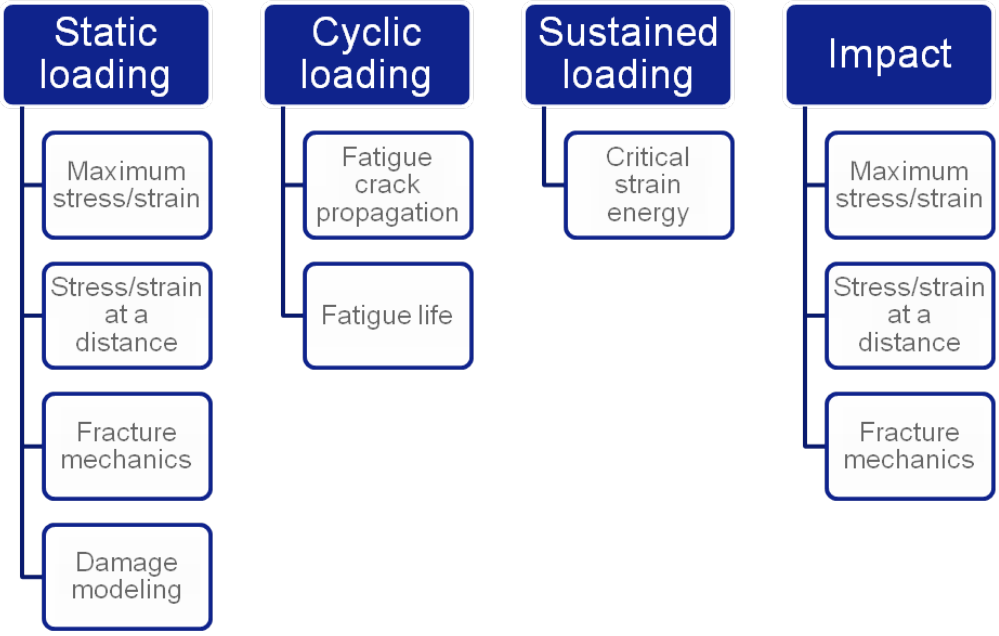

Figure 3.1: Types of loading and failure criteria.

Knowing the failure mode is important for selection of the failure criteria. In general there failure of adhesives can be in tension, shear or peeling. In tension and peel, the stresses near the bond line are very high which is difficult to sustain, so the shear modes of failure is much preferred for design of an adhesive joint.

3.1 Strength based criteria

If there are small plastic strains. This criterion does not include plasticity and assumes linear elastic solid behavior. Strength based classification of criteria is the most simplistic way of defining failure. These can be based on either stress or strain. Either maximum values or average value over the cross section can be considered [42].

1. Average Stress - This approach is too simplistic. Assumes that adherends are rigid, and only adhesive deforms in shear.
2. Maximum Stress - Allows non-uniform stress distribution along bond length and bond thickness. Closed-form analytical and FEM solutions available. FEM has limitations with stress singularity exclusion.
3. Maximum Strain - Developed by Hart-Smith. Accounts for non-linear elastic-plastic deformation. Strength is defined by strain energy in shear. Dependent on shear strain to failure.
4. Von Mises stress, Tresca and Drucker-Prager stress criterion.

3.1.1 Average Stress

Stresses are averaged over the adhesive layer. This approach is too simplistic. The criteria is based on the assumption that the adherends are rigid and also assumes that the adhesives deform on in pure tension or shear.

3.1.2 Maximum Stress

Maximum stress criteria allows us an approach looking at the non-uniform stress distribution along bond length and thickness [7]. Also closed-form analytical & FEM solutions are possible to obtain. Limitations regarding this approach can be overcome by exclusion of the stress singularities. Also maximum stress criteria are the most intuitive starting point for joint strength predictions [12].

Maximum shear stress

1. Appropriate for shear loaded components.
2. For tensile loaded components, predicted strength too low.
3. This failure mode is rare.

Maximum peel stress

1. Can be used for certain configurations.
2. Not accurate where substrate yielding takes place.

Maximum principal stress

1. Fairly accurate using elasto-plastic analysis.

Maximum equivalent stress (Von Mises, Drucker-Prager, Tresca)

1. Relates equivalent adhesive stress to uniaxial yield stress.
2. Commonly used with elastic FE analysis.
3. Neglects hydrostatic component which significantly affects yield and deformation for polymers [24] [54].

3.1.3 Maximum Strain

The maximum strain criteria accounts for non-linear elastic-plastic deformations. The strength is dependent on strain to failure. Strain based failure criteria are generally more accurate than the stress based failure criteria [7].

Maximum shear or peel strains

1. For ductile adhesives, failure best expressed in strains.
2. Dependent on adhesive thickness.
3. Difficult to use with cracked tip models.

Maximum principal strain

1. For toughened adhesives max. principal strain more appropriate than principal strain.

3.1.4 Remarks related to Maximum criteria

1. For non-toughened epoxies the maximum principal stress criteria is found appropriate.
2. For toughened epoxies. Maximum principal stress criteria is accurate for failure in Mode I. And Maximum principal strain criteria for Mode II failure mode.
3. Bi-material geometries result in singular stress/strain fields.
4. Maximum criteria is sensitive to degree of rounding.
5. Maximum criteria is valid with some extent of averaging.

3.1.5 Stress/Strain at a distance

This technique involves use of maximum stress/strain value at a given distance from the point of singularity [42]. Or in some cases we can average this critical value over a region. This distance away from singularity is not a unique parameter. We cannot say if it would be based on material, or adhesive thickness or mode of loading.

3.2 Yield based criteria

These criteria are more accurate for adhesives. Adhesives use are ductile and hence there is yielding expected for these materials. Some of the criteria are mentioned below.

1. Tresca yield.
    - Yielding occurs when maximum shear stress reaches a critical value.
2. Von Mises yield.
    - Interprets yielding as pure shear deformation due to effective shear stress.
    - Yielding occurs when shear strain energy reaches a critical value.
    - The critical strain energy is expressed in terms of principal stresses.
    - Adhesive yielding is sensitive to hydrostatic stress and shear component, there this criteria is not realistic [12].
3. Linear Drucker-Prager yield
    - Includes some sensitivity to hydrostatic stress by introducing parameter (μ)
    - Adhesive yielding is sensitive to hydrostatic stress and shear component, there this criteria is not realistic.
    - Low accuracy under high component of hydrostatic tension. These are common in adhesive joints.
4. Extended Drucker-Prager yield
    - Overcomes shortcomings of Linear DP by introducing another hydrostatic sensitivity parameter (λ).

3.3 Fracture Mechanics

Assumes a pre-existent crack and uses FEA to determine the stress state in the vicinity of the crack tip.

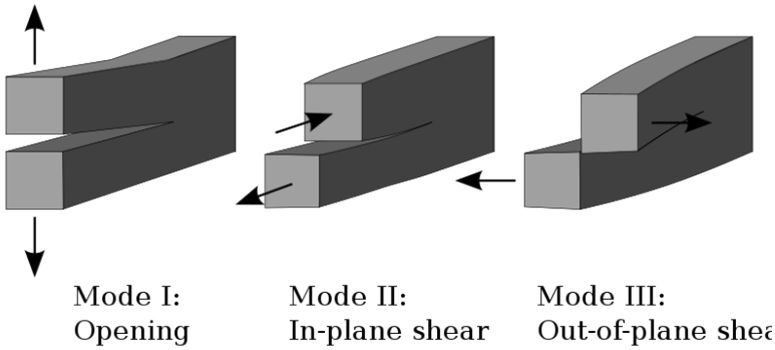

Figure 3.2: Modes of fracture.

This criteria is used for structures that have inherent flaws or cracks. Using this criteria we do not look at local values of peak stress but instead we see if the conditions are suitable for failure. One such parameter we look at is Critical energy release rate (G_c) which is the energy required for crack to propagate. And Critical stress intensity factor (K_c) which is the Fracture toughness. It is a combination of critical value of J integral with crack opening displacements.

3.4 Void nucleation (cavitation) criteria

Cavitation criteria takes into account the cavities present in the adhesive due to locked in air which have a large effect on the failure of these joints. Voids can be trapped which mixing two part adhesives. Careful mixing of adhesives can avoid void nucleation.

- Rubber particle cavitation due to dilatational component in stress tensor.
- Cavitation increases stress concentrations.
- Modified Gurson's yield criterion.

3.5 Description of various criteria used for calculations

When we have ductile adhesives (strain at failure > 0.05), the yield based failure criteria are looked at.

3.5.1 Drucker-Prager criterion

The DRUCKER-PRAGER is a pressure dependent criteria for determining whether a material has yielded or failed. Usually used to study plastic deformation of soils. Also polymers. It is a conical shaped yield surface which if seen in 2D is similar to the Von-Mises but unequal for the tensile and compression stresses. It is similar to Von Mises criteria. Both normal and shear stresses are accounted for failure.

$$S_{yc} \leq (\frac{m-1}{2})(\sigma_1+\sigma_2+\sigma_3) + (\frac{m+1}{2})\sqrt{\frac{(\sigma_1-\sigma_2)^2+(\sigma_2-\sigma_3)^2+(\sigma_3-\sigma_1)^2}{2}} \quad (3.1)$$

where

$$m = \frac{S_{yc}}{S_{yt}} \approx 1.5$$

The value for m for epoxy adhesives ranges between 1.3-1.5. In our research we use $m = 1.5$. Therefore, to use the formula in conjunction with tensile data,

$$S_{yt} \leq (\frac{m-1}{2 \cdot m})(\sigma_1+\sigma_2+\sigma_3) + (\frac{m+1}{2 \cdot m})\sqrt{\frac{(\sigma_1-\sigma_2)^2+(\sigma_2-\sigma_3)^2+(\sigma_3-\sigma_1)^2}{2}} \quad (3.2)$$

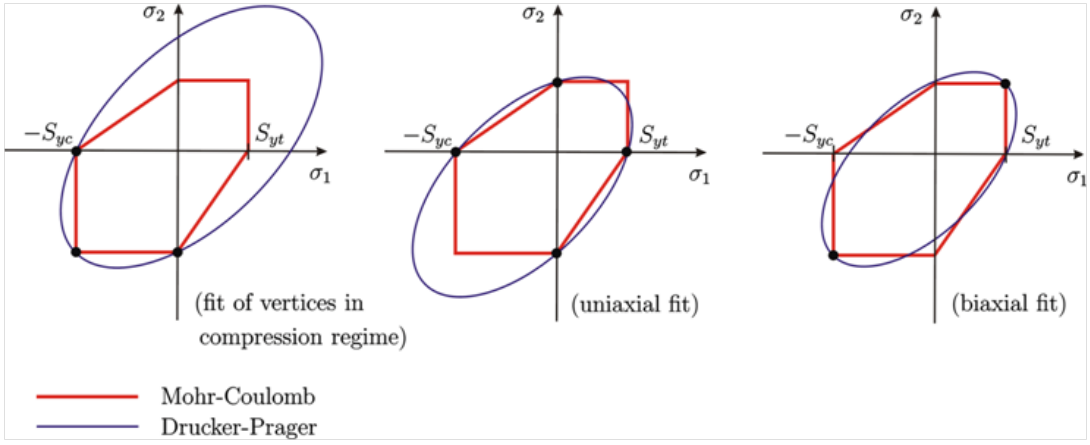

Figure 3.3: Drucker-Prager criteria.

3.5.2 Maximum shear stress criterion

Tresca is also the MAXIMUM SHEAR stress theory. In tensile tests, the failure for ductile materials occurs at slip lines at 45° where we also have the maximum shear stress.To visualize it looks like a prism of 6 sides and running for an infinite length. It means that the material remains elastic if the three principal stresses are equivalent. However as one of the principal stresses becomes larger or smaller, then material is subjected to shearing.

$$S_{yt} \leq \max(|\sigma_1 - \sigma_2|, |\sigma_2 - \sigma_3|, |\sigma_3 - \sigma_1|) \tag{3.3}$$

where, S_{yt} is the material yield stress in uniaxial tension

3.5.3 Mohr-Coulomb criterion

MOHR-COULOMB is usually used for for both ductile and brittle materials. It includes the response of material under shear and normal stresses. Generally applied to material which larger compressive strength than tensile strength.

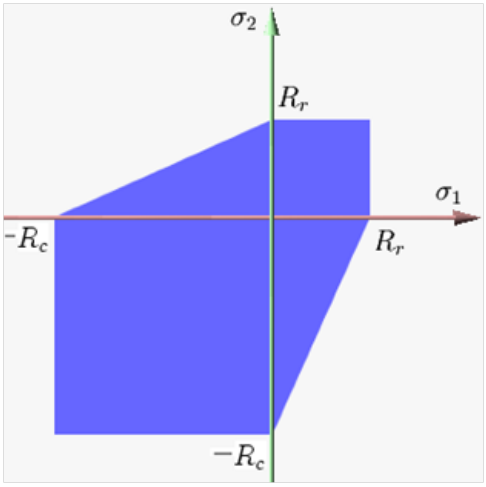

Figure 3.4: Mohr-Coulomb criteria.

$$S_{yt} \leq \frac{m+1}{(2 \cdot m)} \max(|\sigma_1 - \sigma_2| + K(\sigma_1 + \sigma_2), |\sigma_1 - \sigma_3| + K(\sigma_1 + \sigma_3), |\sigma_2 - \sigma_3| + K(\sigma_2 + \sigma_3)) \tag{3.4}$$

where, S_{yt} is the material yield stress in uniaxial tension

$$m = \frac{S_{yc}}{S_{yt}} \quad ; \quad K = \frac{m-1}{m+1}$$

3.5.4 Von-Mises criterion

When strain energy causing distortion of the element exceeds the distortion strain energy from a standard tensile test, the element can be said to have yielded.VON MISES is a circular cylinder of infinite length at an angle equidistant from all the 3 axes. In 2D stress space is looks like an ellipse.

$$S_{yt} \leq \sqrt{\frac{(\sigma_1 - \sigma_2)^2 + (\sigma_2 - \sigma_3)^2 + (\sigma_3 - \sigma_1)^2}{2}} \tag{3.5}$$

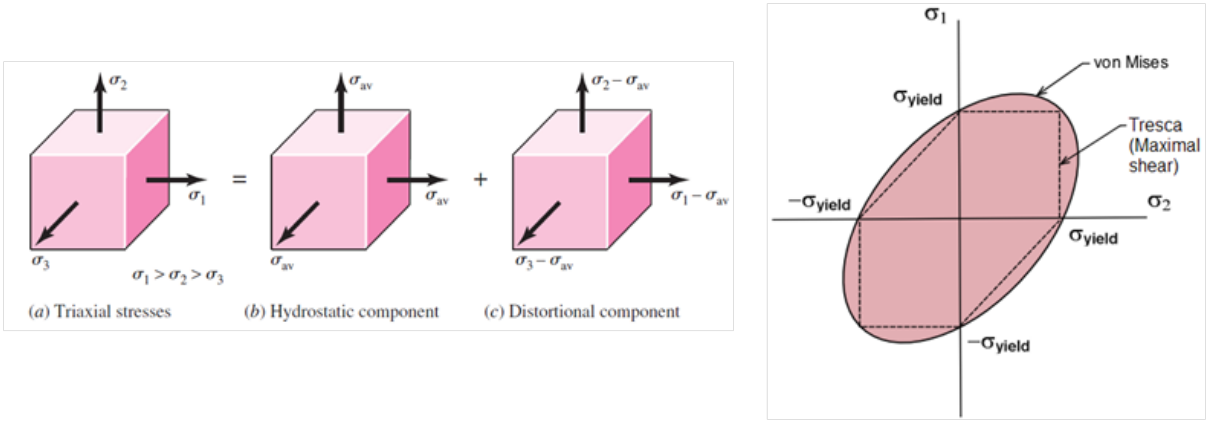

Figure 3.5: Von Mises criteria - Criteria is based on the distortional component of the total stress component. Ignores the hydrostatic stresses. Figure on right gives comparison of the Von-Mises criteria with the Tresca criteria on π plane.

3.5.5 Fracture stress criterion

FRACTURE STRESS criterion is an equivalent stress criterion developed from the combination of in-plane shear stress and the normal stress acting on that plane [37].

$$S_{yt} \leq \sqrt{{\sigma_Z}^2 + {\sigma_{XZ}}^2 + {\sigma_{YZ}}^2} \tag{3.6}$$

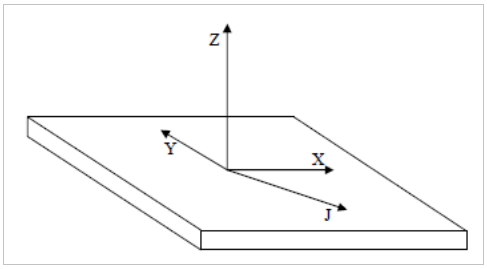

Figure 3.6: Two in-plane and one out-of-plane stresses make up the Fracture stress criterion.

3.5.6 In-plane shear stress criterion

The IN-PLANE SHEAR STRESS is similar to the maximum principal stress except that we only consider the shear stresses in the plane of the shear surface. Referring Fig. 3.6 the criterion is given by,

$$S_{yt} \leq \sqrt{{\sigma_{XZ}}^2 + {\sigma_{YZ}}^2} \tag{3.7}$$

where, S_{yt} is the material yield stress in uniaxial tension

3.5.7 Peel stress criterion

PEEL STRESS is the stress component normal to the surface. In Fig. 3.6 it is represented by σ_Z. The criterion is given by,

$$S_{yt} \leq \sigma_Z \tag{3.8}$$

where, S_{yt} is the material yield stress in uniaxial tension

3.5.8 Mean stress criterion

MEAN STRESS criterion is given by,

$$S_{yt} \leq \frac{\sigma_1 + \sigma_2 + \sigma_3}{3} \tag{3.9}$$

where, S_{yt} is the material yield stress in uniaxial tension

Chapter 4

Research Question

4.1 Research Question

"The goal of the project is to postulate or formulate the best stress based criterion applicable to any adhesive joint to evaluate it's strength or allowable stress accurately. A precise estimation will help avoid the need for bulky safety factors in design. These allowable stresses can be used in conjunction with FEM calculations to design adhesive joints."

4.2 Scope of the Project

One of the problems with using adhesive bonding is that often is it seen that it is difficult to predict the strength of joint based on standard tests. The standard ASME and ASTM tests give us an average F/A as the failure stress value. For these results to be applicable to any generic joint it is then important to perhaps identify a stress component or criterion that more or less has the same value at the point of failure for all geometries and all types of load types. Looking for such a criterion might be too optimistic, but at the least it would lead us to a selection of criteria which could be applicable within a certain scenario.

4.2.1 Linear Elastic Analysis

For the analysis of an adhesive joint, because the results in a linear analysis are scalable, easier to compute and need fewer material properties for tests, we restrict the scope of the project to linear elastic analysis. Although elasto-plastic and more complex material material models will be studied and even formulated to give a comparison.

4.2.2 Approach

The following flowchart explains the skeleton of the approach to be taken for investigating the appropriate failure criteria for analyzing the strength of adhesive joints.
As described in the flowchart, the research starts with deciding which joint geometries need to be tested and for which types of adhesives. Testing would be carried out using the available testing equipment and for some other tests, new test benches would be designed and manufactured.

The test geometry usually has some data that is unreliable due to some unexpected changes in test environment or failure of setup to function as designed. Also sometimes the joints could be damaged in certain samples and could lead to erroneous results. As

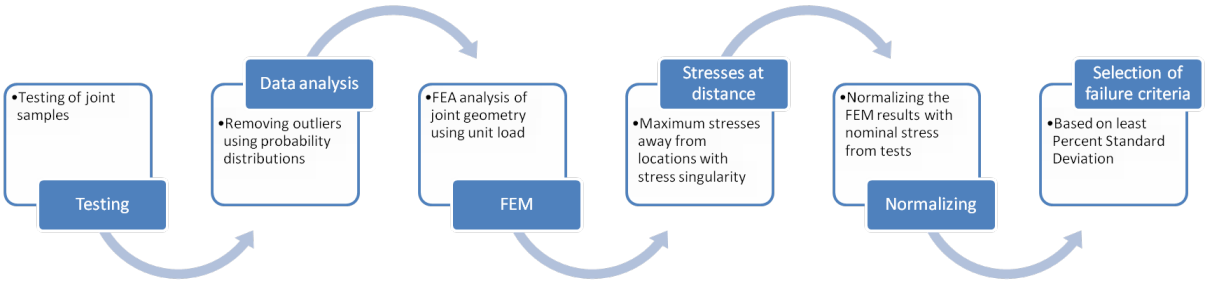

Figure 4.1: Process adopted in the project

such all data outliers need to be identified and eliminated from the final database by carefully observing the tested samples for evidence and motivating the reason for rejection.

Having generated the test database, we then move to the FEM analysis of these test joint geometries. The FEM analysis is essential to study the distribution of stresses along the glued joint. The FEM analysis also helps us determine the variation in the various components of stress which is not available through testing. Testing only gives us the information about the nominal or average stress over the glued area of the joint. The FEM analysis are carried out using unit load. As these analyses are linear elastic, then provide the flexibility to scale the stresses. Further at locations of stress singularity these stresses can be unrealistically high. To avoid this we use the concept of taking stresses at a distance such that they are not influenced by numerical artifices.

The stress results from FEM are normalized using the test results, to obtain the actual value of stress components in the joint at the point of yield failure. These peak stresses in the joint at yield are then combined in the form of various failure criteria, based on strength of materials, or on existing yield criteria used to evaluate metals, or some other criteria specifically popular with polymers. Some other criteria are also formulated based on fracture mechanism in the adhesive.

4.3 Software used

The following list of software were used during the project.

Purpose	Software
Programming	Matlab
Data Analysis	Minitab
Solid Modeling	Unigraphics NX
Meshing	Hypermesh & Ansys
FEM calculations	Ansys

Part II

Material Testing & FEM

Chapter 5

Testing

To be able to identify a general criterion for failure of adhesives, it is important that we have test data that come from tests covering a wide variety of loads that an adhesive joint could encounter during service.

5.1 Types of Loads

The loading can be a single type of load or a combination of such types of loads. In our study we have considered the following types of loads, namely -

1. Tensile
2. Lateral Shear
3. Torsional shear
4. Bending

The selection of these tests is related to the types of tests that can be performed on the existing equipment. The torsional shear test is an additional load type which is performed keeping the test geometry same as for the tensile and lateral shear test with the only modification made to the test pin heads and the way to apply the load.

5.2 Test Setups

To conduct these test types ASML has three types of machines. The types of geometries tested follow directly from the machine type.

5.2.1 IBS Stein

The IBS Precision Engineering company has a test machine that tests 26 pin samples 5mm in diameter that are glued to a substrate.

Figure 5.1: IBS1.

The IBS1 is used for both the tensile, shear and bending tests.

5.2.2 Instron

The Instron on the other hand is able to perform tests on a variety of geometries. In our case we use the lap shear geometry to test using the Instron.

Figure 5.2: Instron.

5.2.3 Customized setup for torsion

The third type is a custom built setup which uses a torque load applied manually to the same geometry as the IBS machine via a coupling and a torque sensor.

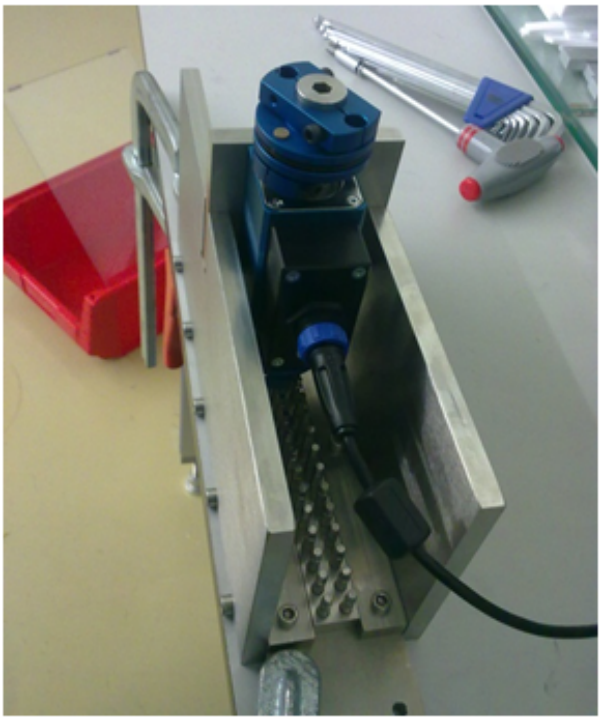

Figure 5.3: Torsion setup. Setup consists of a bar of metal with 26 hexagonal head pins glued to the bar. The torque in imparted with help of a torque wrench. The torque sensor has an USB out and has single couplings on either side for isolating unwanted loading.

5.3 Test data acquisition

In the case of IBS and the Instron, the test data is acquired by the software supplied with the machine. This data in the case of IBS is in nominal stress values that are recorded at a specified frequency. The data from the Instron is more elaborate. It gives us the time, displacement and the force values that are measured by a sensor mounted to one of its chucks.

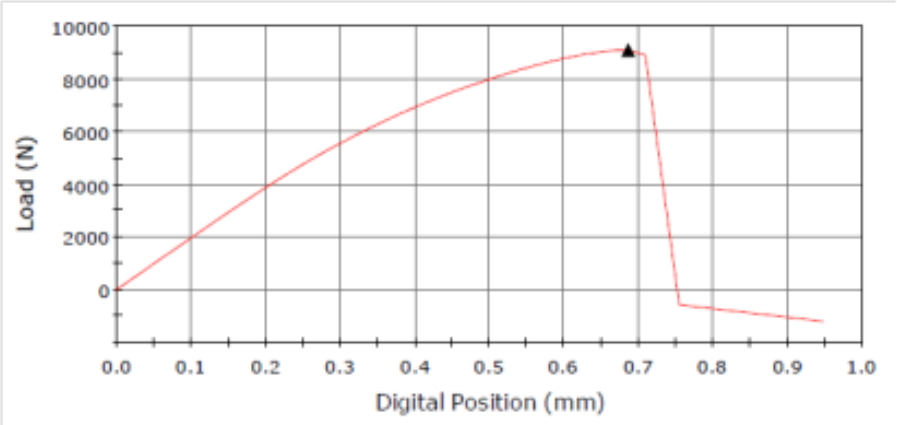

Figure 5.4: Data acquired from Instron.

The torsion setup uses a torque sensor that has a USB connection to a remote computer which records the angle of twist and the torque imparted to the sample. The data again is sampled at a frequency which can give us an idea of the strain rate. The following figure shows a sample of the test data that is acquired from the torque sensor.

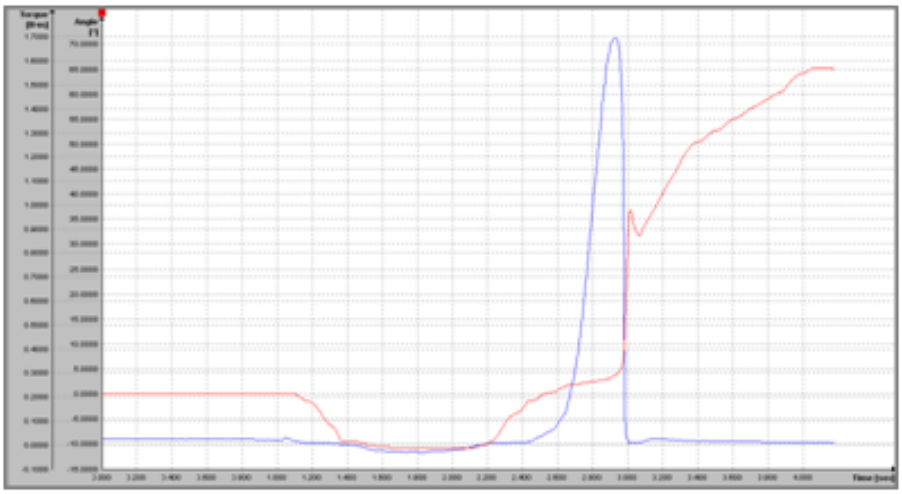

Figure 5.5: Data acquired from Torsion testing. (For illustration purpose only.)

The blue line indicates the loading of the adhesive joint under torsion with respect to time. It reaches a peak until which point we can see that the red line indicating the strain rate (twist angle v/s time) is low. At the point of failure the maximum value of torque

that can be borne by the joint is reached and just after failure a sharp rise in the strain rate is seen confirming failure.

5.4 Bulk adhesive testing

The bulk adhesive test data was available before the start of the research. The Young's modulus and the Poisson's ratio were available for the 2 adhesives used in the calculations. The results of the testing are provided in Section 10.2.

5.5 Adhesive joint testing

Five different adhesive joint tests are carried out on both adhesives, namely Scotweld 9323 and Araldite 2030. The tests and the number of tests carried out are tabulated in Tables 5.1 & 5.2.

Test type for Scotchweld 9323	Number of tests
IBS1 pin lateral shear test	156
IBS1 bending test	156
IBS1 bending test with corner beads	26
IBS1 bending test at 1/10th speed (0.1mm/s)	26
Lap shear test	9
IBS1 tensile test	364
IBS1 bending test for cracked specimen	52
IBS1 bending test at 1/10th speed (0.1mm/s)	26
Torsion test	156

Table 5.1: Table with list of tests and the number of tests conducted for Scotweld 9323.

Test type for Araldite 2030	Number of tests
IBS1 pin lateral shear test	130
IBS1 bending test	156
IBS1 bending test with corner beads	26
IBS1 bending test at 1/10th speed (0.1mm/s)	26
Lap shear test	9
IBS1 tensile test	156
IBS1 bending test for cracked specimen	52
IBS1 bending test at 1/10th speed (0.1mm/s)	26
Torsion test	156

Table 5.2: Table with list of tests and the number of tests conducted for Araldite 2030.

Notes

1. If corner beads is not mentioned, the tests are conducted with 100µ m diameter beads premixed in the adhesive in 1% proportion in mass.

2. If Locked/Unlocked is not mentioned, the tests have been con- ducted with IBS1 in the unlocked position. In the unlocked posi- tion the stiffness is lower and hence the failure loads are higher. This is the default configuration for testing hence the tests results in locked condition need to be increased by a factor of $\approx$ 1.1-1.2.

3. Unless speed is mentioned, the tests are conducted at 10mm/s.

5.6 Correction of test results for damping

Due to minor changes in damping of the setup, the damping needs to be calculated and subtracted from the data obtained from the tests. The Matlab program used for this correction is provided in Appendix A

5.7 Summary of the test results

The a tabular summary of the test results is provided in the Tables 5.3 & 5.4.

Test type for Scotchweld 9323	Nominal stress (MPa)
Torsion test	33
IBS1 tensile test	54
IBS1 pin lateral shear test	27
IBS1 bending test	5
Lap shear test	18
Percent standard deviation in pin tests	66.46
Percent standard deviation in pin and lap shear tests	66.94

Table 5.3: Table with summary of the test results for Scotchweld 9323.

Test type for Araldite 2030	Nominal stress (MPa)
Torsion test	28
IBS1 tensile test	15
IBS1 pin lateral shear test	4
IBS1 bending test	2
Lap shear test	11
Percent standard deviation in pin tests	97.6
Percent standard deviation in pin and lap shear tests	87.02

Table 5.4: Table with summary of the test results for Araldite 2030.

5.8 Adhesive Materials

Two adhesives were used. Both are epoxy polymers. The motivation for choosing the 2 adhesives are,

- Scotchweld 9323 is a widely used and well performing structural adhesive at ASML.
- Araldite 2030 was also popularly used and has a contrasting failure mechanism in comparison. Where SW9323 has a more cohesive failure, Araldite 2030 is mostly seen to fail in adhesion.

5.9 3M — Scotch-Weld 9323 B/A

SW9323 is a two part room temperature curing adhesive offering extremely high strength for structural joints. It has a toughened epoxy as a base material and is mixed in 100:27 ratio by weight with a modified amine which acts as an accelerator for curing of the adhesive. The work life at room temperature is around 2.5 hours for a mix weighing around 55g. The work life decreases with large mixtures.

5.9.1 Description

- High shear strength.
- Service temperature from –55°C to +80°C.
- It is a toughened epoxy system with good elevated temperature resistance.
- High environmental resistance.
- Upon mixing of the two parts, the adhesive is thixotropic for ease of application.
- Also offers high impact resistance.

5.10 Applications

- Used when both toughness and strength is required for the joint.
- Used for bonding various materials, such as metals, glass, ceramics and most thermosets.
- Suited in applications where the joint is required to have resistance to harsh environments such as oil, gasoline, dry heat, etc.

5.11 Huntsman — Araldite 2030

Araldite 2030 is a one part room temperature curing adhesive offering high strength for structural joints.

5.11.1 Description

- High shear and peel strength.
- Tough and resilient.
- Good resistance to dynamic loading.
- Bonding is possible with wide variety of materials.

5.12 Applications

- Multi-purpose adhesive with toughness and strength.
- Suitable for bonding metals, ceramics, glass, rubber and plastics.
- Finds use in industrial and craft applications.

5.13 Joint Test Specimen and Measurement of Properties

In this chapter measurement methods are briefly described for determining true stress and true strain curves for ahesives under tension. Measurements have been made on two adhesives, namely Scotch Weld 9323 and Araldite 2030 which are often used in the ASML machine. Results are analyzed to determine the properties and parameters required to run elastic-plastic material models for simulations using FEM. The measurements are conducted under tension and at rates of 1 mm/s. Measurements at large strains is required to capture the non-linear behavior of the adhesives.
These tensile measurements are used along with measurements under shear that are obtained from literature to derive parameters for Von Mises (Ref. Sec. 7.2.1), Linear Drucker-Prager (Ref. Sec. 7.2.2) and Extended Drucker-Prager models (Ref. Sec. 7.2.3).

5.14 Test Methods

In this section we will consider the various testing methods are employed in our research. We will discuss which tests we will conduct and how we will go about testing the specimen. Finally we will get an overview of the tests performed and discuss the results from the tests.

5.14.1 General considerations

The data requirements for simulating the performance of a adhesive joint using finite element methods depends on the choice of material model used to describe the deformation behavior of the epoxy polymer as well as the approximating assumptions, such as associated with the dependence of properties on strain rate. For the determination of all the parameters in the Drucker-Prager model , measurements of stress/strain behavior are needed to in tension and shear. Results for variation of Poisson's ratio with tensile strain is also needed. The reason we try to use different material models is to assess the applicability of these models and the nature and magnitude of errors associated with their use.

The real case problem that can be considered for validation of this assignment is that of a glued insert that fails under a combined effect of tensile, shear and bending loads. To check that the chosen failure criterion is applicable for most types of failure (peeling, shear, tensile) we plan to experimentally test the adhesive in various ways. We already have the setup to test the adhesive in tension in bulk specimens and also tensile (IBS 1 tests) and shear (Lap shear tests, Instron machine) in joint specimens. The lap shear tests have high stress concentrations at the edges, therefore the napkin ring test or torsional butt joints are also possible.

For shear failure, there are some standardized tests, like the lap shear test. Although the lap shear test is very popular due to its simplicity, it does have high stress concentrations at the adherend-adhesive edges. A better way of testing the adhesive in shear is to use the torsion tests. The napkin ring test is the ideal as it imparts pure shear stress to the adhesive, but manufacturing the samples is more complex and expensive. A simpler butt joint in shear can be alternatively used. The only drawback with butt joints is that the maximum shear stresses and strains (which are at the periphery of the sample) depend largely on the radius of the butt joint sample. Therefore the size of the butt joint is a factor. This problem can be resolved by using the Nadai correction to the Twist-Torque

graph. This enables us to get the true shear stress-true shear strain curve.

For the butt joints we use pins of 5mm diameter glued to a sample bar. The sample pins are easy to manufacture as similar pins are used in another test bench at the company. The only modification needed is that the pin heads need to be redesigned for torque loading (like a hexagonal bolt head) using a torque wrench. We have designed a special test rig for this test. It is important that if a manual-loading torque wrench is used it is in-line with the pin so that no peeling loads are applied, and also that the torque wrench is isolated from the pin in the vertical direction, so that no compressive loads are imparted to the adhesive joint.

Alternatively, instead of a manual torque wrench a variable speed motor can be used for application of the torque so that the problems with the manual wrench can be overcome. In the case of the manual torque wrench, we would be using angular displacement of the wrench; therefore the strain-rate would be kept constant. But in case of an electric motor the input would be force (torque) and it is important that during a test, the strain rate is maintained constant. As the adhesive starts to yield, the strain rate would then increase, and therefore to maintain the same strain-rate we would need to reduce the speed of the motor which would need some sort of a feedback loop.

5.14.2 Tensile Tests

Engineering force/displacement curves are obtained in tension and Poisson's ratios were measured using procedure defined by an ISO standard. The engineering force/displacement data is then converted to engineering stress/strain data and then further to true stress/strain data.

5.14.3 Shear Tests

The adhesives were not able to be tested in shear because there was no test setup available for such a test. The shear stress-strain curve tested at a similar strain rate as that of tensile was found in literature from a paper published from TU/e and Ghent University. These tests are usually performed on an Arcan test setup. One of such test setups along with the design of the test specimens was designed according to an ISO standard. Finite element analysis of the test setup was conducted and it was found that the design would be able to provide good shear force to the tests specimen. But this setup was not possible to be manufactured as it would have amounted to investment of more resources to this activity.

5.14.4 Compression Tests

Compression measurements were also obtained from literature found from papers at TU/e and Ghent. Usually this is done by compaction forces on a block of adhesive of size 10 mm x 10 mm. The end faces of this block are machined smooth and accurately parallel and then compressive force is applied through parallel plates. Alternatively a multi-axial compressive test can also be carried out by having this block of adhesive placed in a liquid (water) and then a piston like arrangement is used to compress the volume of liquid so that equal compressive stress is applied to the block of adhesive. The effect of hydrophobic properties affecting the strength of the adhesive should be considered.

5.15 Results

This section is related to the set of results generated from the testing of the various adhesive joints. (Summary of test results to be included in tabular form).

Chapter 6

Data Analysis

Having acquiring the test data we further need to analyze this data to obtain usable results towards calculations of failure criteria.

6.1 The need to remove outliers

The data that is acquired from the tests has variation. This variation can be a result of various factors. The adhesive joints are prepared with attention that the parameters related to the surface preparation and curing of the adhesive are kept the same for all samples. But this is done manually and there is inherent variation in the process. For instance the surface of the pin is prepared by the user using a sand paper with specific roughness to get rid of the uneven surface from the facing operation and also to impart a roughness to the surface for better adhesion of the glue to the substrate surface. This roughness can vary depending on the condition of the sand paper is use. With prolonged use of the sand paper the grain on the paper lose sharpness and affects the roughness of the pin surface.

Further some adhesives are prepared by mixing an epoxy which is a base material with a modified amine which accelerates the curing. The mixing of the two compounds is sometimes done manually and other times using the centrifuge. This could also pose a variation in the strength of glue produced.

The application of the adhesive is also manually done keeping the flow rate of the adhesive constant during application to the pins. But this flow rate needs to be adjusted depending on the nozzle diameter that is used hence the application of the adhesive can vary from one test batch to the other. Further upon application of the adhesive to the pins the substrate needs to be placed over the pins using alignment pins. It is possible that sometimes there is a slight movement of the substrate after placing over the pins with the adhesive that can move the adhesive to one side of the joint.

Lastly, there are some joints that have either much less amount of adhesive (Fig. 6.1) or are damaged before the test. These tests result in extremely low values of strength and thus including them into our analysis would mean introducing unwanted variation which is not due to the adhesive itself.

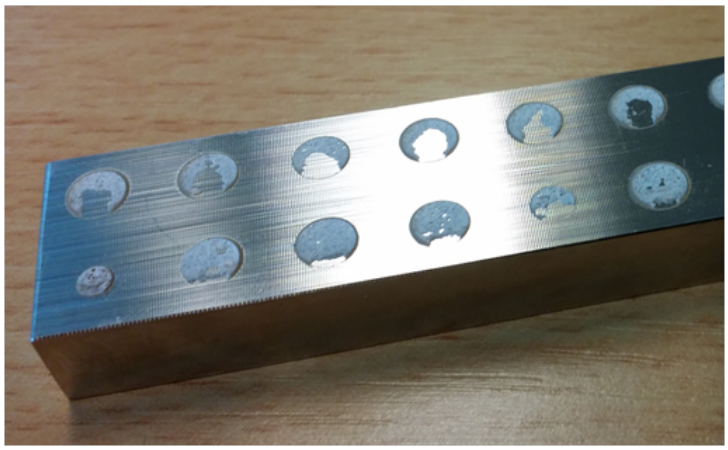

Figure 6.1: In this picture the bottom left most pin was glued with insufficient adhesive resulting in low failure load values.

For all the above reasons, there is a variation in the results that is found. This inherent variation within the adhesive strength needs to be isolated from the variation in the preparation of sample, or test environment or variations in the test setup. For this reason we use some statistical tools to remove the outliers.

6.2 Statistical Analysis

Before we start our discussion about the statistically analysis, it is important that we understand the meaning of some of the values and terms involved [2].

6.2.1 Alpha — Confidence level

Alpha (α) is used by us in hypothesis testing. It is the maximum acceptable level of risk for rejecting a true null hypothesis and is expressed as a probability ranging from 0 to 1. It is also referred to as level of significance. We set alpha before beginning the analysis and then compare the p-value to alpha to determine significance.

- If p-value is less than or equal to alpha, we reject the null hypothesis in favor of the alternative hypothesis.
- If p-value is greater than the alpha, we do not reject the null hypothesis.

The most commonly used alpha value is 0.05. At this level, our chance of finding an effect that does not exist is only 5%. The smaller the alpha value, the less likely we are to incorrectly reject the null hypothesis. However, a smaller value of alpha also means a less chance of detecting an effect if it truly exists.

6.2.2 P-value — Appropriateness of rejecting the null hypothesis

P-value just like alpha also varies from 0 to 1. While using alpha and p-value is it important that we clearly understand what the null hypothesis and the alternative hypothesis is. A p-value greater than alpha value would give the probability of obtaining a statistic that is as extreme as the calculated value, if the null hypothesis is true.

6.2.3 Goodness-of-fit — Whether a statistical model fits your data & Anderson-Darling statistic

We can visually check the fit of data to a certain distribution. Or quantitatively with a hypothesis test such as the Anderson-Darling test (AD statistic).

- The null hypothesis is that the model adequately describes the data.
- The alternative hypothesis is that the model does not adequately describe the data.

We look the least number for the AD statistic which shows the difference between the observed values and their expected values in the model. This difference should be the least for a good fit.

6.3 Use of Minitab for measurement data processing

For cleaning up the data we use the statistical application Minitab. First of all we try and plot the data for each test in a time series plot. This helps us understand how the values for strength have varied over the different tests. Figure 6.2 shows time series plot for the bending test. There were 6 test bars tested that were prepared in 3 batches. We can clearly see that the mean for these three batches varies as such we need to transform the values to the same mean to overcome any process changes that took place from one batch to the other. After adjusting the mean we can then decide which values need to be identified as outliers.

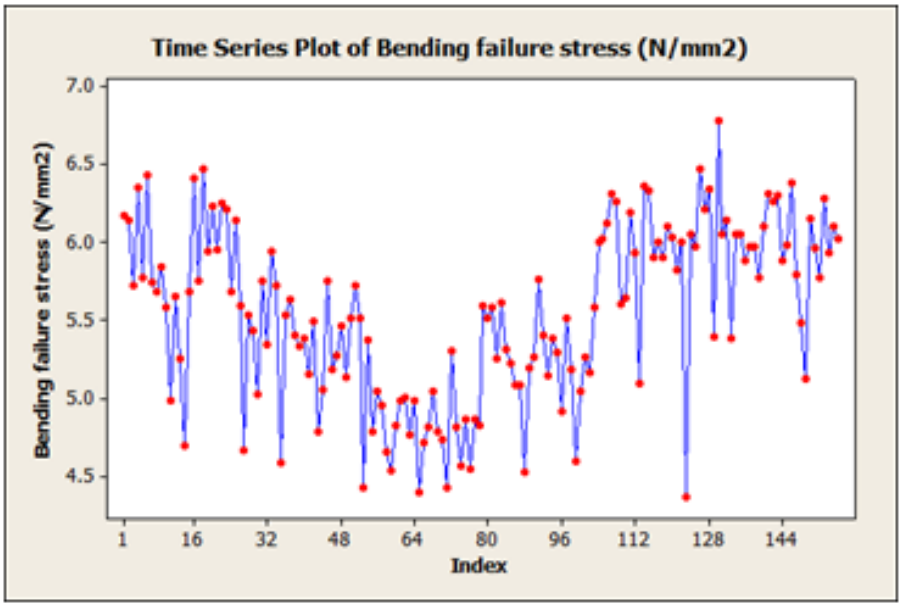

Figure 6.2: Time series plot - Index on x-axis represents the failure stress for individual tests under bending. A batch of 26 tests represent 1 batch of 26 pins. In all 6 such batches (156 pins) are tested.

One of the ways to identify outliers is by trying to fit the data at hand to a distribution. From the literature survey and also after trying to check the fit of the failure values to different distributions we find out that the Weibull distribution show the best fit (Ref. page54) for the data obtained for both the adhesives.
In Fig. 6.3 we can quantitatively determine that the AD statistic is 1.156 which is high and the p-value(<0) is less than the alpha value (0.05). We can also visually identify 4 outliers(Ref. Fig. 6.3). When we remove these outliers and conduct the AD hypothesis test again, we find favorable values for both AD (0.162 in Fig. 6.10) and p-value thus concluding that the data from the shear test fits the Weibull distribution well. This way we take care that the data that does not follow the trend of the distribution has failed for reasons different from the majority of the other tests.

Apart from cleaning up the outliers it is also insightful to see the number of failure mechanisms that are involved for an adhesive for a particular test. For instance for the tension test, if we plot a time series plot but with values sorted in an ascending order,

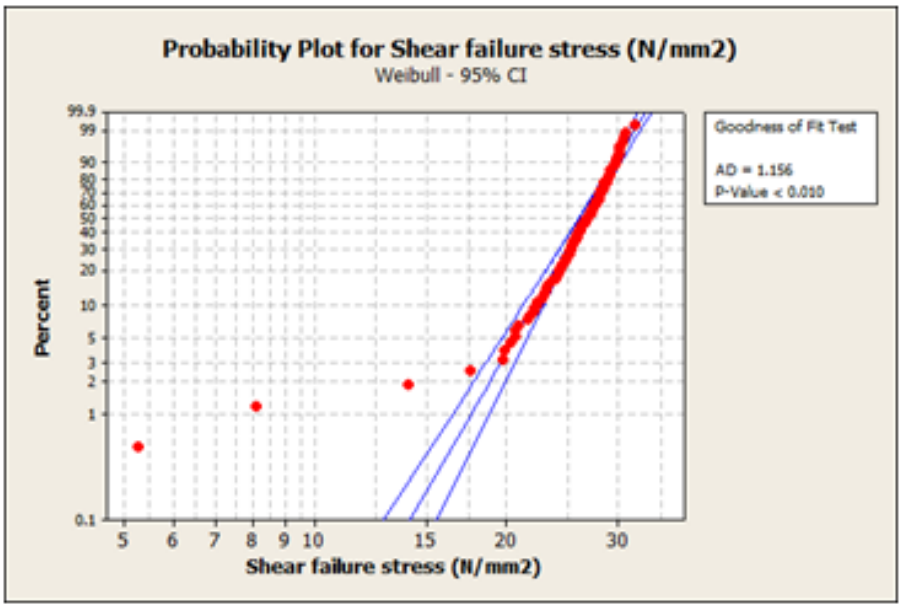

Figure 6.3: Goodness of fit using Weibull. AD = 1.156 & P-value<0. We can see that the fit is not good because of the 4 outliers. Hence we can identify the outliers.

then we get the plot seen in Fig. 6.4.

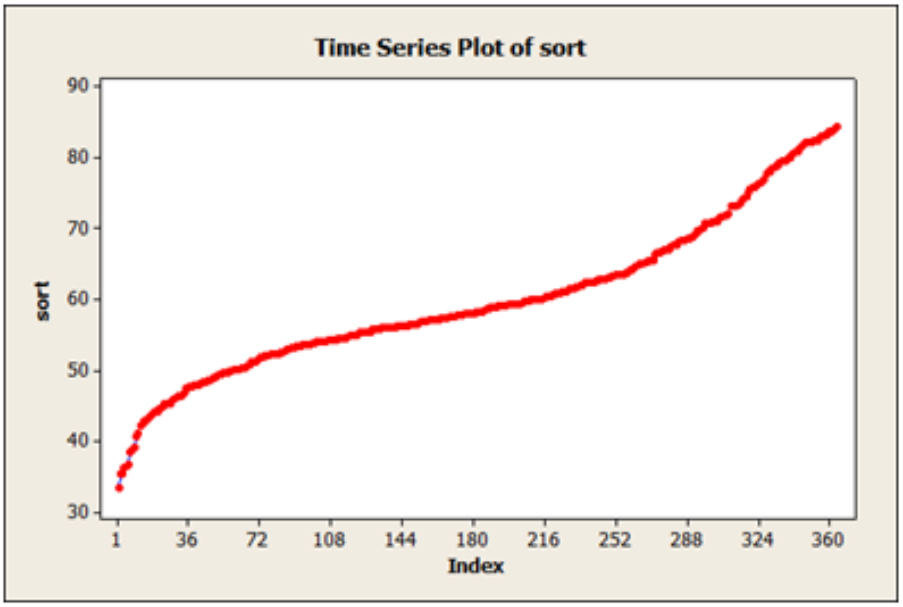

Figure 6.4: Time series plot ranked according to data value.

From the plot in Fig. 6.4 we could possibly say that there is more than just a single mode of failure. Samples are seen either to fail in cohesion within the adhesive layer, or in adhesion, in which case the failure in at the interface between the adhesive and the substrate. Perhaps we could say that these two major types of failures are somewhere represented in the multiple modes that we see from the series plot.

6.3.1 Example of analysis of test data

Data is in a crude form that cannot be directly used. Time series is plotted to identify multiple distributions indicating multiple modes of failure.

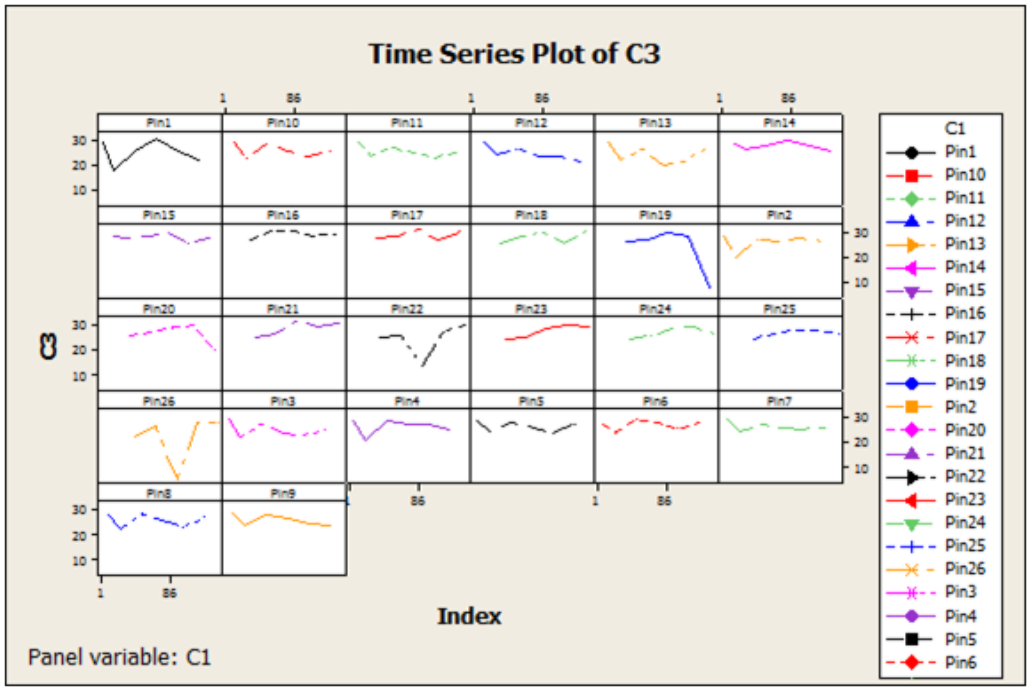

Figure 6.5: Data is plotted per pin to see the trend in the variation in data from one test to the other.

We first look at the first for the data for a number of distributions. First we look at Fig. 6.6. By visual inspection we can see that the data points do not fit well to Lognormal distribution also more importantly AD = 12.419. In comparsion when we look at Fig. 6.7 for Weibull distribution, then we find that AD = 1.156 which is a much better fit.

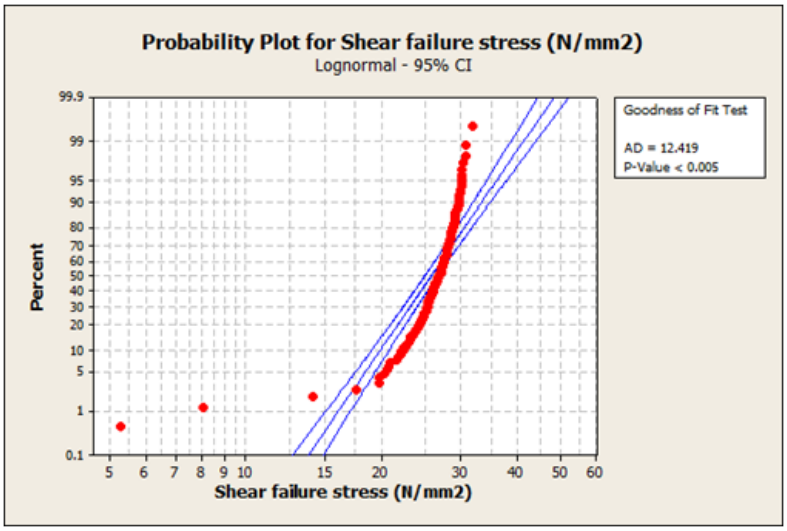

Figure 6.6: Fit for Lognormal distribution.

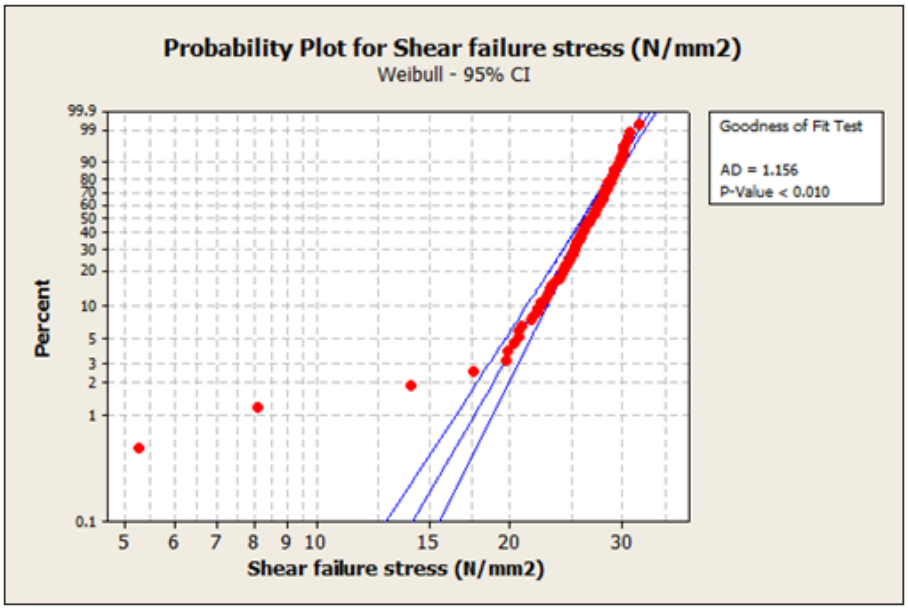

Figure 6.7: Fit for Weibull distribution.

From Fig. 6.7 for Weibull distribution we can also see that there could be 4 possible outlier data points. We can then get back to the actual samples and inspect them to determine any possible reason for failure which are undesirable. For instance one could easily identify if the pin in question failed at unexpectedly low load for lack of adhesive applied. We then move ahead to exclude data points below 17MPa for instance (Ref. Fig. 6.8.

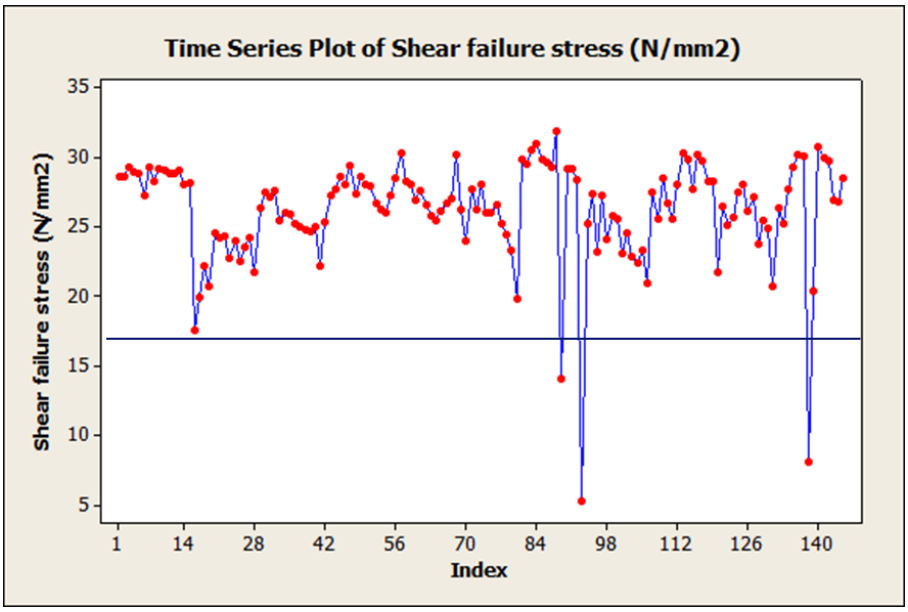

Figure 6.8: Excluding data points below 17MPa.

In Fig. 6.9 we can see that the Box-Cox transformation gives the least AD, but we would rather deal with the real data value than a transformed value.

Goodness of Fit Test

Distribution	AD	P	LRT P
Normal	1.262	<0.005	
Box-Cox Transformation	0.250	0.741	
Lognormal	2.181	<0.005	
3-Parameter Lognormal	1.266	*	0.000
Exponential	53.020	<0.003	
2-Parameter Exponential	32.154	<0.010	0.000
Weibull	0.204	>0.250	
3-Parameter Weibull	0.162	>0.500	0.627
Smallest Extreme Value	0.159	>0.250	
Largest Extreme Value	5.068	<0.010	
Gamma	1.841	<0.005	
3-Parameter Gamma	1.862	*	0.071
Logistic	0.981	0.006	
Loglogistic	1.454	<0.005	
3-Parameter Loglogistic	0.983	*	0.006
Johnson Transformation	0.091	0.998	

Figure 6.9: Goodness of fit test.

3-Parameter Weibull fits well in this case. With AD less than the 2-parameter Weibull the use of the third parameter is justified and also the p-value is greater than 50%, as seen in Fig. 6.10.

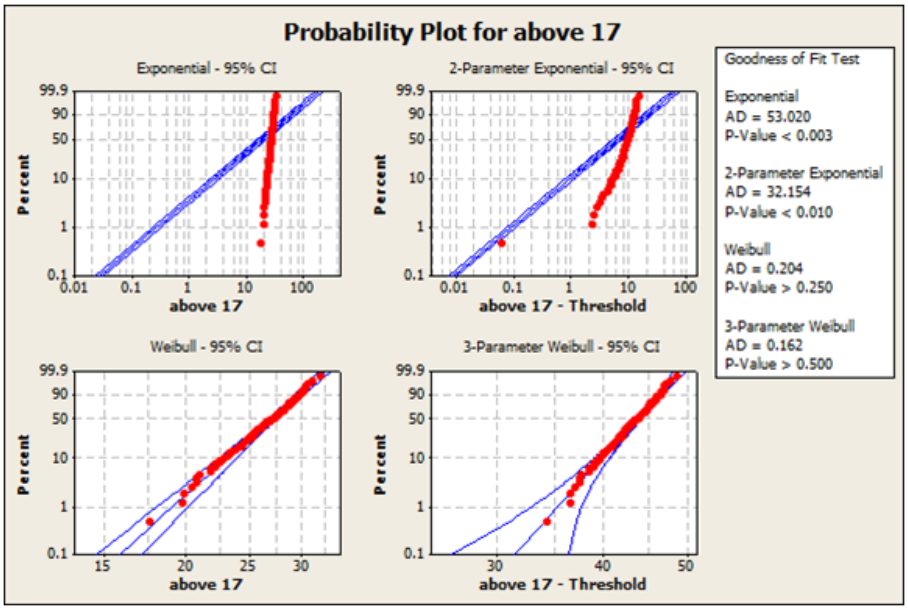

Figure 6.10: Fiting for various probability distributions.

6.4 Identification of yield point for test data from various tests.

The purpose of this chapter is to discuss what stress level on the stress-strain curve is to be considered as yield point for the joint. The important point here is that upon close observation of the stress-strain curve from lap shear test in Fig. 6.13 we see that there are two instances to consider. The first instance is when the plasticity starts at the corners and the second instant is when the plasticity has spread throughout the adhesive layer. The clear deviation from linearity is hard to establish on this curve. Also the deviation from linearity is much clear when the entire adhesive section has yielded. But in actual application especially for very stable adhesive joints we would like to consider the yielding starting at the corners of the lap shear as failure. Thus we conduct an elasto-plastic analysis to identify this yield point.

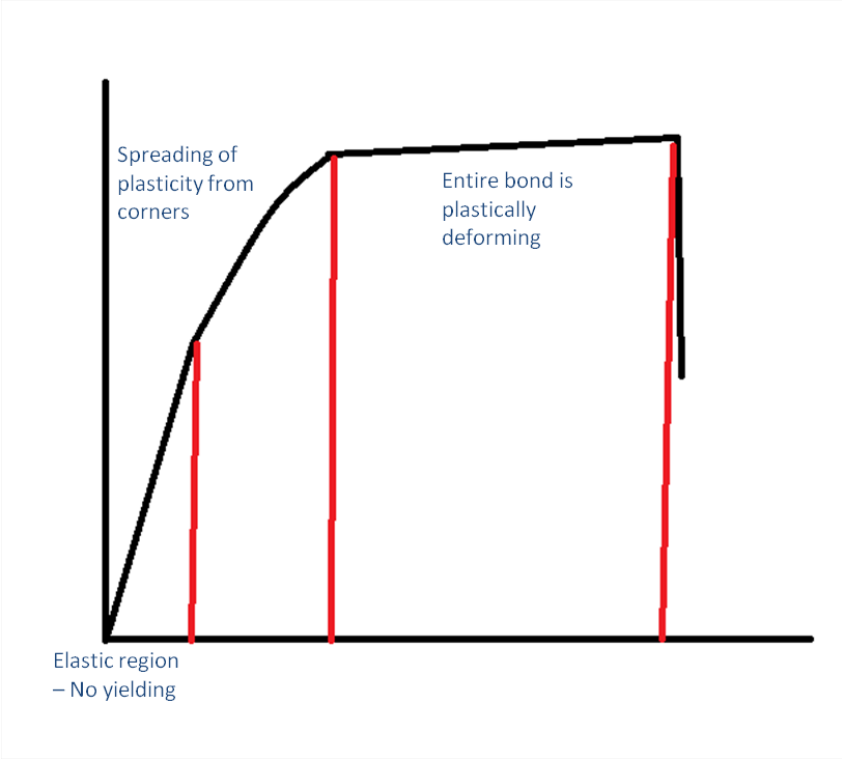

Figure 6.11: Stages of loading and spread of plasticity - Section I represents the elastic region with no plasticity. Section II represents the onset of plasticity at edges. Section III is a plateau where the plasticity has spread throughout the layer and considerable yielding is seen before ultimate failure.

Looking at a typical force-displacement curve (Ref. Fig. 6.11) it can be seen that for some tests the adhesive yields much before it fails. What it indicates is that yielding starts locally and then spreads throughout the adhesive layer and when the entire adhesive has yielded, the material starts flowing until ultimate failure.

Although for determining the strength of the lap shear joint we would consider the ultimate peak load that the joint can sustain, but for our purpose of identifying a common failure criteria it is important to compare values that are comparable. Since some joint tests yield extensively and thus demonstrate higher strength and some others fail with-

out much yielding, we need to consider the yield stress for the tests which yield with the ultimate failure stress for joints that do not yield as much.

The graphs in Fig. 6.12 show yielding in the bending test. The graph on the right zooms on the extent of deviation from linearity and how the yield value is identified. The Matlab code used for the identification of yield as shown in the figure is given in Appendix B.

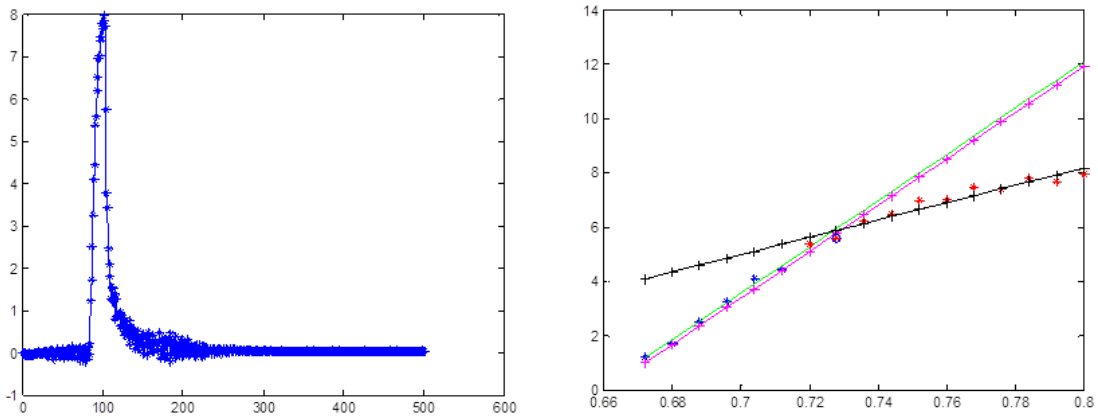

Figure 6.12: Left - Force v/s displacement curve from bending test. Right - Zoomed view of the force-displacement on right, to show the extent of deviation fro linearity during yielding for the bending test.

6.5 Elasto-plastic analysis for correctly identifying yield in lap shear.

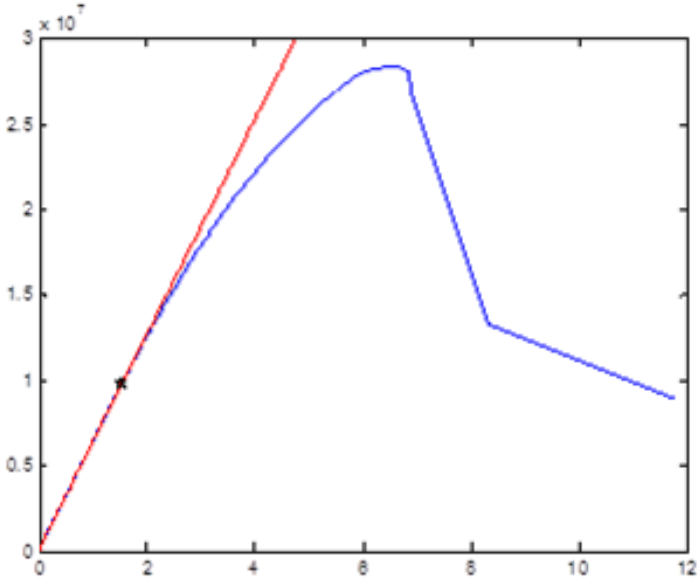

Figure 6.13: Yielding identified on the force-displacement curve from lap shear test.

6.5.1 Test case formulation

We try and formulate an elasto-plastic Bi-linear Isotropic hardening (BISO) curve where one would need to define the yield stress and the tangent modulus. This curve should be defined in such a way that almost the entire adhesive layer would yield at nominal shear stress of 28MPa (nominal Von-Mises of 48.5MPa). Therefore we can say that for almost the entire adhesive layer the nominal Von Mises should be above 48.5MPa for ultimate failure load of about 8750N. If we try and reduce the load, then we expect to see the start of plasticity at around 10MPa say. This would support our graphical method of identifying the yield.

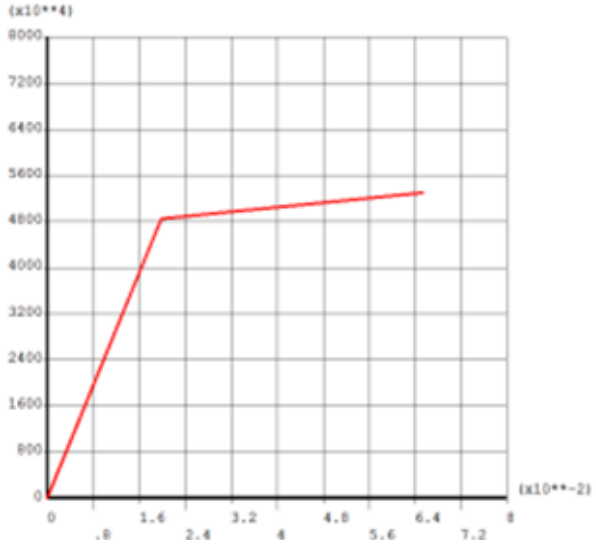

Figure 6.14: Bi-linear isotropic hardening material model.

6.5.2 Solution

The only 2 parameters that can be varied while using BISO are the yield stress and the tangent modulus. The yield stress in this case which is input is 48.5MPa. The tangent modulus chosen is as low as possible, say 0.1GPa, but not zero for ease of convergence.

6.5.3 Results

From the tests we know that the failure occurs at nominal shear stress of 28MPa. This corresponds to a load of 28 x 312.5 = 8750N. We check the nominal Von Mises at load 8750N which is 48.8MPa that we expect to see and which is close to 48.5MPa yield. Therefore according to our definition in the problem formulation we can say that the entire section has yielded.
Now we shift our focus to try and determine the load at which yielding begins in the adhesive layer. For this we could check the load at which the maximum Von Mises stress within the adhesive layer reaches a peak of around 48.5MPa.
For load 3750N we have a peak Von Mises of about 47.2MPa, therefore we can calculate the nominal shear stress for this load as 3750/312.5 = 8.8MPa. We can interpolate

```
 LOAD STEP     1  SUBSTEP=     10
 TIME=   0.87500          LOAD CASE=   0

THE FOLLOWING X,Y,Z STRESSES ARE IN THE GLOBAL COORDINATE SYSTEM.

             ** MEMBRANE **
     SX            SY            SZ            SXY           SYZ           SXZ
0.2206E+07  0.1016E+07  0.1430E+07  0.2817E+08 -0.4875E-07 -0.4676E-09
     S1            S2            S3            SINT          SEQV
0.2979E+08  0.1430E+07 -0.2657E+08  0.5635E+08  0.4880E+08
```

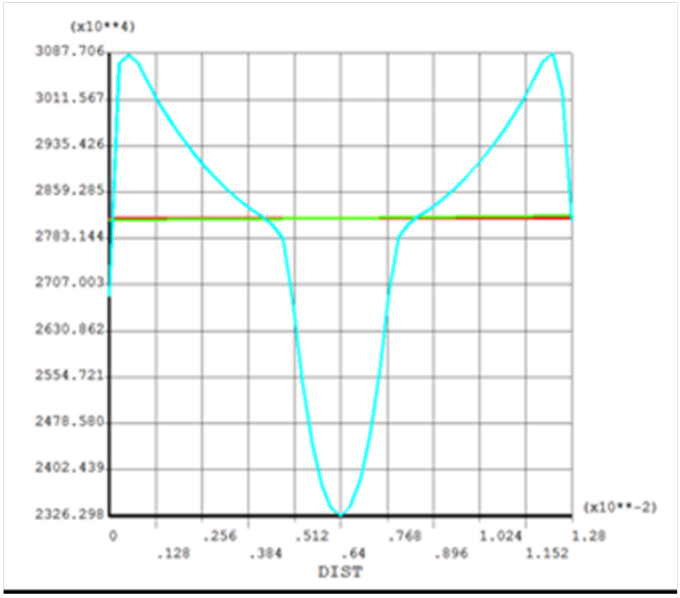

Figure 6.15: Linearized stress results showing plastic plateau.

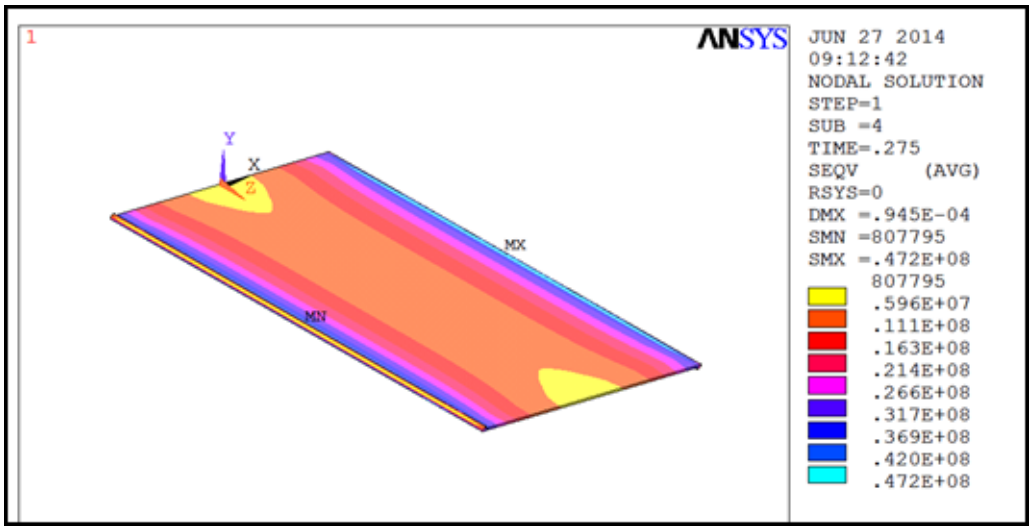

Figure 6.16: Stress distribution showing plasticity.

between the next set of results and find that for load 3101N we have a maximum Von Mises of 48.5. 3101N is 9.9MPa nominal shear.

Chapter 7

Determination of Constitutive material model parameters

In this chapter we will discuss the different material models that can be used to describe the behavior of the adhesives. We will also see what parameters are needed to create this model in a FE program like Ansys. We need to calculate these parameters by using the data we obtain from tests.

7.1 Elastic-Plastic Models

7.1.1 The Von Mises Model

The Von Mises material model is based on the principle that the yield occurs as a result of pure shear deformation. The onset of yielding is said to begin when the effective shear stress which is denoted by σ_e reaches a critical value.

This effective stress is a combination of the principal stresses σ_i for i =1,2,3 and is given by [15],

$$\sigma_e = \sqrt{\frac{(\sigma_1 - \sigma_2)^2 + (\sigma_2 - \sigma_3)^2 + (\sigma_3 - \sigma_1)^2}{2}} \tag{7.1}$$

And the critical limit or critical value for this effective shear stress is taken as the minimum value of the tensile yield stress when proportionality between stress and strain ends and plastic deformation starts. This relation between the yield stress and the plastic strain is defined by hardening rules or hardening functions. The most common rules are that of isotropic and kinematic hardening.

In isotropic hardening, the shape of the yield surface remains the same, but swells up with the increase in stress. We use this hardening rule in our analysis. To give an example of isotropic hardening, we will consider the hardening rule with both Von Mises yield function and the Drucker-Prager yield function.

Firstly, we see the effect on Von Mises yield function. The yield function is defined as,

$$f_0(\sigma_{ij}) = \sigma_e - \sigma_0 = 0 \tag{7.2}$$

$$\tag{7.3}$$

Yield for the Von Mises is defined by a material parameter σ_0. For the Von Mises material model σ_0 is defined as the uniaxial tension yield stress.

$$\sigma_0 = \sigma_T \tag{7.4}$$

Substituting we get,

$$f_0(\sigma_{ij}) = \sigma_e - \sigma_T = 0 \tag{7.5}$$
$$\tag{7.6}$$

As mentioned before for Von Mises the equivalent stress is nothing but the effective shear stress.

$$f_0(\sigma_{ij}) = \sqrt{\frac{(\sigma_1 - \sigma_2)^2 + (\sigma_2 - \sigma_3)^2 + (\sigma_3 - \sigma_1)^2}{2}} - \sigma_T = 0 \tag{7.7}$$
$$\tag{7.8}$$

But the second invariant of the deviatoric stress tensor (J_2) is given by,

$$J_2 = \frac{(\sigma_1 - \sigma_2)^2 + (\sigma_2 - \sigma_3)^2 + (\sigma_3 - \sigma_1)^2}{6} \tag{7.9}$$

Substituting, finally we get the yield function as,

$$f_0(\sigma_{ij}) = \sqrt{3J_2} - \sigma_T = 0 \tag{7.10}$$
$$\tag{7.11}$$

Subsequently as the hardening develops the yield function changes to,

$$f_0(\sigma_{ij}) = \sqrt{3J_2} - \sigma_T - K = 0 \tag{7.12}$$

Where, K is the *hardening parameter* or strength coefficient. The stress-strain behavior in strain hardening is defined in Eq 7.13. n is the *strain hardening exponent*.

$$\sigma = K\epsilon^n \tag{7.13}$$

Therefore in effect the Von Mises yield surface which is a cylinder about the Hydrostatic axis ($\sigma_1 = \sigma_2 = \sigma_3$) with radius $\sqrt{\frac{2}{3}}\sigma_T$ grows in the radial direction with radius $\sqrt{\frac{2}{3}}(\sigma_T + K)$.

Von Mises criterion predicts that the tensile yield stress, shear yield stress and compressive yield stress are related by,

$$\sigma_T = \sigma_C = \sqrt{3}\sigma_S \tag{7.14}$$

7.1.2 The Linear Drucker-Prager Model

Strength calculations based on the Linear Drucker-Prager material model is generally more accurate than strength values for the Von Mises material models [7].

First and foremost, we need to understand the inputs required to build such a constitutive material model to simulate plastic behavior. There are three elements that go into defining this material model. We need the yield function, and along with it the flow rule and lastly we need to define the strain hardening.

Yield function

The yield function defines the onset of plasticity. Essentially it can be imagined as an equation of a surface in 3D space with the three principal stresses as the three respective coordinates for the space. For the linear Drucker-Prager the yield function is given by [15],

$$f_0(\sigma_{ij}) = \sigma_e - \sigma_y = 0 \tag{7.15}$$

where, σ_y is the yield.

Flow rules

Along with the yield function, we need to define the flow rule. For ideal plasticity we have plastic deformation without any strain hardening. This can be written as,

$$d\sigma_{ij} de_{ij}^{(p)} = 0 \tag{7.16}$$

The application of this definition is known as the flow rule. If yielding occurs, we further need to know the rate of deformation to be able to program the complete behavior. This rate of deformation is $\dot{e}_{ij}^{(p)}$. So obtained this rate we say that there exists a potential $h(\sigma_{ij})$ which can be used to derive $\dot{e}_{ij}^{(p)}$,

$$\dot{e}_{ij}^{(p)} = \lambda \frac{\partial h}{\partial \sigma_{ij}} \tag{7.17}$$

where λ is a positive scalar factor. Flow rules can be defined either as associative or non-associative. If this potential $h = f$, the flow is said to be associative and if $h \neq f$, then the flow is said to be non-associative.

These flow rules are used to calculate plastic strain components by relating increments of plastic strain to plastic flow potential F as given in Eq 7.13

$$d\epsilon_{ij}^{p} = d\lambda \frac{\partial F}{\partial \sigma_{ij}} \tag{7.18}$$

where, $d\lambda$ is dependent on the stress state and is determined by ensuring equivalence of plastic work done under all stress states.

Strain hardening

And lastly we need to define the strain hardening. Strain hardening is obviously not needed for defining a perfectly plastic material, but it needs to be defined for a elastic-plastic material. These hardening rules are used to determine the subsequent loading surfaces as plastic flow proceeds. For example if we take metals and we assume that the plastic deformation is not dependent on hydrostatic pressure, that is that the plastic flow is incompressible, then yield surfaces in the principal space are cylinders, but not necessarily with a circular cross-section. These cylinders are usually of infinite length around axis $\sigma_1 = \sigma_2 = \sigma_3 = 0$. The plane perpendicular to this axis is the plane $\sigma_1 + \sigma_2 + \sigma_3 = 0$ and is called the π-plane. Hence the yield surface can also be represented by the intersection of this yield surface with this plane. These intersection curves are 2D envelopes which are always closed, convex and piecewise smooth. They do change their size and shape during the plastic hardening. Under no circumstances is the yield surface parallel to the axis perpendicular to the π-plane.

As discussed in the case of Von Mises criterion, the strain hardening can be isotropic or kinematic. To define strain hardening we need to define the increase in the yield stress with increase in the plastic strain.

Formulation

As compared to the Von Mises material model, the Drucker-Prager model includes the inelastic behavior of adhesives which is pressure dependent. This is done by including hydrostatic stress sensitivity. Just as before the yield function is given by,

$$f_0(\sigma_{ij}) = \sigma_e - \sigma_y = 0 \tag{7.19}$$

For Linear Drucker-Prager unlike Von Mises, the yield includes an adjustment for hydrostatic stress. The inclusion of hydrostatic stress will lower the overall value of yield. Also the yield is based on the shear yield stress and not the Therefore yield is given by,

$$\sigma_y = \text{yield stress - hydrostatic stress} \tag{7.20}$$
$$= \sigma_0 - \mu\sigma_m \tag{7.21}$$

7.1.3 The Extended Drucker-Prager Model

For the linear Drucker-Prager criterion, the yielding on only slightly sensitive to the hydrostatic stress. The criterion is not able to accurate describe the behavior of adhesive under stress states with high component of hydrostatic tension. These high hydrostatic tension states of stress are quite common in adhesive joints where there is high constraint imposed by the adherend under forces directed normal to the interface. The Extended criterion is more accurate under these conditions. The model is written as [15],

$$\sigma_e^2 = \lambda\sigma_T^2 - 3(\lambda - 1)\sigma_T\sigma_m \tag{7.22}$$

where λ is another hydrostatic stress sensitivity parameter and relates stresses σ_C, σ_S and σ_T under uniaxial compression, shear and tension by the equations,

$$\lambda = \frac{\sigma_C}{\sigma_T} \tag{7.23}$$

$$\lambda = \frac{\sigma_C^2}{3\sigma_S^2} \tag{7.24}$$

$$\text{and } \lambda = \frac{3\sigma_S^2}{\sigma_T^2} \tag{7.25}$$

In Ansys we use the extended Drucker-Prager model with the associated flow. It should be noted that a hyperbolic function has been chosen for the flow potential F.

7.2 Determination of Model Parameters

Structural adhesives such as the ones used in this analysis, are tough materials. As such they undergo large strains before final failure. As such it is imperative to study the deformations of these adhesives in the non-linear domain. At high stresses the molecular mobility in these polymeric adhesives is high enough for yielding to occur due to plastic flow. Some non-linear deformations until the stresses are moderate are recoverable, but beyond these moderate stresses, the deformations are non-recoverable. Therefore, to be able to model the true nature of deformation of these adhesives employed under large strains, it is important to use the Elastic-plastic material models.

There are several models that can be used for modeling the adhesive material behavior. Some models are basic and require less input parameters and some more complex models require additional parameters. Parameters for all these tests are obtained from testing the bulk or joint samples of these adhesives. The joint performance under loads that result in large deformations depend on the selection of these material models. Besides the material model, it is also essential that the adhesive in the FE model is meshed well to capture the stresses and strains accurately and also along with any material model it is important to select an appropriate failure criterion.

The models used in this analysis are as below,

Material models	**Data requirements**
Von Mises	Tensile data
Linear Drucker-Prager	Tensile and shear data at same strain rate
Extended Drucker-Prager	Tensile and shear data at the same strain rate
Cavitation model	Tensile, shear and compressive data at the same strain rate

At stress and strain levels above the limit for linear behavior, relationships between stress and strain are non-linear. With elastic-plastic models, calculations of stress and strain distributions at low strains are based on linear elasticity. The onset of non-linearity is due to plastic deformation and occurs at a stress level regarded as the first yield stress. The subsequent increase in stress with strain is associated with the effects of strain hardening. In order to calculate some of the parameters in elastic-plastic models, it is necessary to obtain stress values from different tests under the same state of yielding. Suitable data can be obtained from uniaxial tension, shear or compression tests.

7.2.1 Determination of parameters of The Von Mises Model

The Von-Mises model has been described in the previous section. The parameters needed to define this material model can be obtained from the tensile tests only. There are 3 parameters required –

1. Young's modulus
2. Poisson's ratio
3. Hardening curve (true tensile stress v/s true plastic strain)

Tangent Modulus

When using a bi-linear material constitutive law, one is aiming only for a 'limit analysis'. In such analysis the computed plastic strains have no physical meaning. As a consequence, the value of tangent modulus is really not important, provided a converged solution can be obtained. A typical value one normally uses is the Young's modulus divided by 10000. In our case it should be 2450000000/10000 = 245000 Pa or 0.245 MPa.

On the contrary if one is interested in a less conservative solution, where the plastic strains and material hardening is to be taken into account, the a multi-linear material constitutive law like Kinematic hardening should be used. The input is needed in logarithmic strains and true stresses. The results obtained will also be in logarithmic strains and true stresses. Such material curve can be estimated based only on yield stress, Ultimate tensile strength and Young's modulus. For metals tangent modulus can be estimated as the slope of the stress-strain curve at 0.2% offset strain.

For the FEM analysis we obtain the parameters for the Von Mises model using the data from the tensile tests. This data is obtained by testing bulk adhesive specimen in tension in the Instron machine. The data obtained is in the form of force v/s extension.

7.2.2 Determination of parameters of The linear Drucker-Prager Model

The most commonly used model is based on the Von Mises yield criterion. But tests from literature show that this model doesn't work well in adhesives, such as rubber-toughened adhesives, where plasticity is sensitive to the hydrostatic component of stress[38]. In the commercial FEA software package the linear and exponent forms of the Drucker-Prager materials model are available.

For linear Drucker-Prager we have the criterion as,

$$f_o(\sigma_{ij}) = \sigma_e - \sigma_o + \mu\sigma_m = 0 \tag{7.26}$$

σ_o is a material parameter that is related to the shear yield stress, which is the elastic limit defined as stress at which plastic deformation first takes place.

$$\sigma_o = \sqrt{3}\sigma_s \tag{7.27}$$

And σ_m is the hydrostatic stress given in terms of principal stresses,

$$\sigma_m = \frac{1}{3}(\sigma_1 + \sigma_2 + \sigma_3) \tag{7.28}$$

The equation representing the criterion for linear Drucker-Prager is similar to the one in Ansys.

$$q - \sigma_y(\hat{\epsilon}_{pl}) + \alpha\sigma_m = 0 \tag{7.29}$$

where,

$$q = \sigma_e \quad \mu = \alpha \quad \sigma_o = \sigma_y(\hat{\epsilon}_{pl}) \tag{7.30}$$

The parameter μ depends on the adhesive material and characterizes the sensitivity of yielding to hydrostatic stress. μ is determined from tests under two different states of stress. Using yield stresses from shear and tensile tests,

$$\mu = \tan\beta \tag{7.31}$$

β is the uniaxial asymmetry ratio,

$$\beta = \frac{\sigma_C}{\sigma_T} \tag{7.32}$$

7.2.3 Determination of parameters of The extended Drucker-Prager Model

The Extended Drucker-Prager is a more complex model compared to the Linear Drucker-Prager. It is preferred to describe behavior of materials that have a high component of hydrostatic tension in their stresses [38].

$$\sigma_e^2 = \lambda\sigma_T^2 - 3(\lambda - 1)\sigma_T\sigma_m \tag{7.33}$$

$\lambda = \sigma_C/\sigma_T$ is hydrostatic stress sensitivity.

Data analysis

The following data needs to be calculated from tensile and shear data,

$$\sigma_T\epsilon_T^P \tag{7.34}$$
$$\sigma_S\epsilon_S^P \tag{7.35}$$
$$\tag{7.36}$$

The above values obtained from tensile and shear data are used to obtain equivalent data points for calculation of Drucker-Prager parameters. When the resultant value from a tensile data point equals that from a shear data point, the plastic strain components from

these two points are said to be equivalent. The stresses corresponding to these two points are values that are used to calculate the model parameters.

These values are not unique, there may be other equivalent stress values for given sets of data. How these vary depends on the shape of the stress-strain curves. If the yield stress data shows a plateau region, then yield stresses do not vary much with effective plastic strain.

Equivalent data points

The parameters μ and λ are calculated fro yield stresses obtained from tests under different stress states. The yield stress values used in the calculations must correspond to the same effective plastic strain ϵ^P_{Seff}. Associated with an effective plastic strain is an effective stress σ_{Seff} which is defined with reference to a pure shear stress state by the relationship,

$$\sigma_{eff} = \sqrt{3} J_{2D}^{\frac{1}{2}} \tag{7.37}$$

$$\text{so that} \sigma_{eff} = \sqrt{3}\sigma_S \tag{7.38}$$

Effective stresses and plastic strains σ_{ij} and ϵ^P_{ij} under an arbitrary stress state are then defined such that the plastic work done by this stress state is the same as the effective plastic work so that,

$$\sigma_{ij}\epsilon^P_{ij} = \sigma_{eff}\epsilon^P_{eff} \tag{7.39}$$

In case of shear and tensile stresses,

$$\sigma_S\epsilon^P_S = \sigma_{eff}\epsilon^P_{eff} = \sigma_T\epsilon^P_T \tag{7.40}$$

So from the top equation the effective plastic strain is given by,

$$\epsilon^P_o = \frac{1}{\sqrt{3}}\epsilon^P_S \tag{7.41}$$

Calculation of parameters and generating equivalent stress-strain curve

The calculation of parameters for the Extended Drucker-Prager material model is shown in the Appendix (Chap. D).

Chapter 8

FEM Modeling

8.1 Geometry, mesh and material singularities

FE modeling is done to be able to simulate the tests using FEM. The model is prepared in Ansys and mesh improvement is done using Hypermesh. Simply a lap shear joint can be modeled as below. Even for simple adhesive joints such as the single-lap joint, stresses are of 3D nature.This was investigated by Tsai and Morton [49] who performed 3D linear elastic FE analysis of a single lap joint. These authors showed that 3D regions exist in the specimen. They showed that the adherend and adhesive stress distributions in the overlap, near the free surface, are quite different from those ocurring in the interior [54] [13].

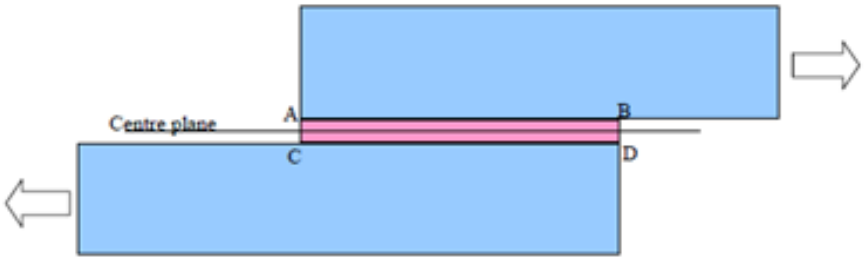

Figure 8.1: Profile geometry of a lap shear joint that is to be modeled in FEM. The boundary conditions are applied such that one of the strips is fixed and a tensile force is applied on the glued strip.

There are some modeling difficulties with these types of joints. Typically a thin layer of adhesive is $100\mu m$ thick with sharp corner leading to singular stresses. There is also singularity due to large differences in material properties of the adhesive and the adherends.

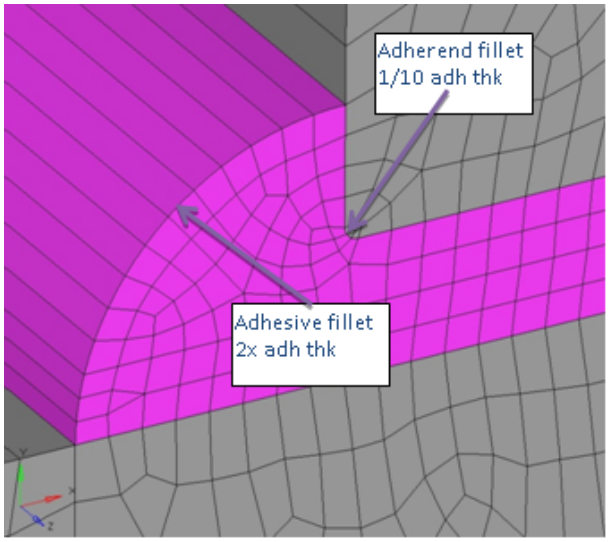

Figure 8.2: Adhesive fillet=2×adhesive layer thickness. Adherend radius=1/10×adhesive layer thickness.

To avoid singularities at the edges we model the glue layer to include the adhesive radius [24] which is a result of excess adhesive pushed outside of the adhesive surfaces. This reflects true geometry of adhesive and also avoids the geometric singularities due to the sharp 90° re-entrants. Roughly this adhesive radius can be 2x the thickness of the adhesive layer thickness. Machined substrates that are glued also do not have sharp edges. There is usually a chamfer or fillet. Adherend radius [24] of the order of 1/10 adhesive thickness also helps in avoiding geometric singularities. All these features and shown in Fig. 8.2.

8.2 Variation in mesh densities

It is advisable to have 2 or more layers of elements to represent the adhesive thickness. There is a high stress gradient through this thickness especially near the corners. This can be accurately captured by having more elements through thickness. It is also advisable to use elements with mid-side nodes for accurate element shape representing geometry and for more accurate results using less number of elements. In the transverse direction, one can take a call on the number of elements keeping in mind a good aspect ratio for the elements. There is less stress gradient in this direction.

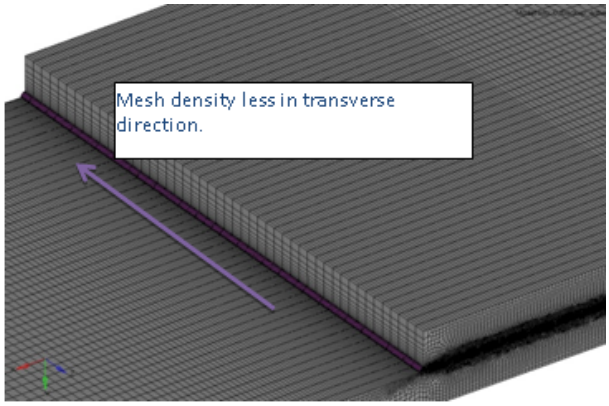

Figure 8.3: Variation in mesh density in transverse direction.

Away from the interest zones, the mesh size can be reduced to avoid very expensive solution times. This is especially critical with non-linear analysis.

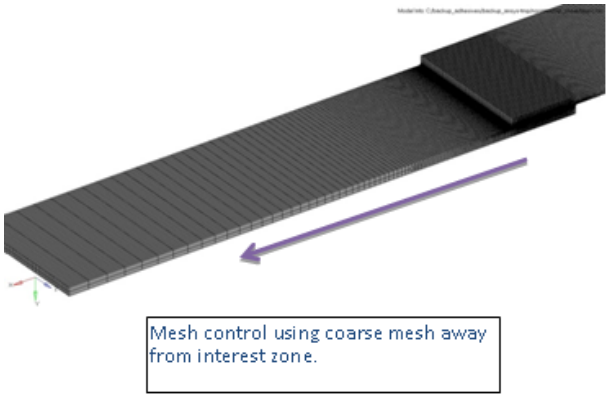

Figure 8.4: Mesh control away from interest zone.

8.3 Locations at which to check stresses

It is important to identify the locations or paths at which we will consider reading stresses. The top in the figure represents a path at the top interface of the adhesive layer. Similarly the middle and bottom represent paths follows at the center of the adhesive layer and bottom interface respectively.

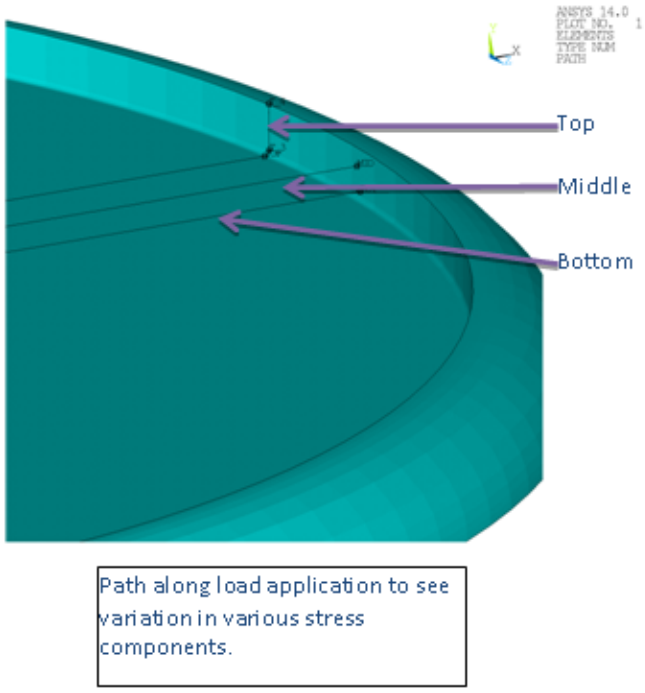

Figure 8.5: Figure shows the geometry of the adhesive layer. The indentation on top is that of the test pin. Top, middle and bottom are paths at which we note stresses.

Due to the presence of difference in material properties between the adherends and the adhesive, there are singular stresses at the interface, especially at the ends. These high stresses are not real and would result in overestimating the factor of safety. Therefore it is better to see the stresses in the mid layer of the adhesive as it is away from these singularity locations.

Another aspect is to see the failure of the joint in tests. If the joint shows a cohesive failure as opposed to an adhesive failure then the mid layer stresses will be more appropriate and vice versa.

It is also important that we check stresses at the same locations in the FEM model as in the tests where the failure has occurred. To explain this point we can use couple of examples. The tests on Scotchweld 9323 show failure mostly within the adhesive layer which can be described as a cohesive failure. Hence it makes sense for us to draw any conclusions about the failure criteria for this adhesive considering the stresses in the center(middle) layer of the adhesive (Ref. Fig. 8.5). Similarly, for Araldite 2030 we mostly see adhesive failure at the interface, as such we need to look at stresses at the top and bottom layers (Ref. Fig. 8.5) of the adhesive to drawn our conclusions from.

8.4 Mesh convergence study

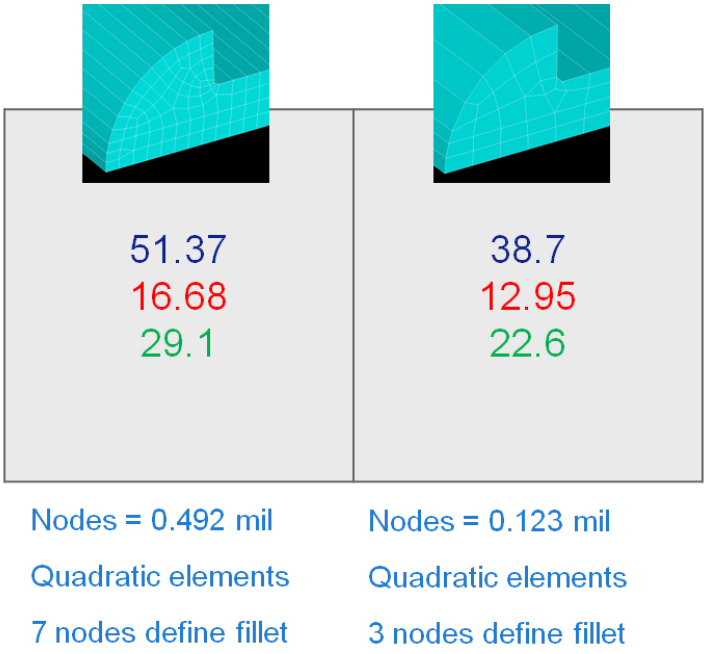

Figure 8.6: Sensitivity to FE mesh.

There is a 30% increase in stresses for 4 times more mesh density. This is due to the fact that as we increase the mesh size the stresses at the singular locations start increasing sharply.

8.5 Sensitivity of FEM results to Young's modulus and Poisson's ratio.

Fig. 8.7 tabulates the change in stress levels with respect to change in Young's modulus and Poisson's ratio.

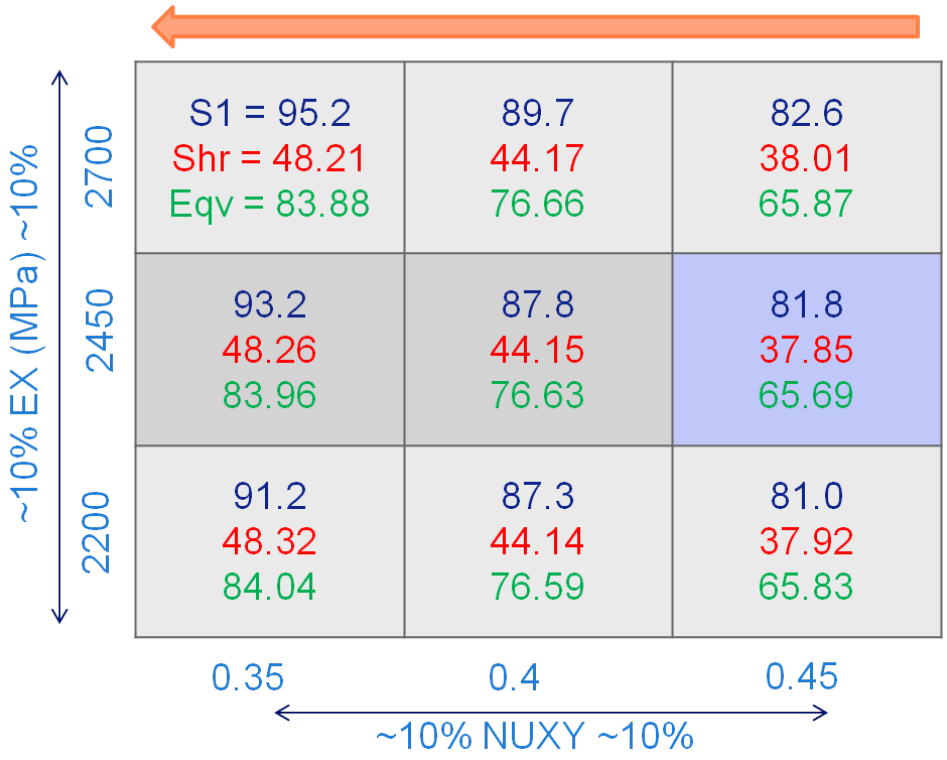

Figure 8.7: Sensitivity to Young's modulus and Poisson's ratio. S1 → Maximum principal stress, Shr → Maximum shear stress, Eqv → Von Mises equivalent stress. Top arrow indicates the trend of increase in stress levels.

The different stress components are inversely related to the Poisson's ratio and change proportional to the Young's modulus. Both results are as expected. Following conclusions can be derived.

- As Young's modulus is increased, the effect of chnage in Poisson's ratio increases.
- This above effect of variation is higher for the maximum shear stress than the maximum principal stress.
- Inaccuracies in Poisson's ratio can results in a variation of 15% in maximum principal and 27% in maximum shear.
- Less sensitivity to Young's Modulus.

Chapter 9

Corrections for data acquired from FEM Analysis

From the various tests conducted we have the values for nominal stress. But for finding which criterion fits best, we need to find the various stress components and their distributions in the layer. For this purpose we model our substrates and the adhesive layer in FEM. We carry out linear FEM analysis using the material properties for the adhesive found from the tensile testing of the dog bone bulk sample. From these tests we calculate the Young's modulus and Poisson's ratio that is to be used in FEM calculations. These calculations are linear which facilitates the ease of scaling the load in FEM by the failure load from the tests and finding the corresponding levels of stress components at this scaled value of load.

The problem with the FEM analysis is the presence of stress singularity (Fig. 9.2 and Fig. 9.4) that is present due to sharp corners in the geometry and at the interface where there is dissimilarity in material properties.

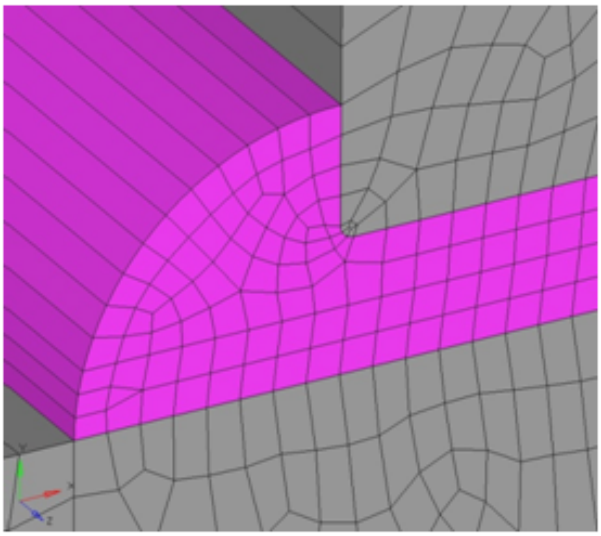

Figure 9.1: Sharp 90° re-entrants.

If we conduct the FEM analysis for the lap shear specimen and plot the criteria for the center layer, we get the plot in Fig. 9.2.
If we take a closer look at the edges of the layer we can see that there is a dotted vertical line which indicates the bifurcation of the layer of adhesive between the substrates which

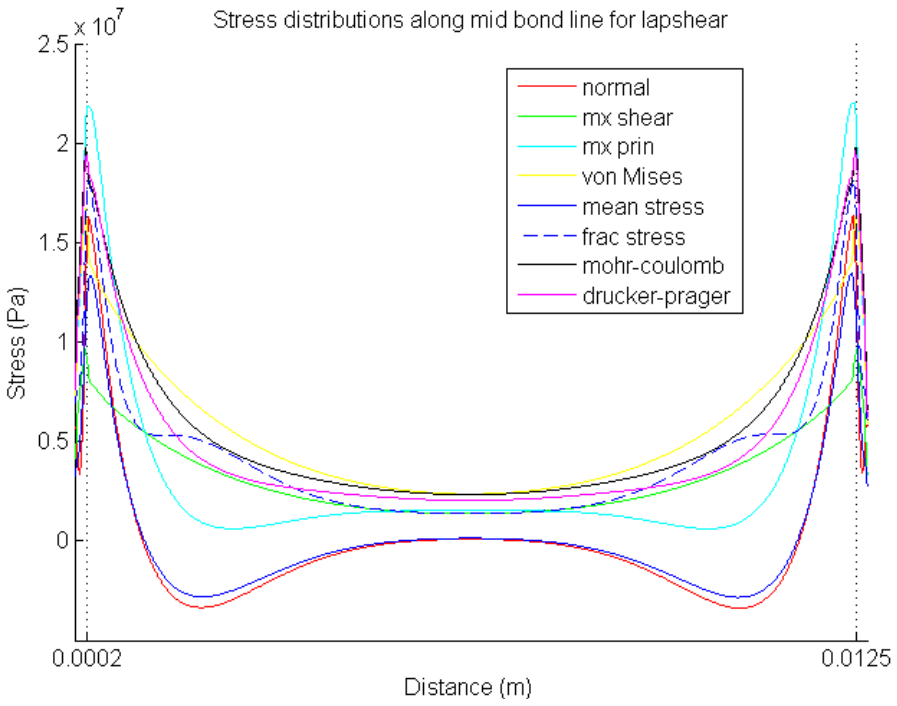

Figure 9.2: Stress distribution for center layer of lap shear.

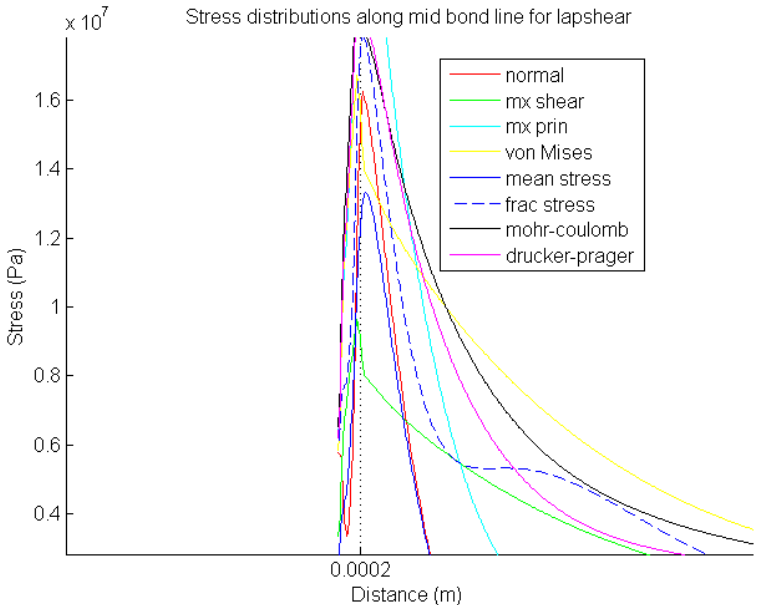

Figure 9.3: Stress distribution for center layer of lap shear near the edge.

is to the right and the layer of adhesive that is outside which is the adhesive that is squeezed out when the substrates are joined.
We can clearly see that stress increases towards the edge of the substrate and this gradient is uniform and no singular stresses are observed.

If we move our attention to the top and bottom layers we see the effects of stress singularity at the edges.

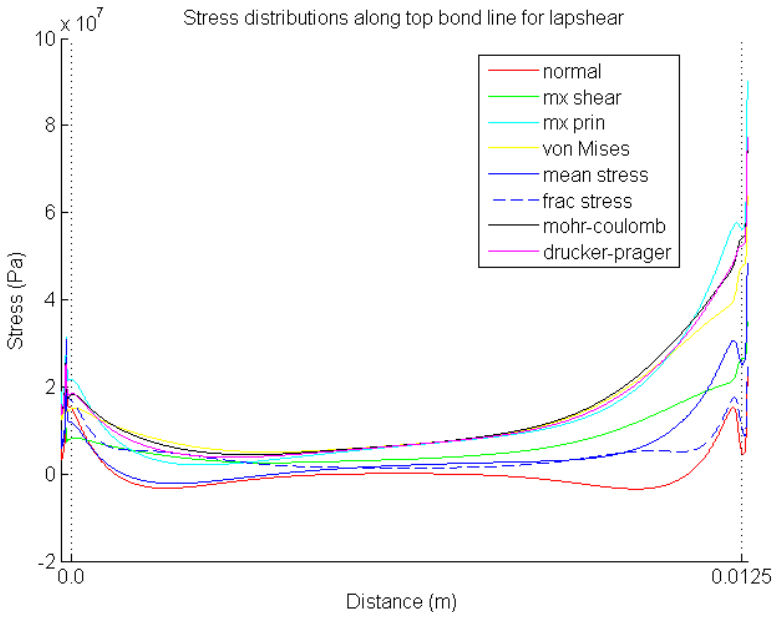

Figure 9.4: Stress distribution for top layer of lap shear.

If we again take a closer look then we identify the singularity to be within 0.025mm from the edge. If we exclude the values beyond what is found in the adhesive layer between the substrates, then we might lose the maximum values for some criteria, hence here we decide to only ignore the nodes contributing to the singular stress values.

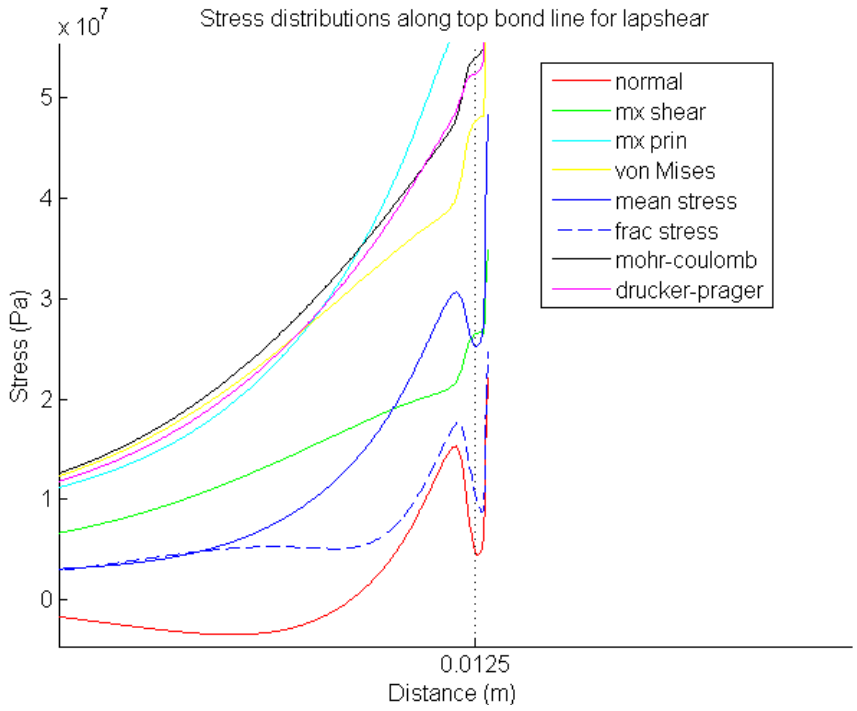

Figure 9.5: Stress distribution for top layer of lap shear near the edge.

The case for the bottom layer is exactly similar as both the edges are symmetric.

Part III

Results & Conclusions

Chapter 10

Analysis of FEM Results

This chapter reviews the FEM results for the different types of tests at the top interface, center of adhesive layer and at the bottom interface (Ref. Fig. 8.5).

10.1 Note

The elastic properties of Araldite 2030 are almost the same as that for Scotchweld 9323 as such the FEM results for Araldite 2030 do not need to be discussed separately. For all purposes we have almost the same linear stress results. As such only FEM results for Scotchweld 9323 are discussed in this chapter.

10.2 Material Properties

The following material properties are tabulated for the 2 adhesives that are used in our analysis. These material properties have been determined by testing bulk samples of the adhesive material. These properties obtained from testing are used as input in our FEM calculations.

SW9323	
Young's modulus (E)	2.45 GPa
Poisson's Ratio (ν)	0.45

Araldite2030	
Young's modulus (E)	2.45 GPa
Poisson's Ratio (ν)	0.44

The adherend used in our research is Stainless steel. The properties used for the adherend are tabulated below.

Stainless steel	
Young's modulus (E)	202.713 GPa
Poisson's Ratio (ν)	0.33

10.3 Tensile Test

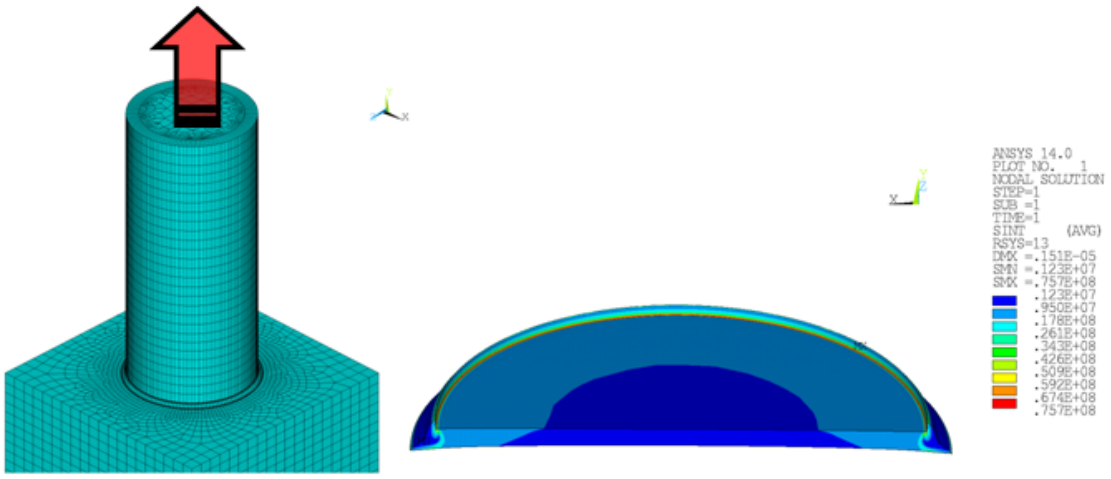

Figure 10.1: Tensile test.

10.3.1 Introduction

The tensile test is carried out on the IBS Stein machine which has 26 pins of diameter 5mm glued to a substrate 10x15x130mm. We choose to model just one of these pins with a block of substrate glued to it. The glue layer is 100µm.

The pin geometry has been simplified as it will not contribute towards the stress analysis. A load of 1KN is uniformly applied to the nodes on the top of the pin in the direction of Y-axis. The nodes at the bottom face of the block are fixed.

10.3.2 Tensile Results

Tensile top layer

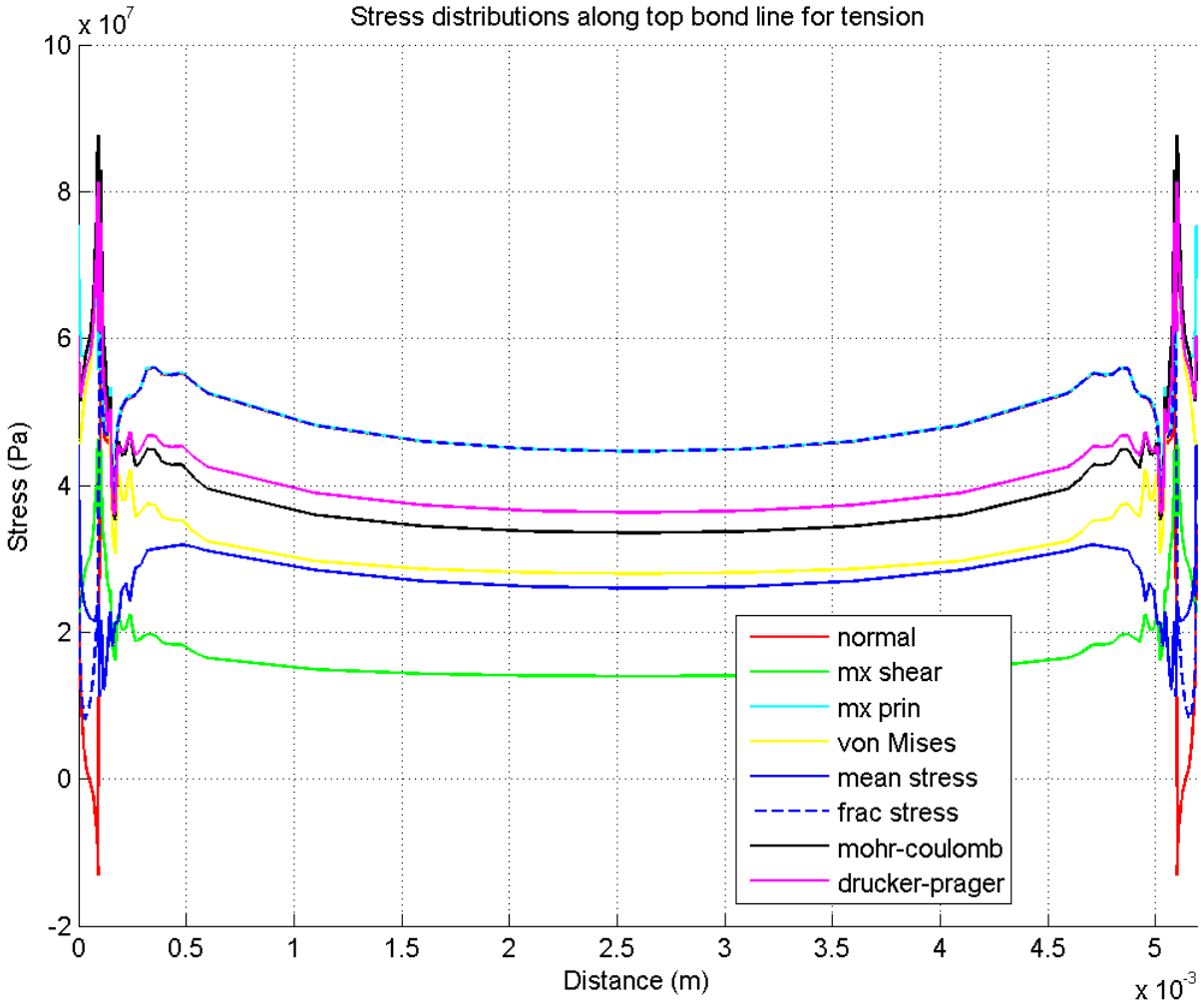

Figure 10.2: Comparison Failure Criteria plot for top layer in tension test.

In the top layer we see that this test being pure tensile the maximum principal stress is the same as the normal stress and is the highest.

Because the maximum shear stress is low, the Fracture stress has contribution only from the normal stress and therefore they have overlapping curves.

The maximum shear is the least as loading is only tensile. The stress distribution is more or less uniform throughout the layer of adhesive. The shear stress increases with a high gradient when we near the fillet radius of the pin. It is highest in the fillet and logically is present in the vertical section of the adhesive attached to the pin.

As there are no compressive stresses, the Drucker-Prager, Mohr-Coulomb and Von-Mises have a similar distribution.

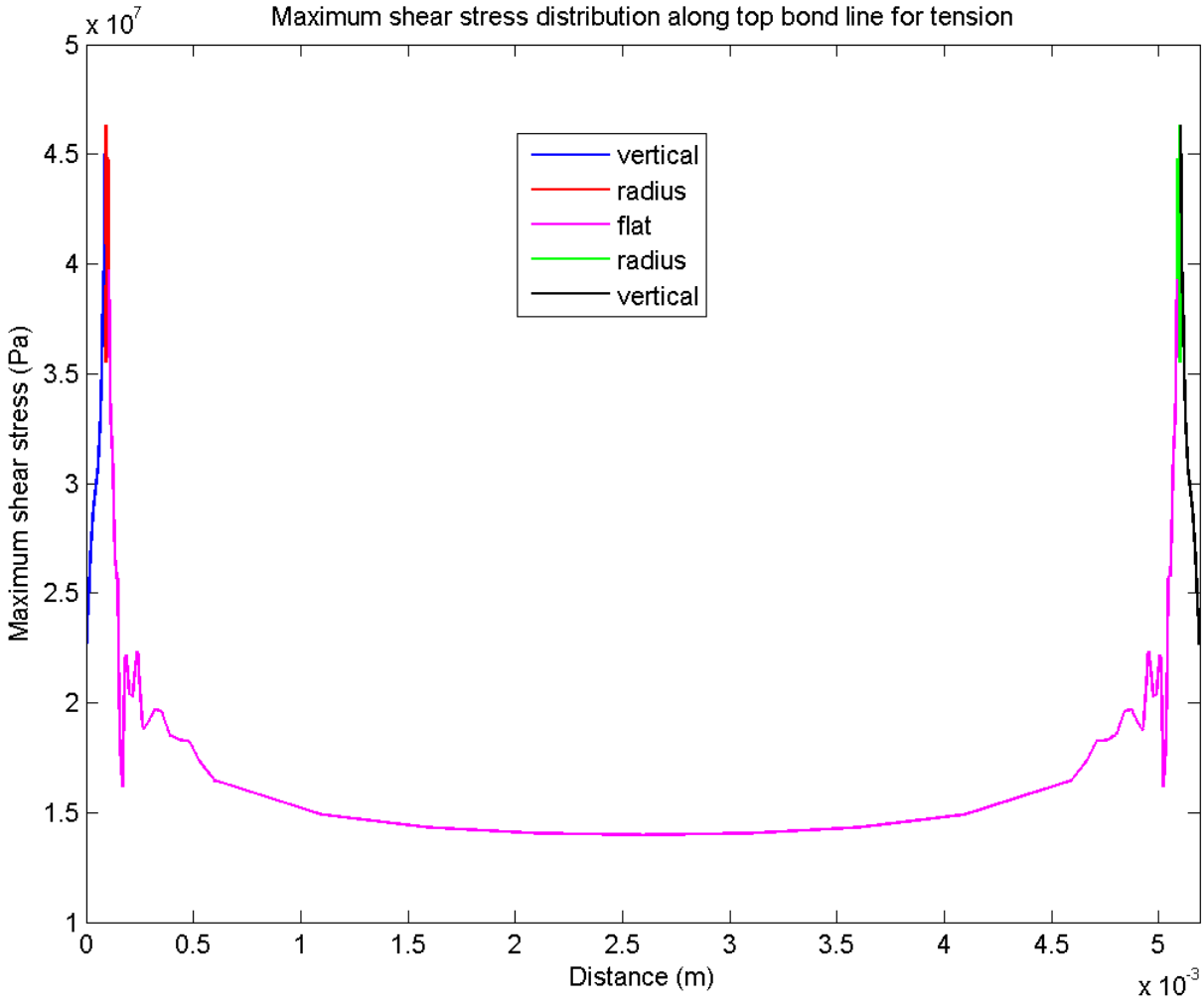

Figure 10.3: An example of the stress singularity at the fillet.

To summarize we can say that most of the stress remains constant throughout the adhesive layer as the load is also applied uniformly to the cross-section. The fillet has the singular stresses which need to be ignored as they are unrealistic. For our calculations we take the part of the results from the nodes away from the fillet so we can obtain more realistic stresses.

Tensile center layer

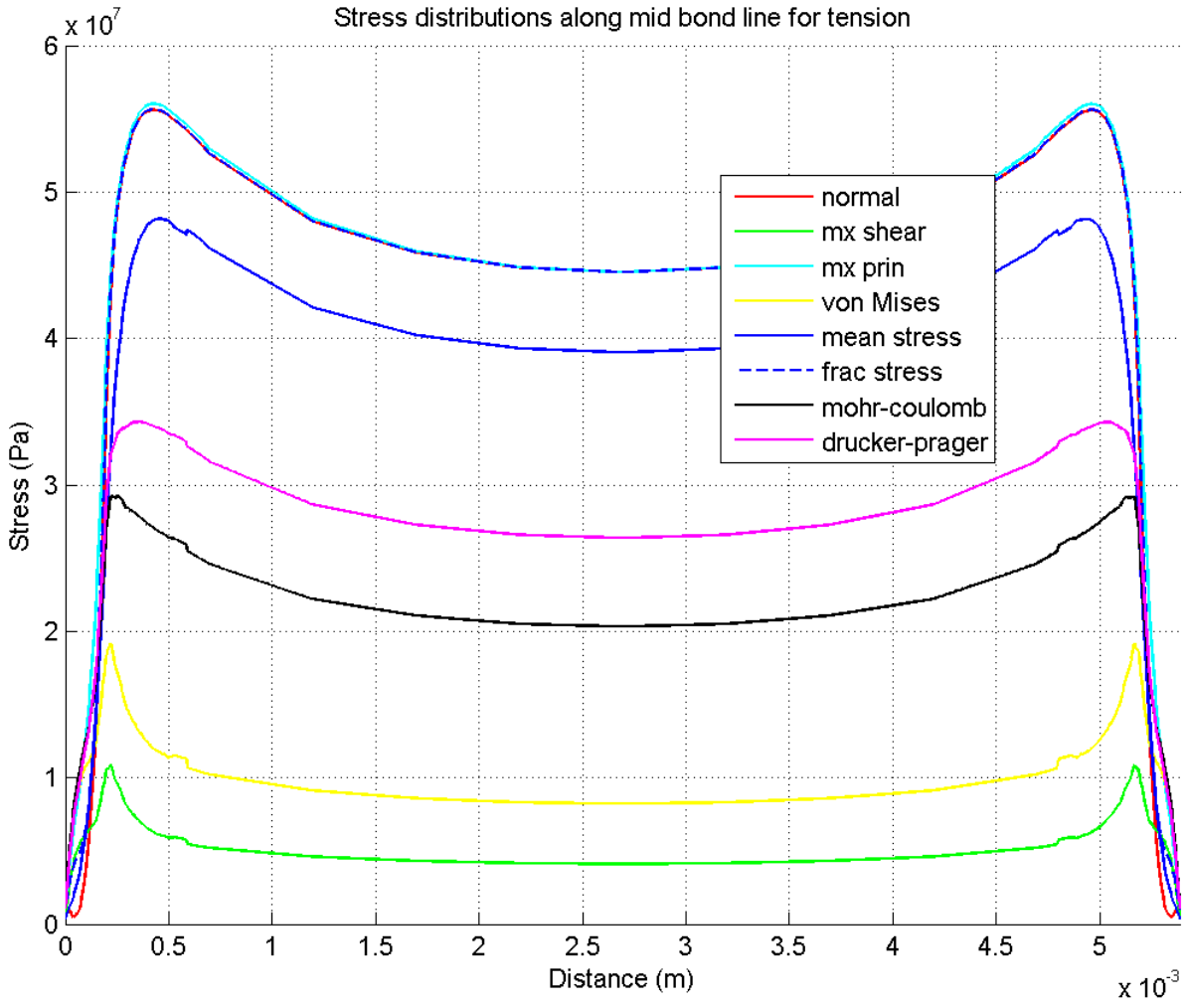

Figure 10.4: Comparison Failure Criteria plot for center layer in tension test.

In the center layer we see that this test being pure tensile the maximum principal stress is the same as the normal stress is the highest.

The maximum shear is the least as loading is only tensile. The stress distribution is more or less uniform throughout the layer of adhesive.

Because the maximum shear stress is low, the Fracture stress has contribution only from the normal stress and therefore they have overlapping curves.

As there are no compressive stresses, the Drucker-Prager, Mohr-Coulomb and Von-Mises have a similar distribution.

Tensile bottom layer

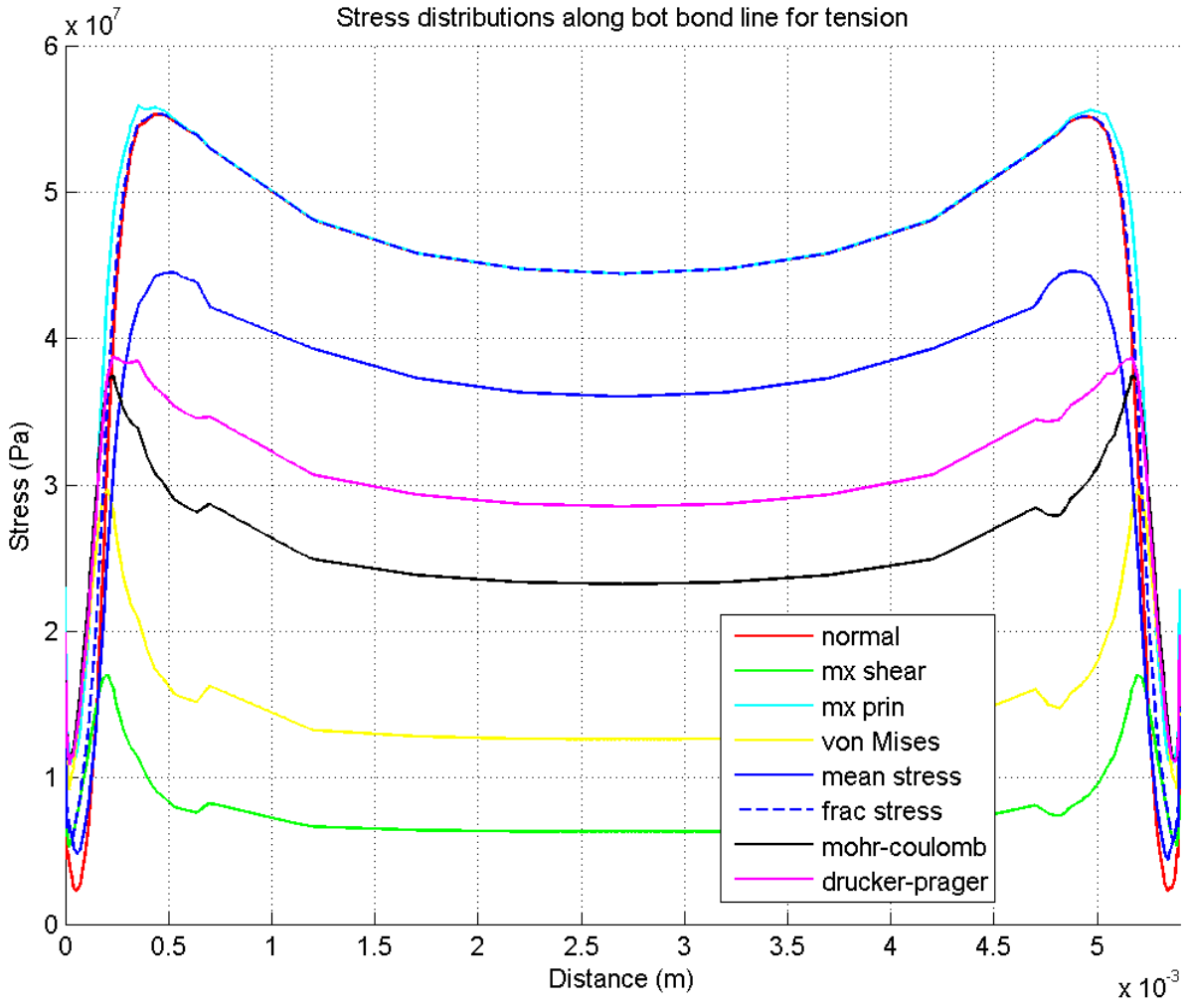

Figure 10.5: Comparison Failure Criteria plot for bottom layer in tension test.

The nature of the stresses is similar to the top and center layer. We see the effect of the singularity near the 90° re-entrant between the glue and the bottom adherend. These stress levels are none the less not as high as the stresses in the interface layer.

The stress levels are similar to the stress levels in the center and top layer. The stresses drop in the adhesive blob just outside the adherent's edge. If we take the stresses from the layer of adhesive between the adherends we still land up capturing the maximum stress level.

10.4 Torsion Test

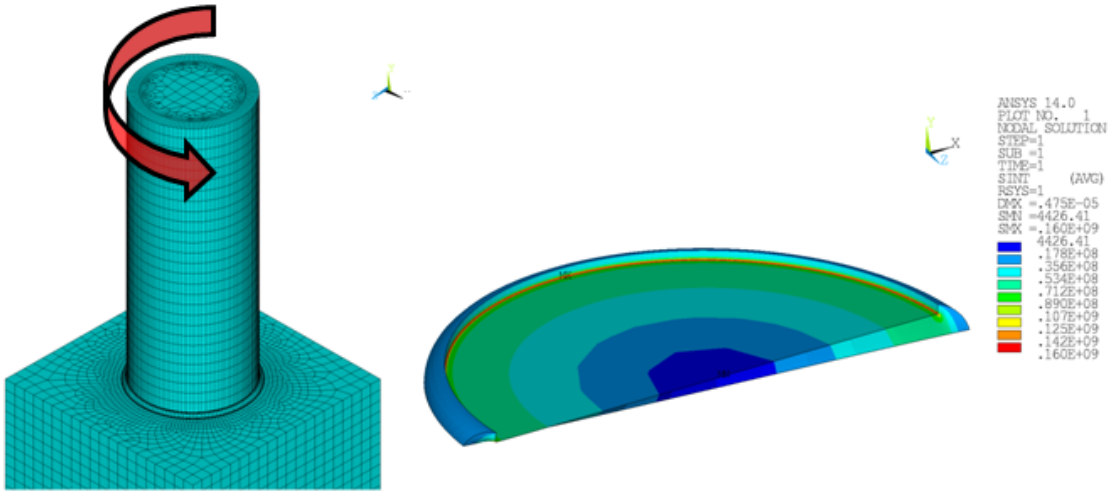

Figure 10.6: Torsion test.

10.4.1 Introduction

The torsion test is carried out on the custom built torsion test setup. The test sample has 26 pins of diameter 5mm glued to a substrate 10x15x130mm. We choose to model just one of these pins with a block of substrate glued to it. The glue layer is 100µm.

The pin geometry has been simplified as it will not contribute towards the stress analysis. A torque of 1Nm is applied uniformly to the external nodes of the top layer of the pin by using Fixed Rigid Zone. The torque is applied about the Y-axis. The nodes at the bottom face of the block are fixed.

10.4.2 Torsion Results

Torsion top layer

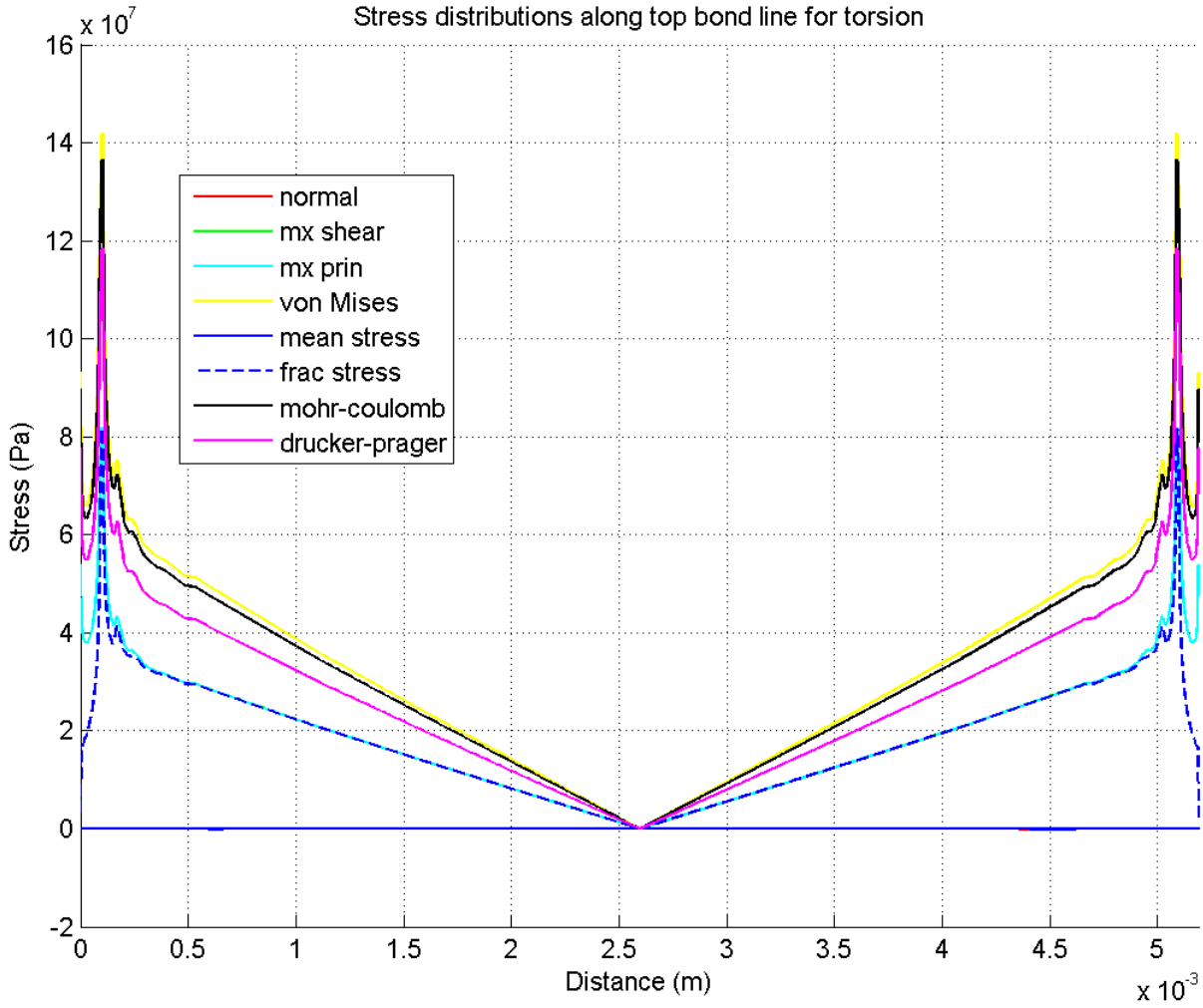

Figure 10.7: Comparison Failure Criteria plot for top layer in torsion test.

The stresses in the top layer are again similar in magnitude and distribution to the center and bottom layers.

The stresses linearly increase with the increase in radius.

The singular stresses in the fillet of the pin are extremely high and are left out of further calculations.

For torsion the maximum principal would be the same as the maximum shear as the load is in the same direction.

Near the fillet the out-of-plane component of shear is higher than the in-plane as such the fracture stress is lower at the edge compared to the maximum shear. Also the normal component of stress is nearly zero. As such the fracture stress is the same as the shear stress.

Torsion center layer

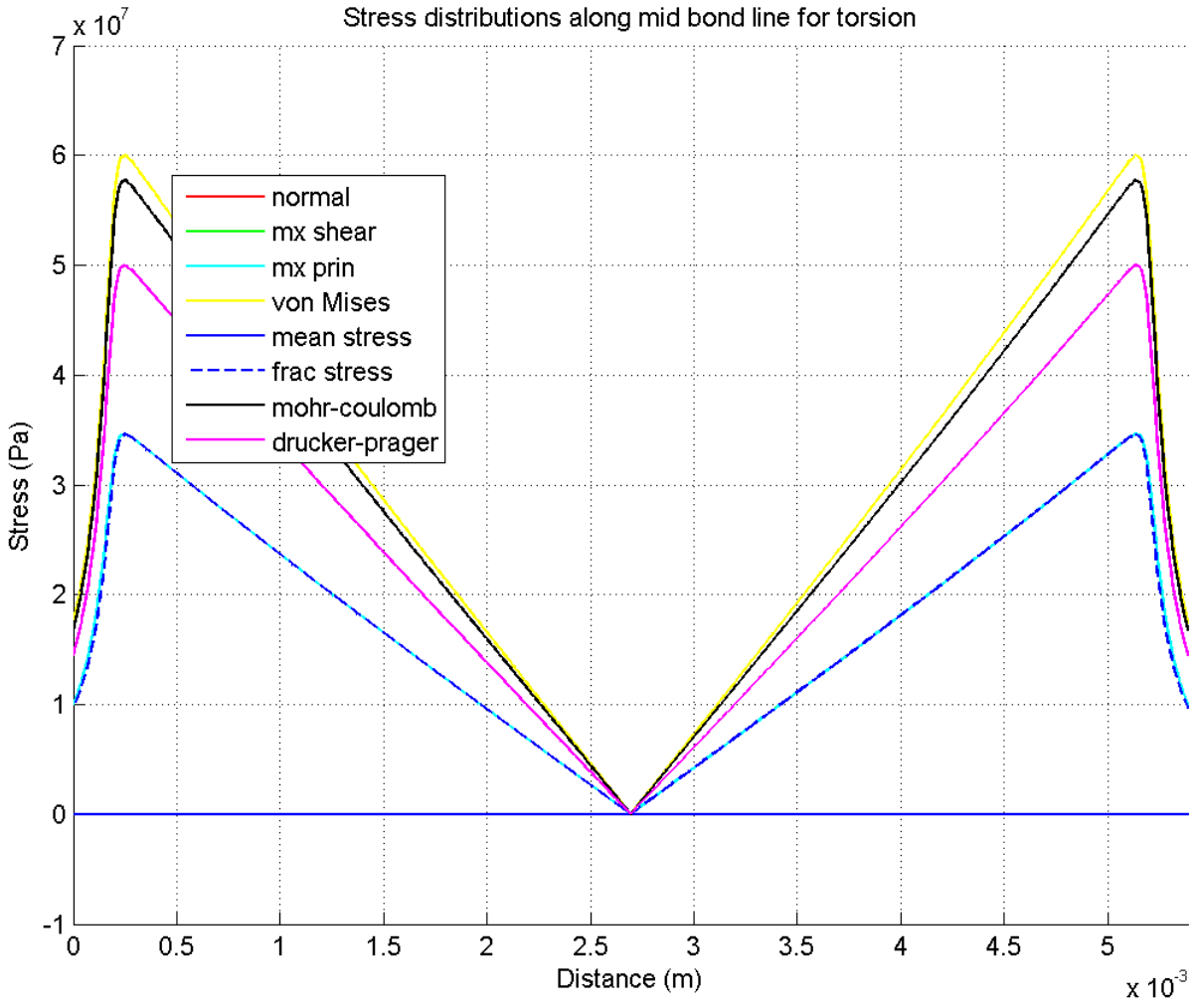

Figure 10.8: Comparison Failure Criteria plot for center layer in torsion test.

As the loading is in torsion we expect the stresses to linearly increase with increase in radius. The normal stress is zero. As such the fracture stress is the same as the shear stress with only the in-plane shear contributing. The load direction which results in the maximum principal stress causes the shear deformation resulting in the same maximum shear stress.

The mean stress is at zero as the nodes on half the path have symmetrically opposite loading to the remaining half of the nodes.

Von-Mises stress is the highest and Drucker-Prager and Mohr-Coulomb stresses are close to each other.

Torsion bottom layer

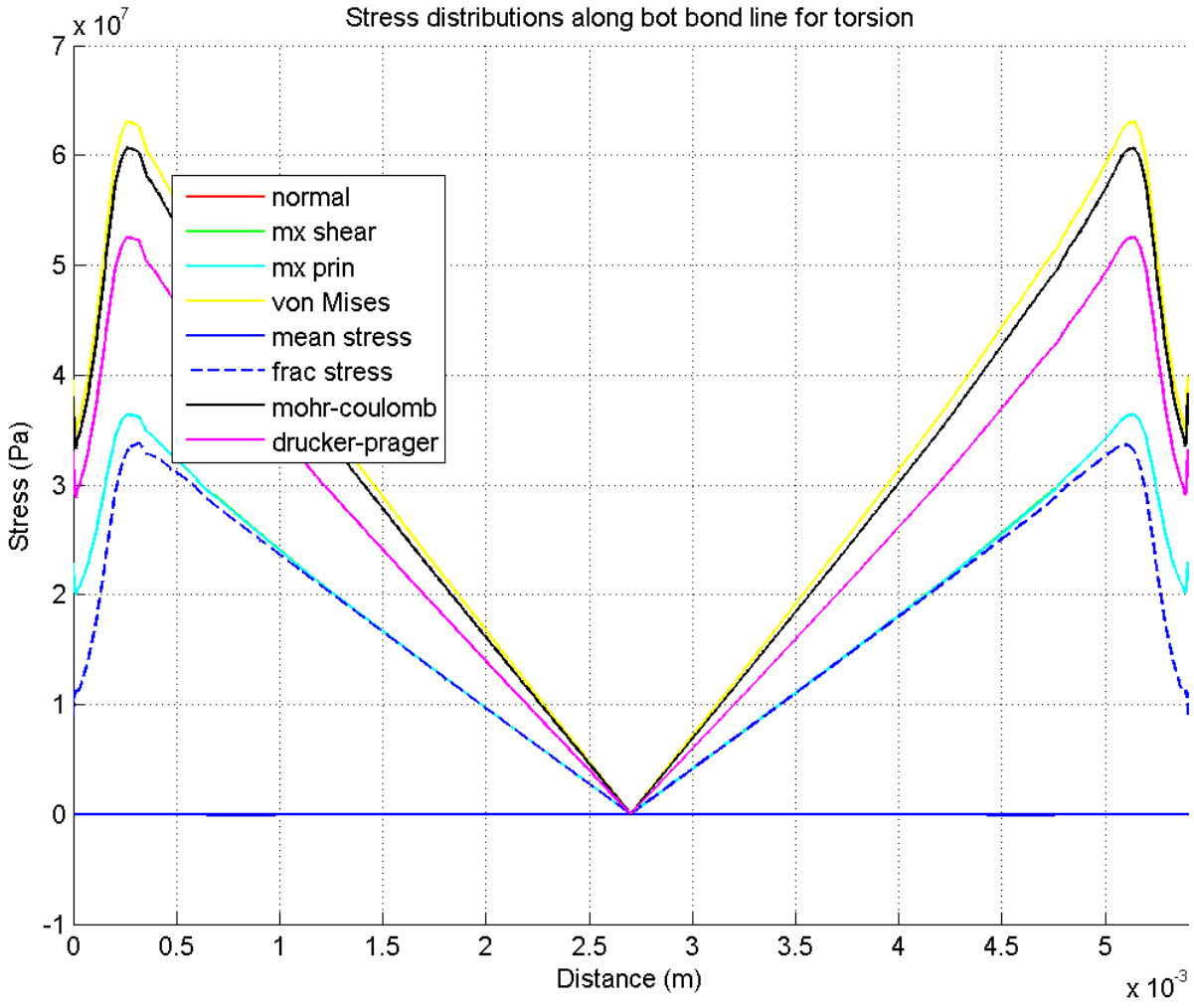

Figure 10.9: Comparison Failure Criteria plot for bottom layer in torsion test.

The bottom layer has stress distribution and magnitude of stresses very similar to the center layer.

The difference only being that at the edge of the interface because of a 90° re-entrant there are singular stresses.

10.5 Shear Test

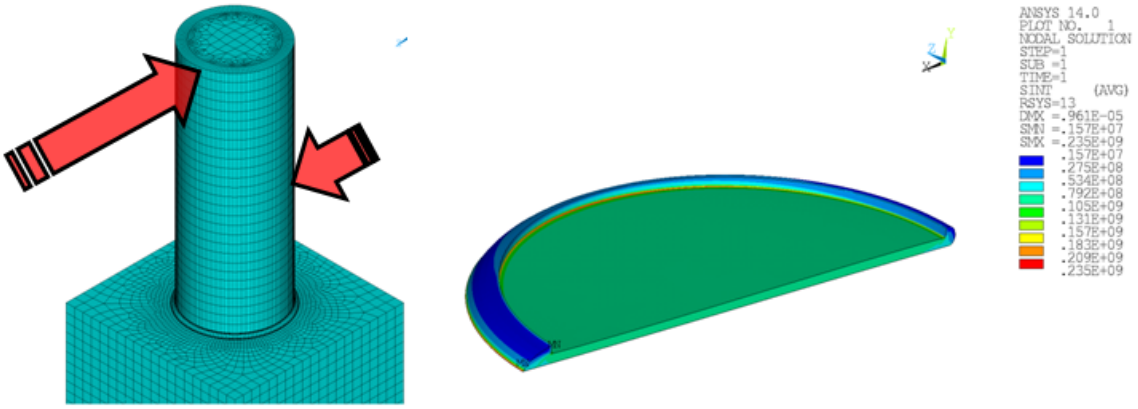

Figure 10.10: Shear test - The pure lateral shear is achieved by applying 2 opposing forces at different height in such a way that the moments of the two forces are canceled and the difference in force magnitudes acts as the shear force applied.

10.5.1 Introduction

The shear test is carried out on the IBS Stein machine which has 26 pins of diameter 5mm glued to a substrate 10x15x130mm. We choose to model just one of these pins with a block of substrate glued to it. The glue layer is 100µm.

The pin geometry has been simplified as it will not contribute towards the stress analysis. A load of 1KN is applied to a circumferential node on the top of the pin in the direction of X-axis. The nodes at the bottom face of the block are fixed.

10.5.2 Shear Results

Shear top layer

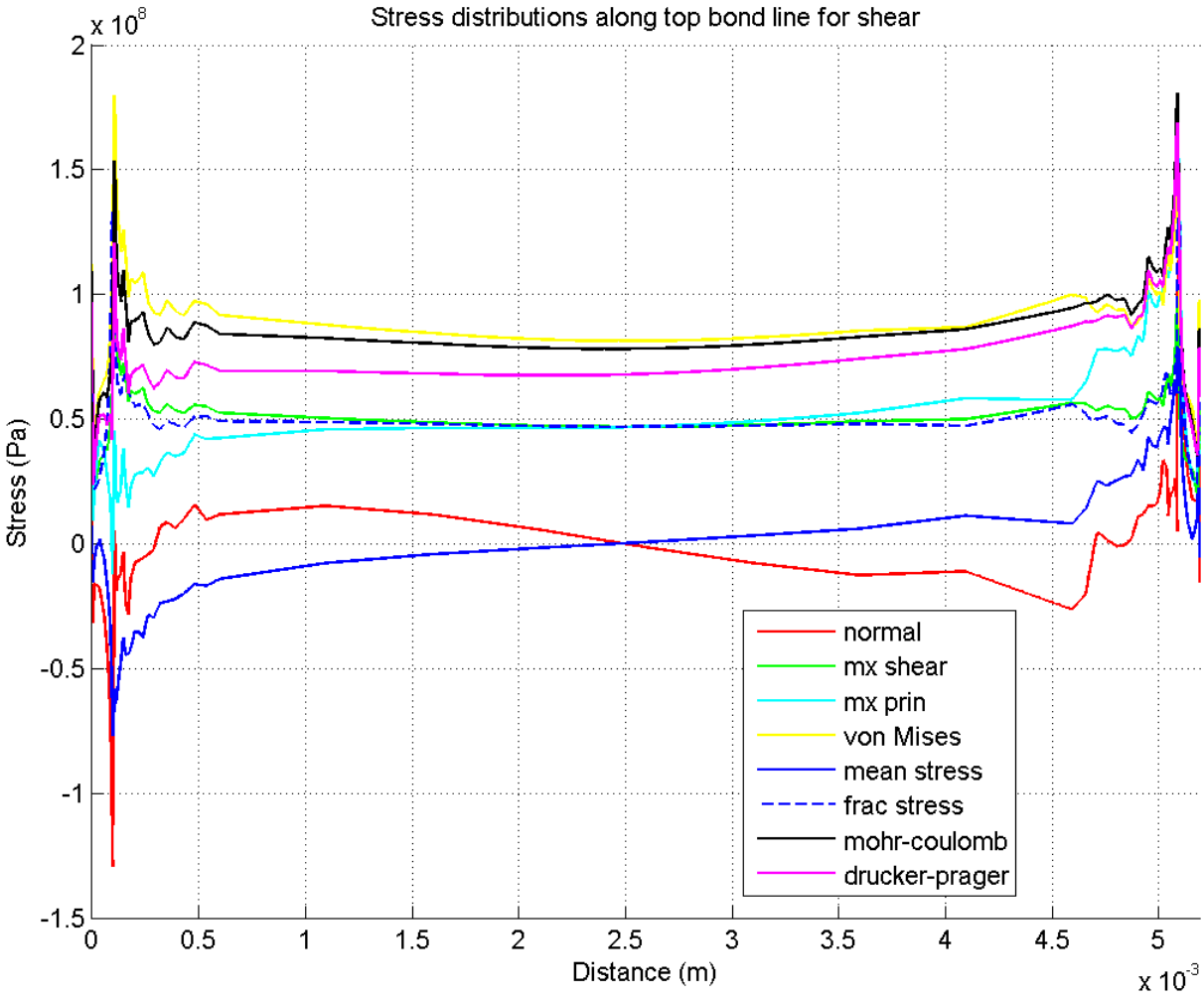

Figure 10.11: Comparison Failure Criteria plot for top layer in shear test.

For the shear load, just as the tensile load the stresses remain uniform throughout the layer of the adhesive for all three layers. The top layer has the obvious stress singularities at the fillet which are neglected as they are not realistic.

The normal stress is zero as load is shear. The mean stress is also zero as due to the load one half of the path is in compression and the other in tensile and they balance each other out.

As normal stress is nearly zero, we have the maximum principal, maximum shear and fracture stresses at the same level. The Von Mises is the highest. This is because there are compressive stresses present in the layer which lower the value of the Mohr-Coulomb and Drucker-Prager.

Shear center layer

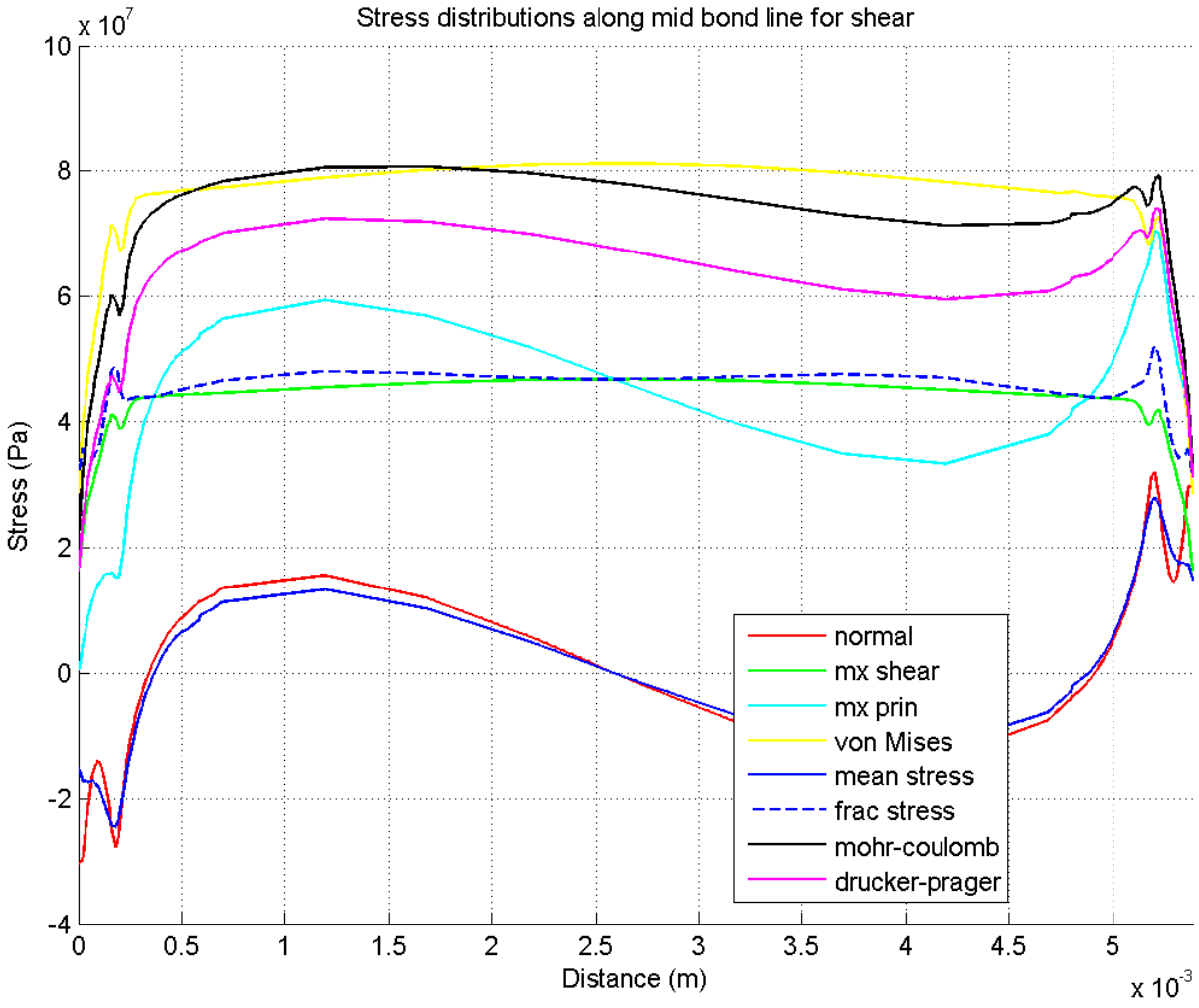

Figure 10.12: Comparison Failure Criteria plot for center layer in shear test.

The center layer here is loaded in shear. As the loading is only in shear we expect to see very low values for normal stresses. It would be ideally zero for a section with constant width, but as this a circular cross section, the shearing force is the same but the area of action decreases as we go to the outer diameter of the pin as such there is a slight bump in the stresses.

For the same reason there is a similar variation in the distribution of the maximum principal stresses.

The maximum shear values are also close to that of the maximum principal stresses. The normal stress is zero as such we expect the fracture stress curve to be close to maximum shear.

Von-Mises represents a high number for stress. The Drucker-Prager and Mohr-Coulomb are also more or less at the same level.

Shear bottom layer

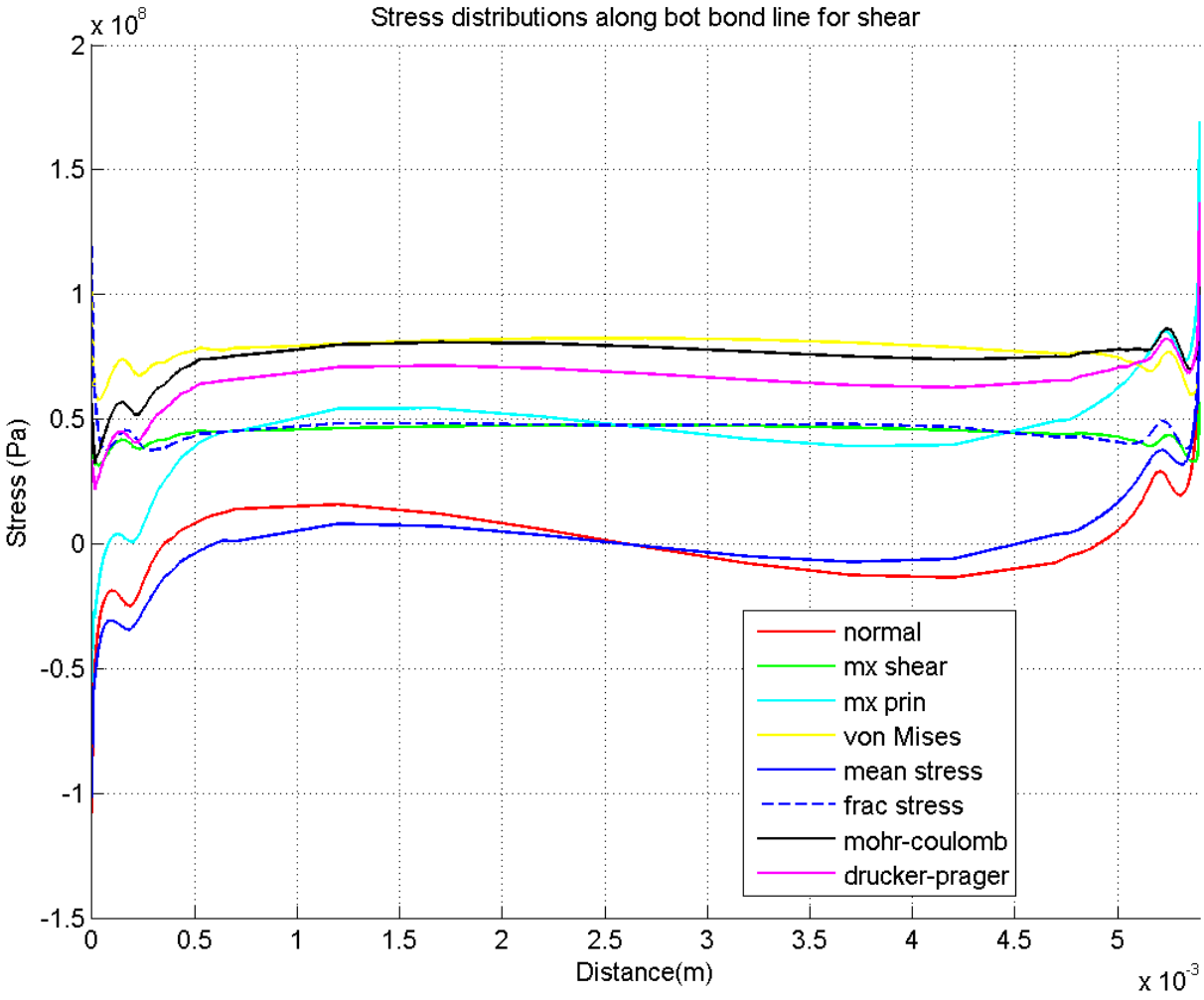

Figure 10.13: Comparison Failure Criteria plot for bottom layer in shear test.

The stress distribution is very similar in top and center layers. The singularities exist at the edges.

The load is applied from the left side and the adhesive layer shears towards the right side. As such the stresses on the left are compressive and are tensile on the right.

The compressive stresses are not as dangerous as such we look at the tensile stresses and we find that they are mostly the singular stresses at the edge. Neglecting we get the peak stress more or less similar to that within the rest of the layer.

10.6 Bending Test

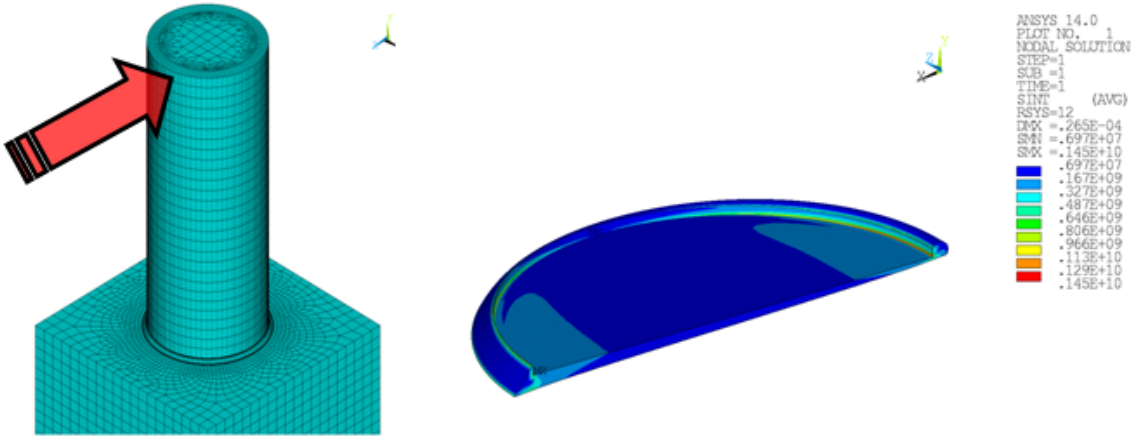

Figure 10.14: Bending test.

10.6.1 Introduction

The bending test is carried out on the IBS Stein machine which has 26 pins of diameter 5mm glued to a substrate 10x15x130mm. We choose to model just one of these pins with a block of substrate glued to it. The glue layer is 100µm.

The IBS is specifically built for tensile and shear tests. The shear setup is modified slightly by changing the width of the tooth that is normally used for shearing the sample. This keeps the test pin from entering the tool and hence avoids the shearing action on the pin.

The pin geometry has been simplified as it will not contribute towards the stress analysis. A load of 1KN is applied to a circumferential node on the top of the pin in the direction of X-axis. The nodes at the bottom face of the block are fixed.

10.6.2 Bending Results

Bending top layer

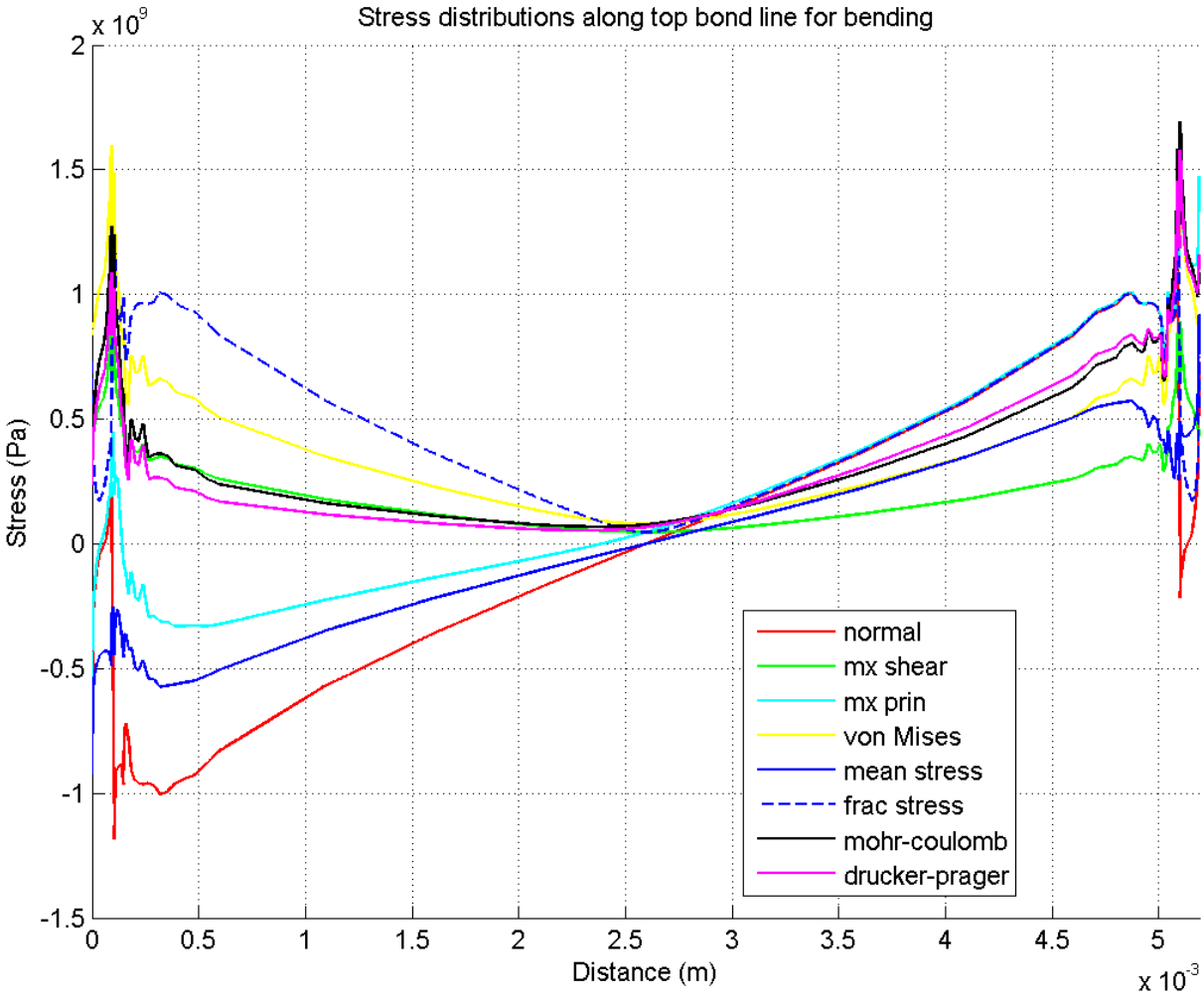

Figure 10.15: Comparison Failure Criteria plot for top layer in bending test.

We can see from the curves that the bending load is applied on the point on the right side where the pin lifts, which is why we have tensile loads on the right side and equally compressive loads on the left side where the pin is pushed into the adhesive which results in compressive loads.

As Mohr-Coulomb and Drucker-Prager are sensitive to tensile and compressive loads differently, we see that the stresses are then lower for the glue in compression as compared to the side where the glue is in tension.

The Von-Mises and Fracture give us an equivalent stress value. The Von-Mises along with the maximum shear is quite low. As the maximum shear is very low, the Fracture stress is mainly from the contribution of the normal stress.

The singular stresses at the fillet are present on both the tensile and compressive side. We ignore these stresses.

Bending center layer

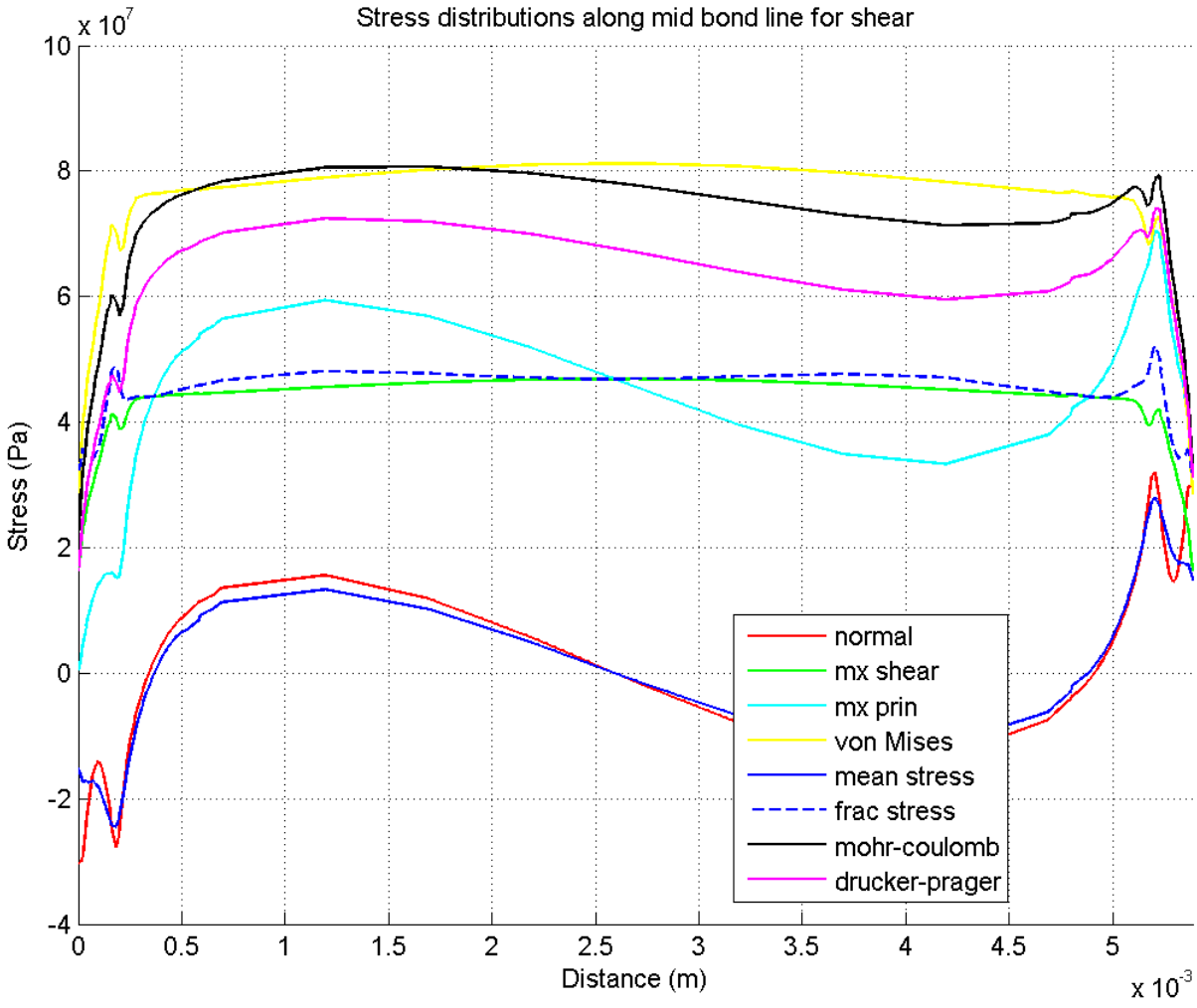

Figure 10.16: Comparison Failure Criteria plot for center layer in bending test.

The center layer has smooth stress gradients indicating no singular stresses.

Otherwise the nature of stress distribution and magnitude of stresses is similar to other layers.

Bending bottom layer

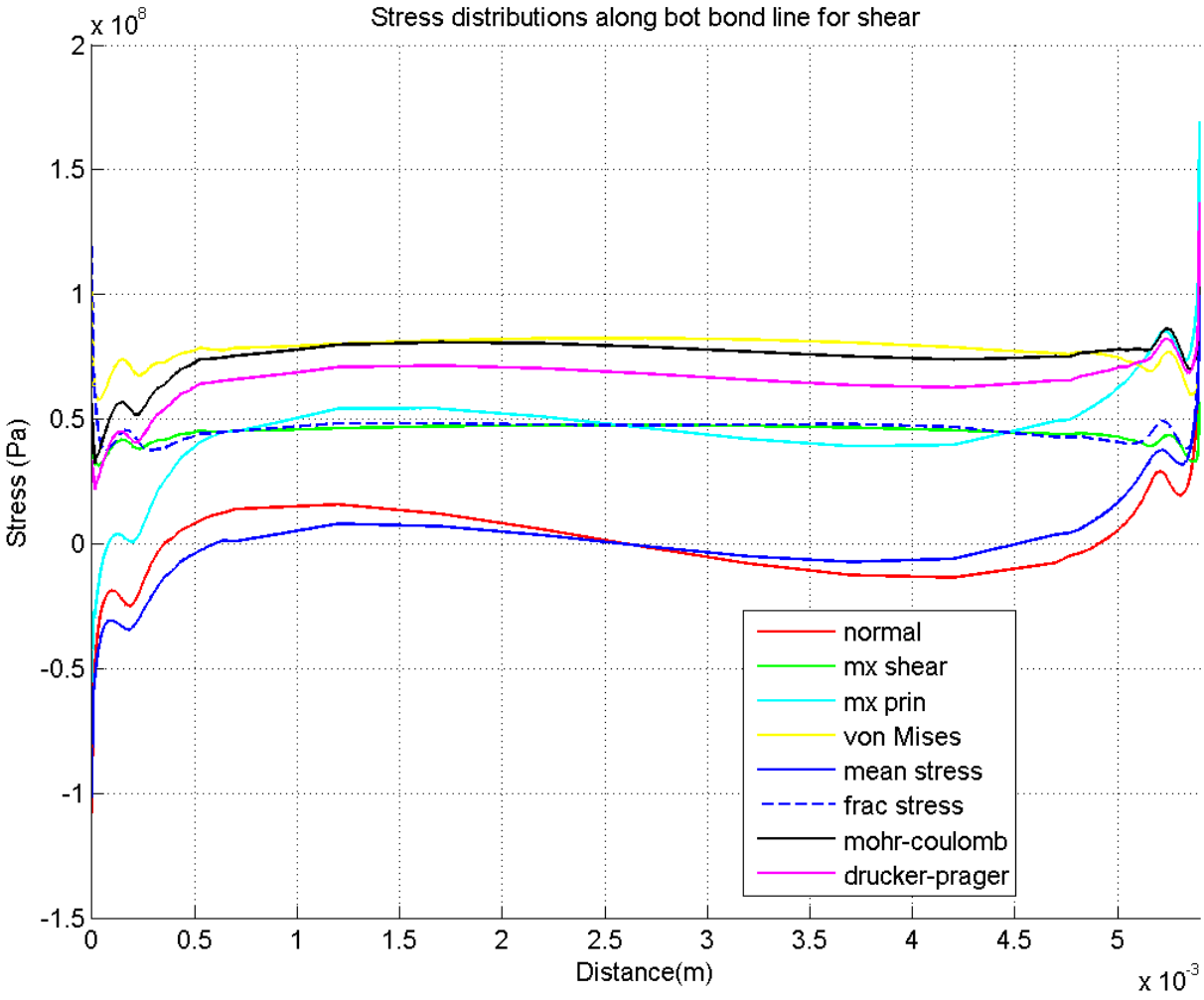

Figure 10.17: Comparison Failure Criteria plot for bottom layer in bending test.

In the bottom layer the stresses are again similar to the center layer. The edge has singular stresses with unrealistic gradient which we ignore. Nonetheless in bending the stresses within the layer are much higher.

10.7 Lap Shear Test

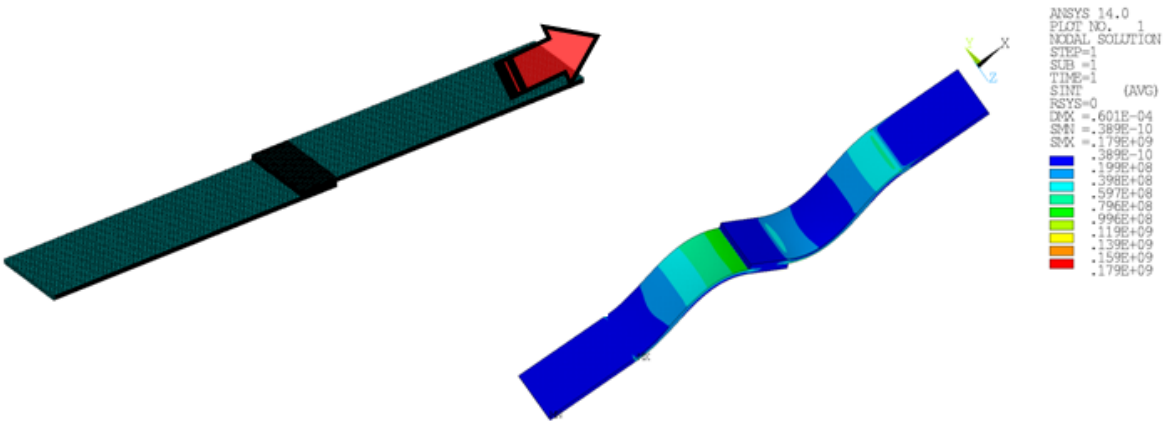

Figure 10.18: Shear test.

10.7.1 Introduction

The lap shear test is carried out on the Instron machine which has 2 jaws to clamp the 2 sides of the sample. One of the clamps is fixed at the bottom, and the top clamp is moved vertically to load the test sample in tension and the adhesive layer in shear.

The test sample is made up of 2 steel substrates 25mm wide that are glued to each other over a length of 12.5mm resulting in a total glued area of 312.5mm^2. The glue layer is 100µm.

A load of 1KN is applied to the nodes on end face of one of the substrates along X-axis. The nodes on the end face of the other substrate are fixed.

10.7.2 Lap Shear Results

Lap Shear top layer

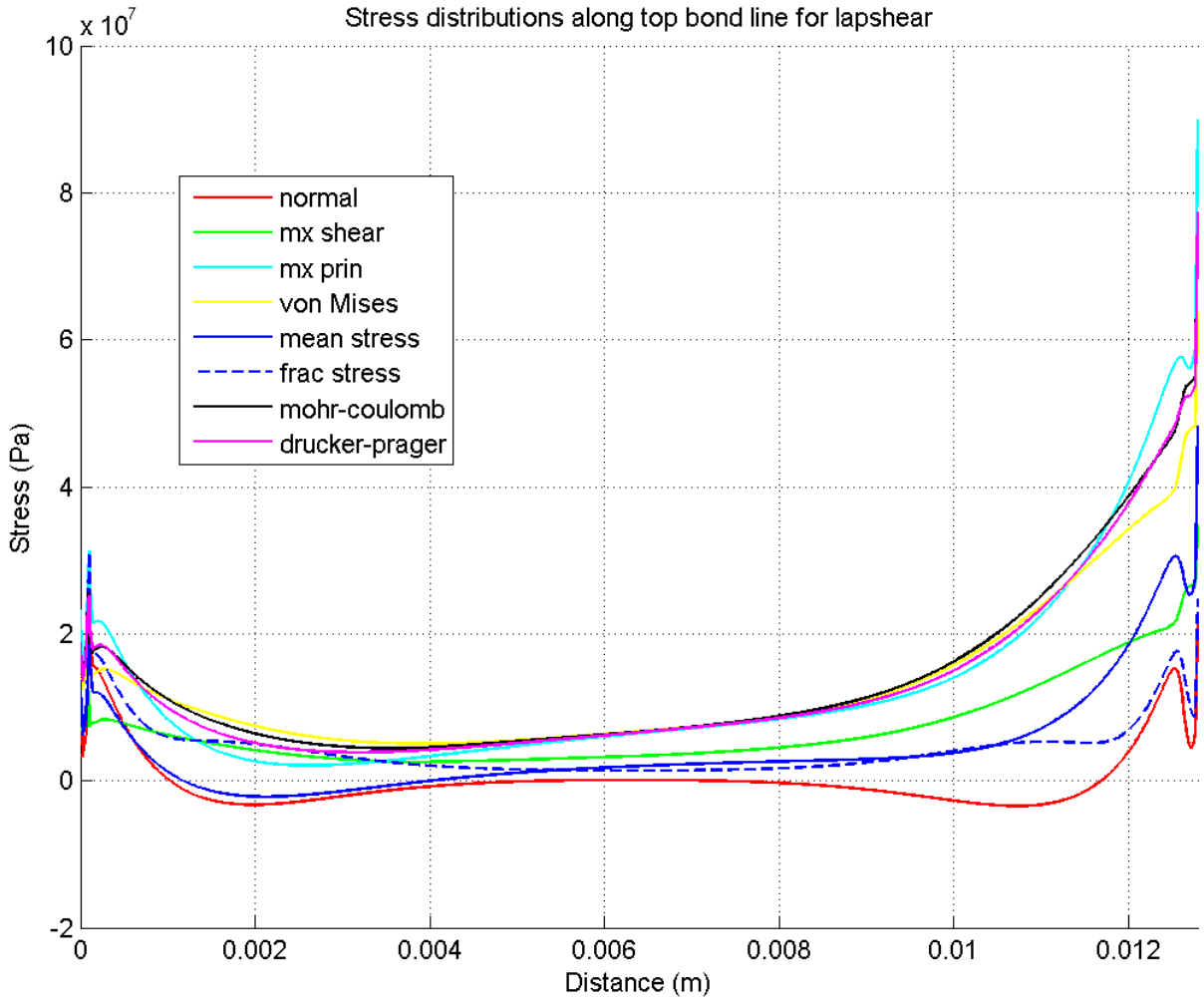

Figure 10.19: Comparison Failure Criteria plot for top layer in lap shear test.

The lap shear is a shear test, but as the 2 substrates are not in line with each other there is bending in the joint at the edges of the adhesive. This bending means that the maximum principal is highest at the edges.

The maximum shear increases very uniformly from the center towards the outer edge.

For the normal stress it is peculiar to see that the adhesive is actually in compression just after the high tensile stress at the edge and before it dives to almost zero at the middle of the adhesive overlap.

The Drucker-Prager, Mohr-Coulomb and Von-Mises have similar distributions. But the D-P and M-C have peak values slightly higher than Von-Mises because of the high tensile component due to bending.

The stresses in the fillet are singular but yet much lower than the stresses in the adhesive layer. The singular stresses at the edge with the 90° re-entrant are highest. These are only due to the edge in the mesh and sharp change in material properties of the adhesive and substrate. These singular stresses are very easily isolated and the more realistic high stresses in the layer are taken into consideration.

Lap Shear center layer

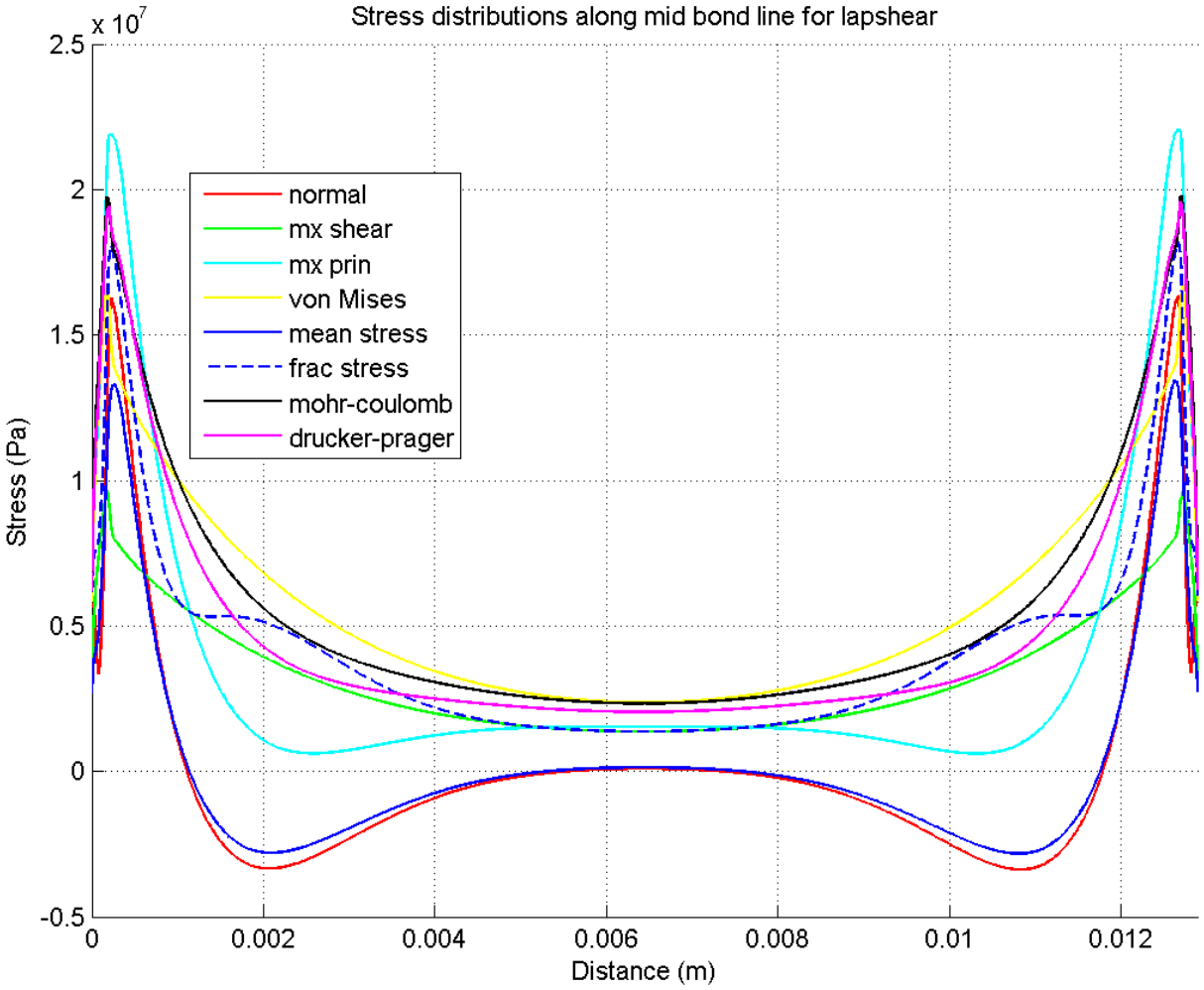

Figure 10.20: Comparison Failure Criteria plot for center layer in lap shear test.

The center layer is free from any singular stresses. All stress components are low in the middle of the layer and peak towards the edges. This leads to an important conclusion that when the adhesive starts to yield near the edge the bulk of the material in the middle is not yet stressed. Only as the yielded part is no longer able to sustain the increased load, the material in the middle starts to support the load and then yield.

Lap Shear bottom layer

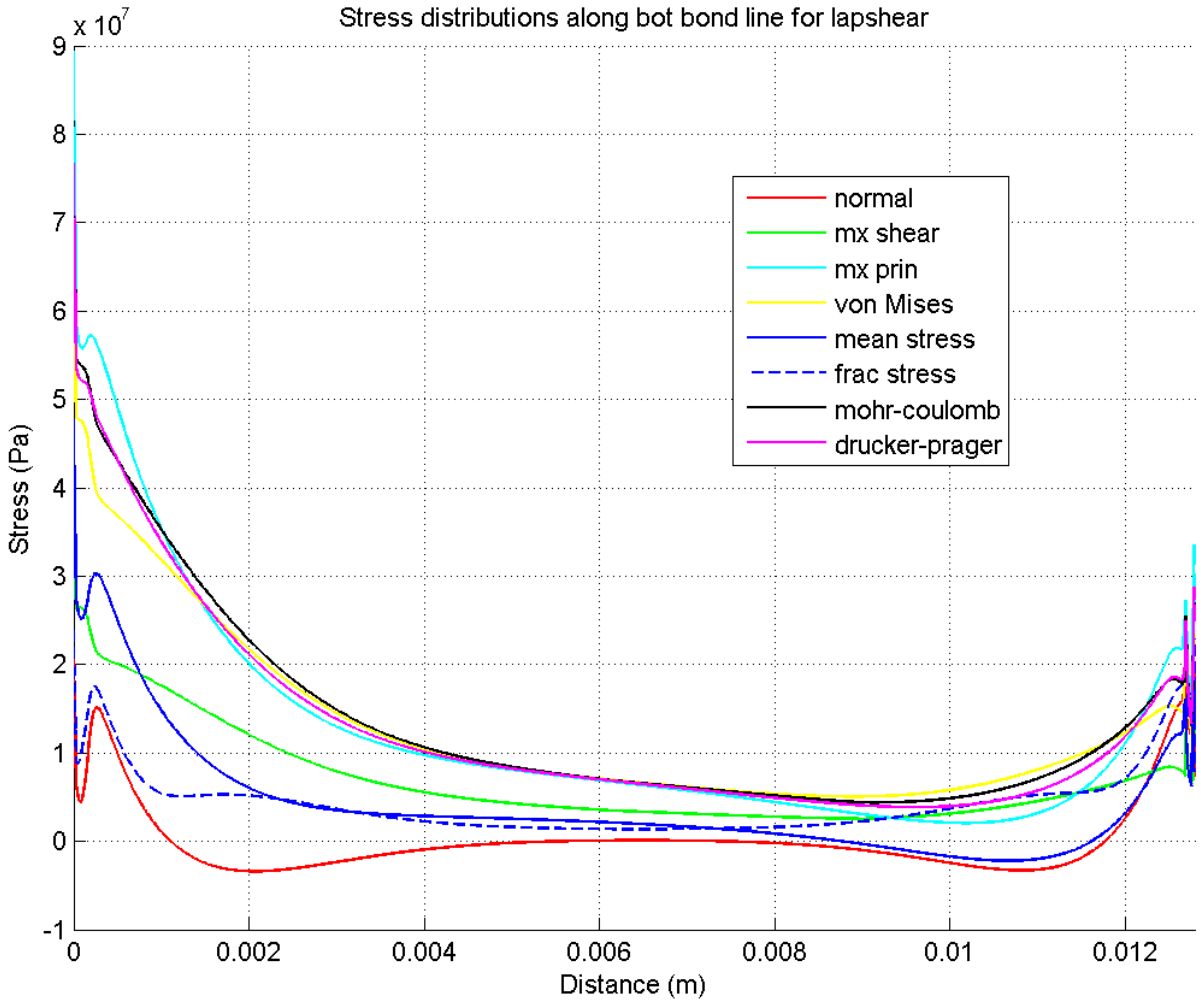

Figure 10.21: Comparison Failure Criteria plot for bottom layer in lap shear test.

The bottom layer is symmetric to the top layer as such the results are similar.

Chapter 11

Results for Failure criteria

11.1 For SW9323

The tests are carried out on approximately 180 samples for the tensile, shear, bending and the torsion tests and about 8 samples for the lapshear test. The test results are combined with the finite element analysis results to obtain distributions for all stress components at the three critical locations at the adhesive joint. These three locations are also the locations where the actual failure in the joint has taken place during testing. They are the top and bottom interface between the adhesive and the substrate in case of adhesion failures and the center layer of the adhesive where the cohesive failure occurs for an adhesive joint. For SW9323 we have observed cohesive failure and for Araldite2030 we have only observed adhesion failure.

The Fig 11.1 tabulates the results in a compact format. From amongst the criteria investigated that few of them which accurately describe the failure of the adhesive joint in all the different tests have been shown. The first three columns describe the different locations, the failure criteria used to describe the state of stress, the average value of failure stress over all the tests. The second to last column contains the computed Percent Standard Deviation based on all the results compiled from all the IBS1 tests. The last column contains the Percent Standard Deviation including the Lap Shear test. This Percent Standard Deviation is calculated based on the mean values of failure stresses from the IBS1 and Lap Shear tests. This is done because the number of samples tested for the Lap Shear test is smaller than that for the IBS1, hence the statistics considering all individual tests will not be able to reflect the true variation in the stresses. This last column has been compiled to illustrate firstly how the combination of tests with different geometries affects the Deviation in stress results and secondly to give a more realistic estimate of the Standard Deviation value when the joint under consideration may not be easily classified into one of the standard test/load types.

Location	Criteria	Torsion	Tensile	Shear	Bending (Yield)	Lap Shear (Yield)	Percent STD (Excl. Lap Shear)	With lap (with means)
Top	Maximum Principal	86	60	71	97	184	21.00	49.49
	Maximum Shear	86	35	41	57	83	39.69	39.17
	Equivalent von Mises	150	61	71	101	151	39.09	39.58
	Peel	0	60	17	96	49	83.47	84.38
	In-plane shear	76	13	34	19	35	73.44	68.76
	Mean stress	0	34	33	55	96	66.07	81.06
	Fracture stress	29	60	36	96	55	46.66	48.16
	Mohr-Coulomb stress	48	63	75	106	172	30.34	52.95
	Drucker-Prager stress	42	57	72	97	169	31.73	57.14
Middle	Maximum Principal	56	60	37	99	69	34.00	35.26
	Maximum Shear	56	12	25	21	30	64.04	58.26
	Equivalent von Mises	97	20	42	37	52	63.34	57.64
	Peel	0	59	17	97	51	84.41	84.77
	In-plane shear	56	9	25	18	30	70.98	64.06
	Mean stress	0	51	15	83	42	83.90	84.92
	Fracture stress	28	59	27	97	57	51.48	53.29
	Mohr-Coulomb stress	47	31	42	56	62	23.60	25.11
	Drucker-Prager stress	41	37	39	63	61	24.47	26.74
Bottom	Maximum Principal	59	60	51	99	183	27.57	61.22
	Maximum Shear	59	18	25	32	83	50.02	62.17
	Equivalent von Mises	102	32	43	56	150	49.78	64.00
	Peel	0	59	28	96	50	77.01	76.96
	In-plane shear	55	18	25	32	35	47.23	42.67
	Mean stress	0	47	29	78	95	72.95	75.96
	Fracture stress	28	59	32	97	56	48.78	50.39
	Mohr-Coulomb stress	50	40	45	70	171	24.01	73.01
	Drucker-Prager stress	43	41	43	72	168	26.57	73.90
Interface	Maximum Principal	73	60	61	98	183	25.29	54.47
	Maximum Shear	73	26	33	45	83	50.28	47.61
	Equivalent von Mises	126	46	57	79	150	49.98	48.72
	Peel	0	59	23	96	50	80.22	80.29
	In-plane shear	65	15	30	25	35	63.25	55.18
	Mean stress	0	41	31	66	95	72.16	77.28
	Fracture stress	28	59	34	97	56	47.72	49.22
	Mohr-Coulomb stress	49	52	60	88	171	33.68	60.99
	Drucker-Prager stress	42	49	57	85	168	33.44	64.10
Test	Nominal stress	33	54	27	5	18	68.46	66.94

Table 11.1: Results for SW9323. Grouped according to the layer they belong to. The numbers in the table represent the mean value of failure stress (MPa) for each test and for each criterion. The last 2 columns have the Percent standard deviations for all test results combined, without lap shear and with lap shear respectively. The last row has nominal stress results from the tests for comparison.

Before we discuss the results for the different failure criteria, it is also important to know where and how the result is obtained for the various tests. For the IBS1 tests, the maximum stress in the top layer is obtained by excluding the vertical and fillet portion of the interface. It is observed that the vertical face contains nodes which are close to the mesh singularities in the model, then the gradients in stress are unrealistically high, but also the stress levels are not the maximum in this region. The second area which is excluded is the fillet area. The fillet radius is 0.01 millimeters which is very small. This results in very high stresses as we go on refining the mesh in this region. The high stresses are very local. In another observation it was found that if stresses from this region were ignored, then the maximum stresses found were a good approximation of stress values if the stresses were extrapolated from non-singular locations. As such for the top layer, the maximum stress was obtained from within the flat portion of the joint. Similarly for the bottom layer, there is an almost 90° re-entrant corner which results in very high peak stresses, especially in the lap shear and the bending tests. These singular stresses are easily excluded by excluding a few nodes from the re-entrant corner. In our case it was identified that these singular stresses were present within a distance of 0.025mm from the outer edge. Excluding 4 corner nodes gave an accurate value of maximum stress if mesh singularities would not have influenced the value of stress. For the middle/center layer though, the entire layer could be used for finding the peak stress, as there were no un-explicable stresses present.

The data in the above table has been reported for SW9323. For this adhesive, the failure observed was due to loss in cohesion. As substrate surfaces for both SW9323 and Araldite2030 were prepared similarly, therefore we can say that the adhesion between SW9323 and stainless steel was less sensitive to the surface preparation. If we look closely at the values for the center layer, we have a few criteria which best describe the stress state at failure. Both Mohr-Coulomb and Drucker-Prager criteria give us around 23% spread in stresses from amongst all IBS1 tests with different load types as compared to around 65% for the currently used Von-Mises criteria for instance. A 23% spread around the mean would indicate a factor of 2.3 to be included in the margin for safety ideally for a generic adhesive joint similar to that of the IBS1 for any type and combination of loading. This factor of 2.3 which covers the uncertainty in estimating the failure stress arises from a combination of factors related to adhesive joint surface preparation, variations in joint testing and approximation from finite element analysis results. This factor coupled with a factor of 2 for variations in design should result in an overall factor of safety of 5 for the adhesive joint.

If we choose to dwell a little deeper we might see what makes these criteria a good choice to consider. The Mohr-Coulomb yield surface in 3D stress space is a tapering cone like surface with 6 individual surfaces connecting first, second and third principal stresses. The provision for differentiating between the tensile and the compressive yield strength of the material is what differentiates this criterion from the Tresca criterion. Although the Tresca is dependent on the Maximum shear stress, the Mohr-Coulomb includes response of the material under shear and normal stresses. It is generally applied to materials with large compressive strength than the tensile strength. In our case, we have this ratio approximated at 1.5 which is derived directly from the literature studied and also from the data for rubber-toughened SW9323 found in another literature study.

The second most likely criteria for SW9323 in the center layer, seems to be the Drucker-

Prager criterion. The Drucker-Prager is a pressure dependent criterion. It is popularly used for describing the deformations of soils and polymers. It is again a conical shaped envelope which represents an ellipse in 2D stress space similar to the Von-Mises criterion. The difference here again is that the hydrostatic pressure sensitivity can be included by introducing the ratio of the compressive yield to the tensile yield. We can conclude that the failure for SW9323 in the center layer is a combination of both the peel and shear stresses if we were to consider multiple types of loading.

Having discussed about the failure of SW9323 at the center layer, it is essential to mention that since the tests showed no failure at the interface, a discussion about criteria at the interface is at the most a speculation hence avoided.

11.2 Including Lap Shear results

Finally when we include the results from the lap shear tests into the picture, we again get Mohr-Coulomb and Drucker-Prager criteria as the best criteria for the center layer. The spread is around 25% from the mean. This will result in a factor of safety of 2.5. The Fracture criterion is also a very logical criterion in general for adhesives. It is based on the premise that if a defect at the layer of adhesive we are considering is present then the defect will try to open in Mode I as well as Mode II of failure. The Mode I will depend on peeling forces and Mode II will depend on magnitude of shear forces. If such a criterion is developed with takes into account equally the effect of these two types of stresses, then we have the Fracture criteria which is given by equivalent in-plane shear and the normal or peel stress at a location.

11.3 Araldite2030

Location	Criteria	Torsion	Tensile	Shear	Bending (Yield)	Lap Shear (Yield)	Percent STD (Excl. Lap Shear)	With lap (with means)
Top	Maximum Principal	74	17	11	36	198	65.66	114.83
	Maximum Shear	74	10	7	22	90	83.53	95.82
	Equivalent von Mises	129	17	12	38	162	82.93	96.52
	Peel	0	17	3	35	53	112.04	104.50
	In-plane shear	65	4	6	7	38	106.27	113.86
	Mean stress	0	9	5	20	103	108.24	156.51
	Fracture stress	25	17	6	35	59	45.83	72.51
	Mohr-Coulomb stress	41	18	12	40	185	45.99	120.61
	Drucker-Prager stress	36	16	12	36	182	45.28	125.75
Middle	Maximum Principal	48	17	6	36	74	52.93	74.65
	Maximum Shear	48	3	4	8	32	98.74	104.18
	Equivalent von Mises	83	6	7	15	56	98.24	103.67
	Peel	0	16	3	35	55	112.81	106.30
	In-plane shear	48	3	4	7	32	103.38	108.67
	Mean stress	0	14	2	29	45	112.23	105.36
	Fracture stress	24	16	4	35	61	47.04	76.31
	Mohr-Coulomb stress	41	9	7	21	66	64.22	86.26
	Drucker-Prager stress	35	10	6	24	66	56.03	84.94
Bottom	Maximum Principal	51	17	8	36	197	53.57	125.79
	Maximum Shear	51	5	4	12	89	91.28	115.92
	Equivalent von Mises	88	9	7	20	161	91.04	117.61
	Peel	0	16	4	35	54	111.27	102.28
	In-plane shear	47	5	4	11	37	89.82	94.96
	Mean stress	0	13	5	28	102	110.64	141.96
	Fracture stress	24	16	5	35	60	46.73	73.94
	Mohr-Coulomb stress	43	11	7	26	184	59.65	136.76
	Drucker-Prager stress	37	12	7	26	180	54.27	138.45
Interface	Maximum Principal	62	17	10	36	197	63.08	119.61
	Maximum Shear	62	7	5	17	89	90.42	103.80
	Equivalent von Mises	108	13	9	29	161	89.98	105.03
	Peel	0	16	4	35	54	111.66	103.78
	In-plane shear	56	4	5	9	37	101.43	104.38
	Mean stress	0	11	5	24	102	112.58	148.60
	Fracture stress	24	16	5	35	60	46.28	73.39
	Mohr-Coulomb stress	42	15	10	33	184	53.02	128.04
	Drucker-Prager stress	36	14	9	31	180	49.96	131.63
Test	Nominal stress	28	15	4	2	11	97.60	87.02

Table 11.2: Results for Araldite2030. The numbers in the table represent the mean value of failure stress (MPa) for each test and for each criterion. The last 2 columns have the Percent standard deviations for all test results.

Araldite2030 has failure of the bond at the top and bottom interface which is observed from the tests. Hence the results from tests on Araldite2030 will prove conclusive towards determining a failure criterion at the interface.

We first look at the results for the top layer. Although there are geometric complexities, we still consider only the part which is away from these complexities. The Fracture stress is the best candidate as failure criterion for this layer. After excluding the stress singularity at the outer edge for the bottom layer, the rest of the layer also has Fracture stress as a good choice for criterion. Therefore overall the Fracture stress simply is the best criteria to describe the stresses at the interface.

11.4 Factor of Safety

From the result Tables 11.1 & 11.2 we can see which criteria performs the best as far as predicting the strength of the adhesive irrespective of the type of loading or geometry. This helps the problem of accurately predicting the failure and in turn designing efficient joints with respect to strength.

This being said, for the designer or the analyst it is also important to know what factor of safety is to be used while designing, keeping in mind a certain criteria. From our tests on the joint specimen we obtain the nominal stresses. If these stresses are then compared with the stresses from the criteria, then the factor obtained is the factor of safety that you need to multiply your nominal stresses from the tests to obtain the comparable stress values in the FEM.

But we also need to add that there is a variation in these stress values of criteria depending on the type of loading and geometry. This window of uncertainty is as we see from the table about 25% for the center layer. For example if we are looking at a Drucker-Prager stress value of 28MPa then we have a spread from 21-35MPa.

At the same time if we look at results for Von Mises criterion, we have a spread of 65%. This means that we will need a factor of safety of almost 3 times for Von Mises criteria than for Drucker-Prager criteria.

Depending on the classification of the purpose of the joint, whether for strength until failure or stability of the joint we can choose to be either conservative (stable) or be aggressive and go for a more optimized design of the joint (strength).

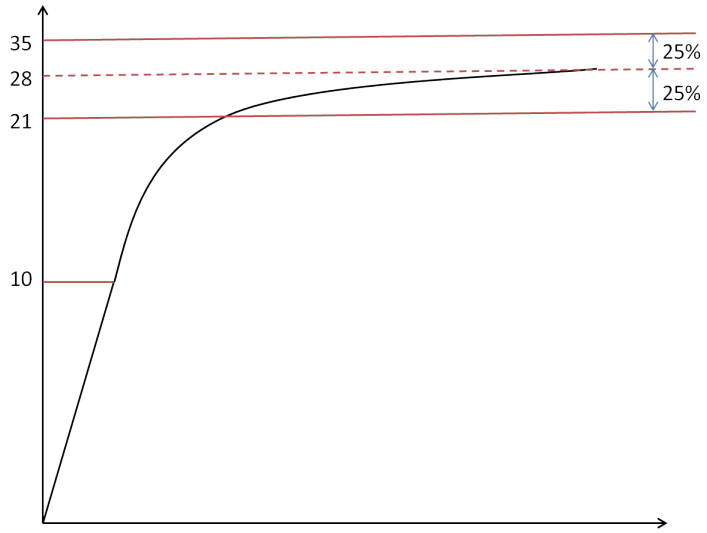

Figure 11.1: Band for Factor of Safety. The graph is a stress-strain curve. 10 MPa on the graph represents the nominal failure stress obtained from the tests. 28 MPa represents the calculated Drucker-Prager stress. The band from 21-35 MPa represents the spread that is possible in the D-P value due to spread in the strength from tests.

11.5 Summary

11.5.1 For Center layer

For the center layer the Drucker-Prager stress criteria and the Mohr-Coulomb criteria are equally effective. As the results from Araldite for the center layer has better results when using the Drucker-Prager criteria we select it as the preferred criteria.

Criteria	Torsion	Tensile	Shear	Bending	Lap	STD	w/ lap
Max. Principal	56	60	37	99	69	34.00	35.26
Maximum Shear	56	12	25	21	30	64.04	58.26
Von Mises	97	20	42	37	52	63.34	57.64
Peel	0	59	17	97	51	84.41	84.77
In-plane shear	56	9	25	18	30	70.98	64.06
Mean stress	0	51	15	83	42	83.90	84.92
Fracture stress	28	59	27	97	57	51.48	53.29
Mohr-Couloumb	47	31	42	56	62	**23.60**	**25.11**
Drucker-Prager	41	37	39	63	61	**24.47**	**26.74**

Table 11.3: Summary of results for center layer. These results are the results of center layer for Scotchweld 9323. STD represents Percent standard deviation for results for each criterion. Last column includes the lap shear results in the STD calculations.

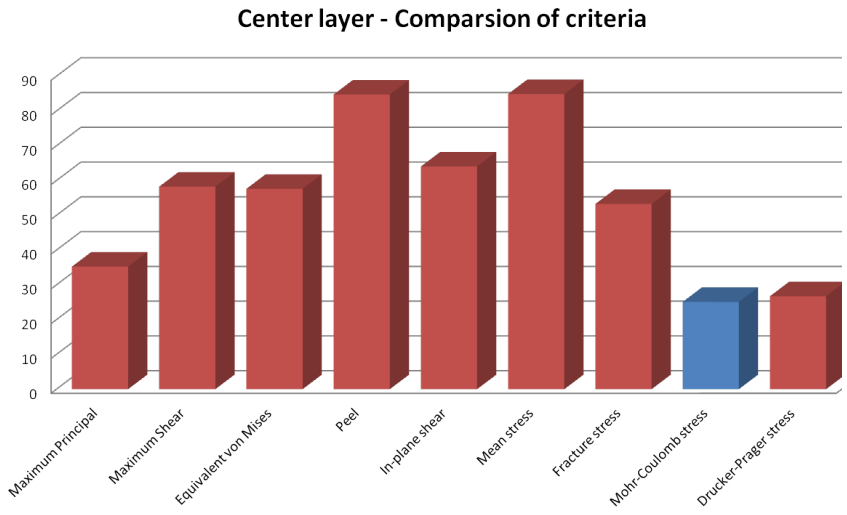

Figure 11.2: Chart showing the Percent standard deviations for various criteria for center layer in a bar chart format to pictorially indicate how Drucker-Prager and Mohr-Coulomb criteria outperform the other criteria.

11.5.2 For Interface layer

For the interface layer the Fracture stress criteria is the preferred criteria.

Criteria	Torsion	Tensile	Shear	Bending	Lap	STD	w/ lap
Max. Principal	62	17	10	36	197	63.08	119.61
Maximum Shear	62	7	5	17	89	90.42	103.80
Von Mises	108	13	9	29	161	89.98	105.03
Peel	0	16	4	35	54	111.66	103.78
In-plane shear	56	4	5	9	37	101.43	104.38
Mean stress	0	11	5	24	102	112.58	148.60
Fracture stress	24	16	5	35	60	**46.28**	**73.39**
Mohr-Couloumb	42	15	10	33	184	53.02	128.04
Drucker-Prager	36	14	9	31	180	49.96	131.63

Table 11.4: Summary of results for interface layer. These results are a combination of the results from top and bottom layer results for Araldite 2030. STD represents Percent standard deviation for results for each criterion. Last column includes the lap shear results in the STD calculations.

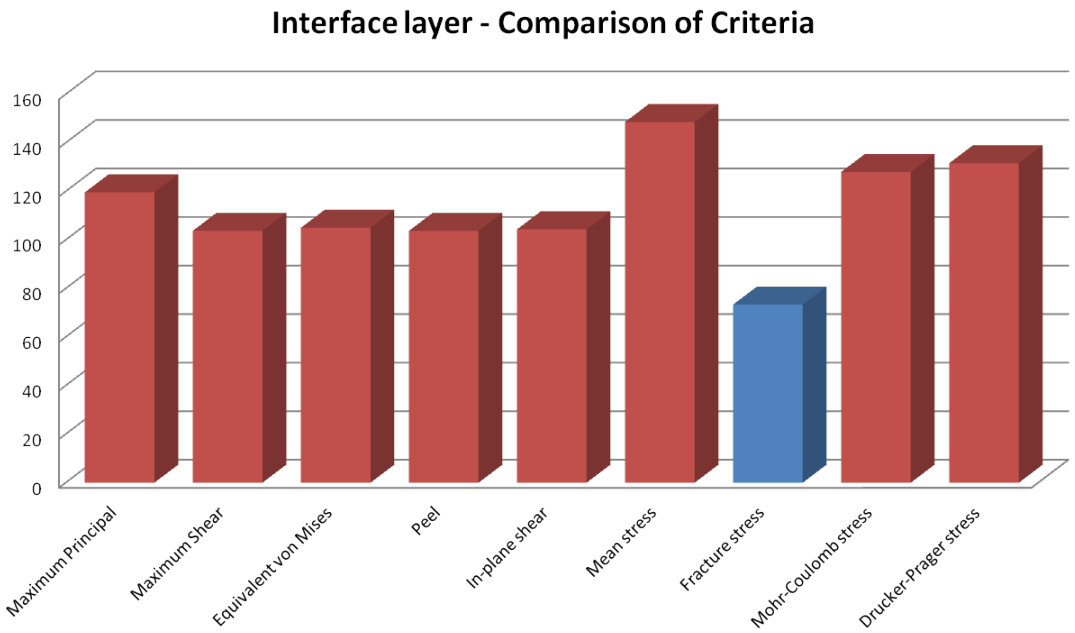

Figure 11.3: Chart showing the Percent standard deviations for various criteria for interface layer in a bar chart format to pictorially indicate how Fracture criterion outperforms the other criteria.

Chapter 12

Conclusions

12.1 Considering IBS1 tests - Same geometry different loads

1. In the center layer of the adhesive, the criterion that best describes the failure in all different load cases is the Mohr-Coulomb or the Drucker-Prager. Essentially these are Maximum shear and Von-Mises but with a factor to differentiate between tensile and compressive stresses.

2. For the top layer which has to deal with the material singularity and the small pin radius, and the bottom which also has singularity due to the 90 entrants at the adhesive and substrate interface, the Fracture stress is a good criterion because failure in this layer will be the result of a combination of Mode I & II failures (peeling and shear).

3. Compared to the Von Mises criterion in practice, the Drucker-Prager or Mohr-Couloumb criteria gives a 3-fold narrower spread in results, giving us a 1/3rd reduced Factor of Safety in comparison with Von Mises for cohesive failures.

4. Compared to the Von Mises criterion in practice, the Fracture stress criterion gives a 2-fold narrower spread in results, giving us a halved Factor of Safety in comparison with Von Mises for adhesive failures.

12.2 Considering IBS1 & lap shear results together - Different geometries different loads.

1. In the center layer of the adhesive, again the criteria that best describe the failure in test cases including the lap shear are the Mohr-Coulomb or Drucker-Prager criteria.

2. For the top and bottom locations, the Fracture stress is again the best overall.

12.3 FEM conclusions

1. The 'stresses at a distance' away from the location of stress singularities gives a more realistic estimate of stresses near the edges.

2. The rounding of the adhesive and the adherend also help avoid unrealistic steep stress gradients.

12.4 Miscellaneous conclusions

1. Results from cohesive failure tests should most likely be the same for different substrates.

2. While adhesive failures must certainly be substrate-dependent.

Chapter 13

Way of Working with Failure Criteria

This chapter tries to pictorially summarize the way of working for a simulation engineer at ASML. This is done with the help of all the conclusions drawn from the results of this research. Ideally a simulation engineer would follow the prescribed steps to calculate an allowable stress value from the tensile test data and also depending on the criterion selected. This way the engineer would be able to ascertain if the adhesive joint is safe or would fail.

13.1 Algorithm for way of working for center layer

1. Check D-P stress in center layer.
2. Compare it with nominal yield strength in cohesion obtained from tests.

13.2 Algorithm for way of working for interface layer

1. Check maximum principal stress or fracture stress at the interface.
2. Compare with adhesion strength from tests.

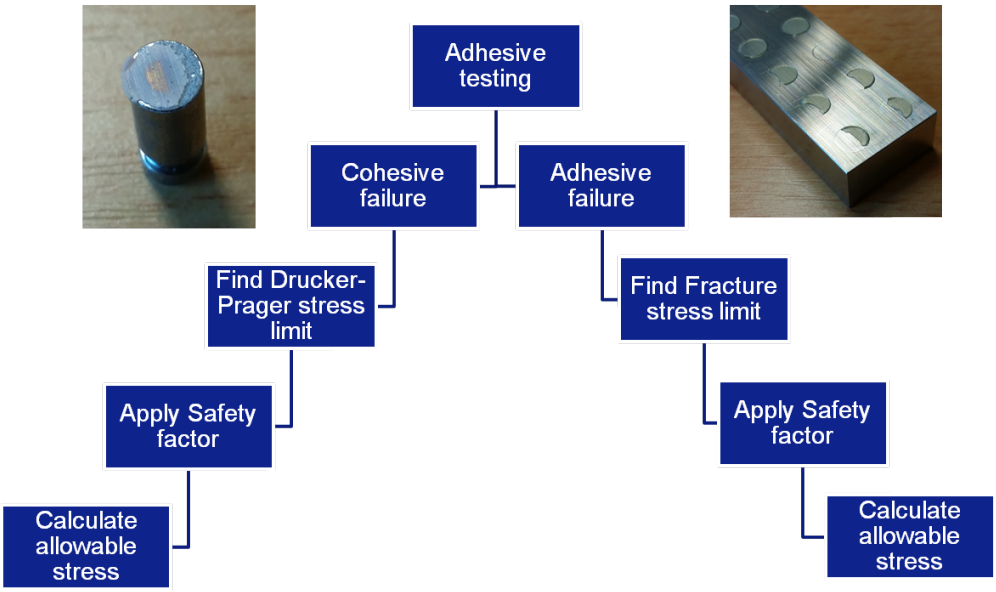

Figure 13.1: Algorithm describing way of working to obtain allowable stress for design.

Chapter 14

Overall Conclusion

"The selection of Failure criteria is dependent on the mode of failure of the joint. For cohesive failure, the Drucker-Prager criterion is recommended and for interface/adhesive failure of joints a newly developed Fracture stress criterion is recommended to be used.

The Drucker-Prager stress criterion and Fracture stress criterion need a much smaller factor of safety to be used during design in comparison with the currently used Von Mises stress criteria for adhesives at ASML. This therefore would enable more efficiently designed adhesive joints. Efficient adhesive designs are critical not only from weight optimization point of view, but are more stable in environments such as vacuum. "

Chapter 15

Future work & Recommendations

This research has explored all possibility related to linear FEM calculations. The natural step ahead would be to test the adhesives more accurately to obtain precise stress-strain curves until failure under shear testing. This would help us formulate the Extended Drucker-Prager model more accurately. Also in my opinion it would lead to better convergence for the FEM calculations. This would certainly help is narrowing the uncertainty further and lower factors of safety would be needed to be applied. Also with more precise strain measurements the strain criteria could be evaluated.

15.1 Testing

1. Lap shear is a popular test replicating reality of such joints. Alternate tests can be looked into like Arcan for instance.

2. More accurate measurement of strains need additional setting up of gages, but considering strain criteria might be interesting.

3. For bulk tests, tensile data is available through Instron, but strain data lacks accuracy because of machine strain is present in total strain.

4. Even though machine strain can be calculated, it's still approximate and can be critical while calculating Poisson's ratio. Stresses are more sensitive to Poisson's ratio.

5. Also Scotch weld yields, therefore behaves non-linearly. For accurate calculation of non-linear Poisson's ratio[24] [54], transverse stresses need to be measured using gages or probes.

15.2 FEM

1. Non-linear analysis has already been tried and is computationally very expensive. To increase the efficiency to solve models, the equivalent curve needs to be accurately calculated.

2. None the less in the quest for a more accurate failure criterion for high precision adhesive joints, not just a non-linear material model, but also difference in response of adhesive under tensile/shear/compressive loads is to be taken into account. A good example is the Drucker-Prager material model which is popularly used for polymers and soils.

Bibliography

[1] *Ansys Help 14.0*.

[2] *Minitab 17 Help*.

[3] Robert D Adams, William C Wake, and John Comyn. *Structural adhesive joints in engineering*, volume 2. Springer, 1997.

[4] W. Brockmann, P.L. GeiÃ§, J. Klingen, and B. SchrÃűder. *Adhesive Bonding: Materials, Applications and Technology*. 2009. cited By (since 1996)34.

[5] Bill Broughton. Measurement good practice guide no. 28: Durability performance of adhesive joints. *National Physical Laboratory*, 2000.

[6] Bill Broughton and Mike Gower. Measurement good practice guide no. 47: Preparation and testing of adhesive joints. *National Physical Laboratory*, 2001.

[7] WR Broughton, LE Crocker, and JM Urquhart. *Strength of adhesive joints: a parametric study*. National Physical Laboratory, 2001.

[8] WR Broughton and RD Mera. Npl report cmmt (a) 61. *Review of durability test methods and standards for assessing long term performance of adhesive joints*, 1997.

[9] Steve Abbott Bruce Duncan and Richard Roberts. Measurement good practice guide no. 26: Adhesive tack. *National Physical Laboratory*, 1999.

[10] D Castagnetti and E Dragoni. Standard finite element techniques for efficient stress analysis of adhesive joints. *International Journal of Adhesion and Adhesives*, 29(2):125–135, 2009.

[11] MN Charalambides and A Olusanya. The consititutive models suitable for adhesives in some finite element codes and suggested methods of generating the appropriate materials data. *NPL Report No. CMMT (B)*, 130, 1997.

[12] AD Crocombe and AJ Kinloch. Review of adhesive bond failure criteria, 1994.

[13] Lucas FM da Silva, Paulo JC das Neves, RD Adams, and JK Spelt. Analytical models of adhesively bonded jointsâĂŤpart i: Literature survey. *International Journal of Adhesion and Adhesives*, 29(3):319–330, 2009.

[14] Lucas FM da Silva, Paulo JC das Neves, RD Adams, A Wang, and JK Spelt. Analytical models of adhesively bonded jointsâĂŤpart ii: Comparative study. *International Journal of Adhesion and Adhesives*, 29(3):331–341, 2009.

[15] G Dean and L Crocker. The use of finite element methods for design with adhesives. August 2001.

[16] G Dean, G Lord, and B Duncan. *Comparison of the measured and predicted performance of adhesive joints under impact*. National Physical Laboratory. Great Britain, Centre for Materials Measurement and Technology, 1999.

[17] G Dean and R Mera. *Determination of material properties and parameters required for the simulation of impact performance of plastics using finite element analysis*. National Physical Laboratory, 2004.

[18] GD Dean and LE Crocker. *A proposed failure criterion for tough adhesives*. National Physical Laboratory. Great Britain, Centre for Materials Measurement and Technology, 1999.

[19] GD Dean, Bryan Eric Read, and BC Duncan. *An evaluation of yield criteria for adhesives for finite element analysis*. National Physical Laboratory, 1999.

[20] Greg Dean and Louise Crocker. Measurement good practice guide no. 48: The use of finite element methods for design with adhesives. *National Physical Laboratory*, 2001.

[21] Greg Dean and Bruce Duncan. Measurement good practice guide no. 17: Preparation and testing of bulk specimens of adhesives. *National Physical Laboratory*, 1998.

[22] David A Dillard and Alphonsus V Pocius. *The mechanics of adhesion*. Elsevier Amsterdam, 2002.

[23] Jonas Dispersyn, Jan Belis, Vincent Dias, and Christoph Odenbreit. Determination of the material properties of an epoxy and ms-polymer for adhesive point-fixings. In *COST Action TU0905, Mid-term Conference on Structural Glass*, pages 485–492. Taylor & Francis Group, 2013.

[24] BC Duncan and GD Dean. Quantifying design properties of adhesives. 2001.

[25] BC Duncan, Teddington (United Kingdom). Centre for Materials Measurement National Physical Lab., and Technology;. *Performance of Adhesive Joints Programme Project PAJ1: Failure Criteria and Their Application to Visco-elastic/visco-plastic Materials; Final Report*. National Physical Laboratory. Great Britain, Centre for Materials Measurement and Technology, 1999.

[26] Bruce Duncan and Louise Crocker. Measurement good practice guide no. 45: Characterization of flexible adhesives for design. *National Physical Laboratory*, 2001.

[27] Bruce Duncan and Louise Crocker. *Review of tests for adhesion strength*. National Physical Laboratory, 2001.

[28] Amos Gilat, Robert K Goldberg, and Gary D Roberts. Strain rate sensitivity of epoxy resin in tensile and shear loading. *Journal of Aerospace Engineering*, 20(2):75–89, 2007.

[29] Jan Godzimirski and Sławomir Tkaczuk. Numerical calculations of adhesive joints subjected to shearing. *Journal of Theoretical and Applied Mechanics - Warsaw*, 45(2):311, 2007.

[30] JPM Goncalves, MFSF De Moura, and PMST De Castro. A three-dimensional finite element model for stress analysis of adhesive joints. *International Journal of Adhesion and Adhesives*, 22(5):357–365, 2002.

[31] Hans L Groth. Viscoelastic and viscoplastic stress analysis of adhesive joints. *International Journal of Adhesion and Adhesives*, 10(3):207–213, 1990.

[32] Gerd Habenicht. *Applied adhesive bonding: A practical Guide for Flawless Results*. John Wiley & Sons, 2008.

[33] EMP Huveners, F van Herwijnen, F Soetens, and H Hofmeyer. Mechanical shear properties of adhesives. *Polyurethane*, 3(1):23, 2007.

[34] Mladen Ignjatovic, Peter Chalkley, and Chun Wang. The yield behaviour of a structural adhesive under complex loading. Technical report, DTIC Document, 1998.

[35] JP Jeandrau. Analysis and design data for adhesively bonded joints. *International Journal of Adhesion and Adhesives*, 11(2):71–79, 1991.

[36] Anthony James Kinloch. *Adhesion and adhesives: science and technology*. Springer, 1987.

[37] Ilja Malakhovsky. *GID Mechanical Design Criteria*, 2012.

[38] NPL. *Manual for the Calculation of Elastic-Plastic Materials Models Parameters*, 2007.

[39] Je Hoon Oh. Nonlinear analysis of adhesively bonded tubular single-lap joints for composites in torsion. *Composites science and technology*, 67(7):1320–1329, 2007.

[40] Je Hoon Oh. Strength prediction of tubular composite adhesive joints under torsion. *Composites science and technology*, 67(7):1340–1347, 2007.

[41] A Olusanya. A criterion of tensile failure for hyperelastic materials and its application to viscoelastic-viscoplastic materials. *NPL Report CMMT (B)*, 130, 1997.

[42] René Quispe Rodríguez, William Portilho de Paiva, Paulo Sollero, Marcelo Ricardo Bertoni Rodrigues, and Éder Lima de Albuquerque. Failure criteria for adhesively bonded joints. *International Journal of Adhesion and Adhesives*, 37:26–36, 2012.

[43] DE Richardson, GL Anderson, and DJ Macon. Improved multi-axial, temperature and time dependent (matt) failure model. 2002.

[44] Joseph Edward Shigley, Charles R Mischke, Richard G Budynas, Xiangfeng Liu, and Zhi Gao. *Mechanical engineering design*, volume 89. McGraw-Hill New York, 1989.

[45] Stanley S Smeltzer III. Paper title: Analysis method for inelastic, adhesively bonded joints with anisotropic adherends. 2003.

[46] S Srinivas. Analysis of bonded joints. Technical report, DTIC Document, 1975.

[47] Scott E Stapleton, Anthony M Waas, and Brett A Bednarcyk. Modeling progressive failure of bonded joints using a single joint finite element. *AIAA journal*, 49(8):1740–1749, 2011.

[48] Liyong Tong and Grant P Steven. Analysis and design of structural bonded joints. Technical report, Univ. of Sydney, New South Wales (AU), 1999.

[49] MY Tsai and J Morton. Three-dimensional deformations in a single-lap joint. *The Journal of Strain Analysis for Engineering Design*, 29(2):137–145, 1994.

[50] Ijsbrand Jan van Straalen. Development of design rules for structural adhesive bonded joints-a systematic approach. 2001.

[51] Richard van Wifferen. *PIR Thermal and equivalent stress in adhesive bondings*, 2003.

[52] Charles Yang, John S Tomblin, and Zhidong Guan. Analytical modeling of astm lap shear adhesive specimens. Technical report, DTIC Document, 2003.

[53] XX Yu, AD Crocombe, and G Richardson. Material modelling for rate-dependent adhesives. *International journal of adhesion and adhesives*, 21(3):197–210, 2001.

[54] M Zgoul and AD Crocombe. Numerical modelling of lap joints bonded with a rate-dependent adhesive. *International journal of adhesion and adhesives*, 24(4):355–366, 2004.

[55] Y Zhu and K Kedward. Methods of analysis and failure predictions for adhesively bonded joints of uniform and variable bondline thickness. Technical report, May 2005.

Appendices

Appendix A

Sample Adhesive joint test data

A.1 Sample test data

Shear strength test report

Date	: 07-02-2014
Operator	: Sainath
Adhesive name	: Araldite2030
Batch number	:
Layer thickness	:
Curing conditions	: 100um at corner
Storage time	: 3days cleanroom
Storage conditions	: Clean room
Material testbar	: Stainless steel
Surface treatment test bar	: from stock
Cleaning test bar	: Acetone
Material test rod	: AISI 303
Surface treatment test rod	: Sand paper_Acetone
Cleaning test rod	: acetone - scratch - acetone
Diameter test rod	: 5.00
Tensile speed	: 0.10
Sensor type	: sensor type 1
Sample frequency	: 150000.00
Remarks	:

Breakpoints: 26

1:1.13	8:1.39	15:1.41	22:1.46
2:0.86	9:1.64	16:1.42	23:1.44
3:1.10	10:1.12	17:1.71	24:1.57
4:1.56	11:1.34	18:1.16	25:1.50
5:1.50	12:1.04	19:1.43	26:1.36
6:1.37	13:1.50	20:1.67	
7:1.22	14:1.20	21:1.54	

Statistics

Characteristic life(eta)	1.46
Shape factor(beta)	7.12
max	1.71
min	0.86
Reliability 99%	0.77
Reliability 99.9%	0.55

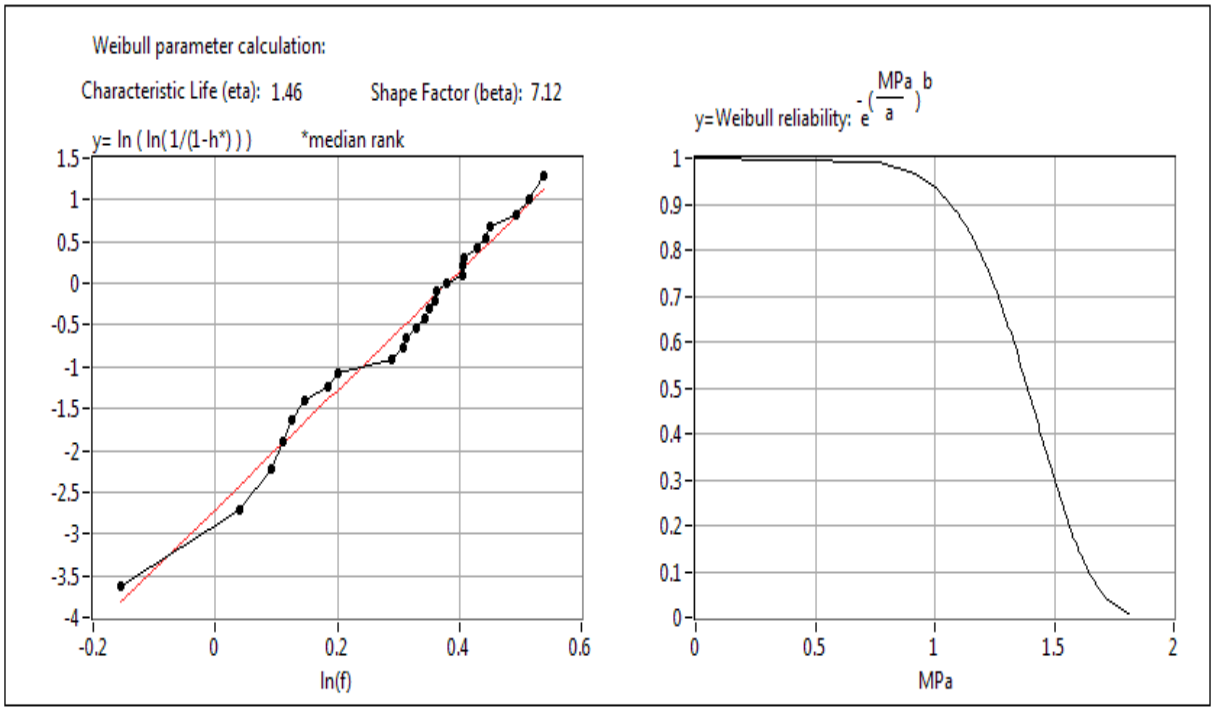

ASML

A.2 Sample Matlab code for damping correction for test data

Listing A.1: Sample Matlab code for breakpoint correction for damping

```
% function [b] = extract_data(filename)
clear all
close all
clc
fid = fopen('bend_sw_t7_cb.txt');
%%
%*****************************************************************
%*************** STRUCTURING THE TEST RESULTS   ******************
%*****************************************************************
for ii = 1:26
    b.t7_cb.sprintf('p%d',ii) = [];
end
jj = 0;
while ¬feof(fid),
  line=deblank(fgetl(fid));
  if ¬isempty(line)
      if strcmp(line(1:3), '[pr') == 1 ,
          jj = jj+1;
      end
      [data,¬,errmsg,¬]=sscanf(line,'%f');
      if isempty(errmsg),
      b.t7_cb.(sprintf('p%d',jj))= ...
          [b.t7_cb.(sprintf('p%d',jj));data(1)];
      end
  end
end
%%
%*****************************************************************
%***  BREAKPOINT CORRECTION FOR DAMPING DURING MEASUREMENT   ****
%*****************************************************************
b.t7_cb.mx = [];
b.t7_cb.bs = [];
for ii = 1:26
    [b.t7_cb.(sprintf('mx%d',ii)),id] = ...
        max(b.t7_cb.(sprintf('p%d',ii)));
        b.t7_cb.mx = [b.t7_cb.mx ; b.t7_cb.(sprintf('mx%d',ii))];
    % Initializing first 5 sample values
    sample = [0;1];
    % Updating sampled values
    while max(sample) - min(sample) > 0.5          %MPa value is ...
       critical
    sample = [];
        for kk = 1:5           %sample size is critical,normal=5,...
           other=30
        sample = [sample; b.t7_cb.(sprintf('p%d',ii))(id+kk)];
        id = id+kk;
        end
    end
    base = [];
        for mm = 1:100
        base = [base; b.t7_cb.(sprintf('p%d',ii))(id+mm)];
        end
    b.t7_cb.(sprintf('bs%d',ii)) = mean(base);
```

```
52      b.t7_cb.bs = [b.t7_cb.bs ; b.t7_cb.(sprintf('bs%d',ii))];
53      b.t7_cb.dmx = b.t7_cb.mx-b.t7_cb.bs;
54
55
56  end
57  fclose(fid);
58
59  save('t7_cb.mat','-struct','b');
```

Appendix B

Sample Matlab code for correction of stresses to identify yield

Listing B.1: Sample Matlab code for correction of stresses to identify yield

```
clear all
close all
clc
% % Find the index and value when residual increases beyond a certain...
    limit
data = cell(6,1);
data{1} = 'sw.b.t1_lk';
data{2} = 'sw.b.t2_lk';
data{3} = 'sw.b.t3_lk';
data{4} = 'sw.b.t4_lk';
data{5} = 'sw.b.t5';
data{6} = 'sw.b.t6';
data{7} = 'sw.b.t7_cb';
data{8} = 'sw.b.t8_cb_01';
load('db_test_backup_for_restore.mat');
h = waitbar(0,'Please wait...');
counter = 0;
for ii = 5
    for jj = 5
        counter = counter+1;
        waitbar(counter/208);
        filnam = strcat(data{ii},sprintf('.p%d',jj));
        col = eval(filnam);
        figure(1);
        plot(col,'*-');
        hold on;
        [maximus,idx] = max(col);
        sz = length(col);
        strain_lc = 0.008;
        B = (0:strain_lc:((idx-1)*strain_lc))';
        A = col(1:idx);
        coll_1 = A(A>0.6);%select pts between 1 and the max
        xx_start = find(A == coll_1(1));
        xx = B(xx_start:(end));
        y = coll_1(coll_1(1) & coll_1<0.65*coll_1(end));
        x_end = find(A == y(end));
        x = B(xx_start:x_end);
        [poly,struct] = polyfit(x,y,1);
        [yfit,Δ] = polyval(poly,xx,struct);
        x_intercept = roots(poly);
        diff = abs(yfit-coll_1);
        w = xx(length(x)+1:length(xx));
        z = coll_1(length(x)+1:length(xx));
```

```
43          [poly2,struct2] = polyfit(w,z,1);
44          [yfit2,a2] = polyval(poly2,xx,struct2);
45          poly_pl = [poly(1),-(poly(1)*(x_intercept+0.002))];%proof ...
                stress line
46          plasticity_curve = polyval(poly_pl,xx);
47          figure(2)
48          plot(x,y,'*b')
49          hold on;
50          plot(xx,yfit,'-g');
51          hold on;
52          plot(xx,plasticity_curve,'-+m');
53          hold on;
54          plot(w,coll_1(length(x)+1:length(xx)),'*r');
55          hold on;
56          plot(xx,yfit2,'-+k');
57          hold on;
58          if (atan(poly_pl(1))-atan(poly2(1)))*180/pi > 0.1   %angle ...
                difference for plasticity
59              %new better modified intersection
60              inter = find(abs(flipud(yfit2) - flipud(plasticity_curve)...
                    ) < 0.254, 1);
61              flip_xx = flipud(xx);
62              flip_yfit2 = flipud(yfit2);
63              px = flip_xx(inter);
64              py = flip_yfit2(inter);
65              coll_2 = A(A<py);
66              eval(strcat('dbb.',data{ii},sprintf('.cmx(%d,1) = coll_2...
                    (end);',jj))) %the corrected max values for bending
67              %that crucial point
68              iiidx = find(A == coll_2(end));
69              plotx = B(iiidx);
70              plot(plotx,coll_2(end),'o');
71          else
72              eval(strcat('dbb.',data{ii},sprintf('.cmx(%d,1) = coll_1...
                    (end);',jj)))
73          end
74          %some output to monitor
75          angle(jj,ii) = (atan(poly_pl(1))-atan(poly2(1)))*180/pi;
76      end
77  end
78  close(h);
79  % %%%
80  % %%%Comparison charts to see which values were corrected
81  for kk = 1:4
82  figure(kk+2)
83  plot(eval(sprintf('dbb.sw.b.t%d_lk.cmx-sw.b.t%d_lk.bs',kk,kk)),'*r');
84  hold on;
85  plot(eval(sprintf('sw.b.t%d_lk.dmx',kk)),'ob');
86  end
87  for kk = 5:6
88  figure(kk+2)
89  plot(eval(sprintf('dbb.sw.b.t%d.cmx-sw.b.t%d.bs',kk,kk)),'*r');
90  hold on;
91  plot(eval(sprintf('sw.b.t%d.dmx',kk)),'ob');
92  end
93  %%%%%%%%%%%%%%%
94  %%%%%%%%%%%%%%%
95  data{1} = 'ar.b.t1_lk';
96  data{2} = 'ar.b.t2_lk';
```

```
97  data{3} = 'ar.b.t3_lk';
98  data{4} = 'ar.b.t4_lk';
99  data{5} = 'ar.b.t5_lk';
100 data{6} = 'ar.b.t6_lk';
101 data{7} = 'ar.b.t7_cb';
102 data{8} = 'ar.b.t8_cb_01';
103 h = waitbar(0,'Please wait...');
104 counter = 0;
105 for ii = 1:8
106     for jj = 1:26
107         counter = counter+1;
108         waitbar(counter/208);
109         filnam = strcat(data{ii},sprintf('.p%d',jj));
110         col = eval(filnam);
111         figure(1);
112         plot(col,'*-');
113         hold on;
114         [maximus,idx] = max(col);
115         sz = length(col);
116         strain_lc = 0.008;
117         B = (0:strain_lc:((idx-1)*strain_lc))';
118         A = col(1:idx);
119         coll_1 = A(A>0.27);%select pts between 1 and the max
120         xx_start = find(A == coll_1(1));
121         xx = B(xx_start:end);
122         y = coll_1(coll_1(1) & coll_1<0.65*coll_1(end));
123         x_end = find(A == y(end));
124         x = B(xx_start:x_end);
125         [poly,struct] = polyfit(x,y,1);
126         [yfit,Δ] = polyval(poly,xx,struct);
127         x_intercept = roots(poly);
128         diff = abs(yfit-coll_1);
129         w = xx(length(x)+1:length(xx));
130         z = coll_1(length(x)+1:length(xx));
131         [poly2,struct2] = polyfit(w,z,1);%second order polynomial
132         [yfit2,Δ2] = polyval(poly2,xx,struct2);
133         poly_pl = [poly(1),-(poly(1)*(x_intercept+0.002))];%proof ...
              stress line
134         plasticity_curve = polyval(poly_pl,xx);
135         figure(2)
136         plot(x,y,'*b')
137         hold on;
138         plot(xx,yfit,'-g');
139         hold on;
140         plot(xx,plasticity_curve,'-+m');
141         hold on;
142         plot(w,coll_1(length(x)+1:length(xx)),'*r');
143         hold on;
144         plot(xx,yfit2,'-+k');
145         hold on;
146         if (atan(poly_pl(1))-atan(poly2(1)))*180/pi > 0.2
147             %new better modified intersection
148             inter = find(abs(yfit2 - plasticity_curve) < 0.419, 1);
149             px = xx(inter);
150             py = yfit2(inter);
151             coll_2 = A(A<py);
152             eval(strcat('dbb.',data{ii},sprintf('.cmx(%d,1) = coll_2...
                  (end);',jj))) %the corrected max values for bending
153             %that crucial point
```

```
154                 iiidx = find(A == coll_2(end));
155                 plotx = B(iiidx);
156                 plot(plotx,coll_2(end),'o');
157             else
158                 eval(strcat('dbb.',data{ii},sprintf('.cmx(%d,1) = coll_1...
                        (end);',jj)))
159             end
160             %some output to monitor
161             angle(jj,ii) = (atan(poly_pl(1))-atan(poly2(1)))*180/pi;
162         end
163     end
164     close(h);
165     %%%
166     %%%Comparison charts to see which values were corrected
167     for kk = 1:6
168     figure(kk+2)
169     plot(eval(sprintf('dbb.ar.b.t%d_lk.cmx-ar.b.t%d_lk.bs',kk,kk)),'*r');
170     hold on;
171     plot(eval(sprintf('ar.b.t%d_lk.dmx',kk)),'ob');
172     end
173     %%%%%%%%%%%%%%%
174     %%%%%%%%%%%%%%%
175     db.ar = ar;
176     db.sw = sw;
177     db.sw.b.t1_lk.cmx = dbb.sw.b.t1_lk.cmx;
178     db.sw.b.t2_lk.cmx = dbb.sw.b.t2_lk.cmx;
179     db.sw.b.t3_lk.cmx = dbb.sw.b.t3_lk.cmx;
180     db.sw.b.t4_lk.cmx = dbb.sw.b.t4_lk.cmx;
181     db.sw.b.t5.cmx = dbb.sw.b.t5.cmx;
182     db.sw.b.t6.cmx = dbb.sw.b.t6.cmx;
183     db.sw.b.t7_cb.cmx = dbb.sw.b.t7_cb.cmx;
184     db.sw.b.t8_cb_01.cmx = dbb.sw.b.t8_cb_01.cmx;
185     % % %
186     db.ar.b.t1_lk.cmx = dbb.ar.b.t1_lk.cmx;
187     db.ar.b.t2_lk.cmx = dbb.ar.b.t2_lk.cmx;
188     db.ar.b.t3_lk.cmx = dbb.ar.b.t3_lk.cmx;
189     db.ar.b.t4_lk.cmx = dbb.ar.b.t4_lk.cmx;
190     db.ar.b.t5_lk.cmx = dbb.ar.b.t5_lk.cmx;
191     db.ar.b.t6_lk.cmx = dbb.ar.b.t6_lk.cmx;
192     db.ar.b.t7_cb.cmx = dbb.ar.b.t7_cb.cmx;
193     db.ar.b.t8_cb_01.cmx = dbb.ar.b.t8_cb_01.cmx;
194     % % %
195     save('db_test.mat','-struct','db');
```

Appendix C

Sample Matlab code for identifying outliers in data

Listing C.1: Sample Matlab code for identifying outliers in data

```
clear all
close all
clc
%
load('shr_test.mat');
load('ten_test.mat');
load('tor_test.mat');
load('lap_test.mat');
load('bnd_test.mat');
%
mean_shr_test = mean(shr_test,1);
mean_ten_test = mean(ten_test,1);
mean_tor_test = mean(tor_test,1);
mean_lap_test = mean(lap_test,1);
mean_bnd_test = mean(bnd_test,1);
%
stdev_shr_test = std(shr_test,1);
stdev_ten_test = std(ten_test,1);
stdev_tor_test = std(tor_test,1);
stdev_lap_test = std(lap_test,1);
stdev_bnd_test = std(bnd_test,1);
%
m1std_shr_test_high = mean_shr_test + stdev_shr_test;
m1std_shr_test_low = mean_shr_test - stdev_shr_test;
m1std_ten_test_high = mean_ten_test + stdev_ten_test;
m1std_ten_test_low = mean_ten_test - stdev_ten_test;
m1std_tor_test_high = mean_tor_test + stdev_tor_test;
m1std_tor_test_low = mean_tor_test - stdev_tor_test;
m1std_lap_test_high = mean_lap_test + stdev_lap_test;
m1std_lap_test_low = mean_lap_test - stdev_lap_test;
m1std_bnd_test_high = mean_bnd_test + stdev_bnd_test;
m1std_bnd_test_low = mean_bnd_test - stdev_bnd_test;
%
logical_array_shr_test =¬ (shr_test > m1std_shr_test_low & shr_test <...
    m1std_shr_test_high);
rows_keep = logical_array_shr_test == 0;
shr_test_m1std = shr_test(rows_keep,:);
stdev_shr_test_m1std = std(shr_test_m1std,1);
save('shr_test_m1std.mat','shr_test_m1std');
%
logical_array_ten_test =¬ (ten_test > m1std_ten_test_low & ten_test <...
    m1std_ten_test_high);
rows_keep = logical_array_ten_test == 0;
```

```
ten_test_m1std = ten_test(rows_keep,:);
stdev_ten_test_m1std = std(ten_test_m1std,1);
save('ten_test_m1std.mat','ten_test_m1std');
%
logical_array_tor_test =¬ (tor_test > m1std_tor_test_low & tor_test <...
    m1std_tor_test_high);
rows_keep = logical_array_tor_test == 0;
tor_test_m1std = tor_test(rows_keep,:);
stdev_tor_test_m1std = std(tor_test_m1std,1);
save('tor_test_m1std.mat','tor_test_m1std');
%
logical_array_lap_test =¬ (lap_test > m1std_lap_test_low & lap_test <...
    m1std_lap_test_high);
rows_keep = logical_array_lap_test == 0;
lap_test_m1std = lap_test(rows_keep,:);
stdev_lap_test_m1std = std(lap_test_m1std,1);
save('lap_test_m1std.mat','lap_test_m1std');
%
logical_array_bnd_test =¬ (bnd_test > m1std_bnd_test_low & bnd_test <...
    m1std_bnd_test_high);
rows_keep = logical_array_bnd_test == 0;
bnd_test_m1std = bnd_test(rows_keep,:);
stdev_bnd_test_m1std = std(bnd_test_m1std,1);
save('bnd_test_m1std.mat','bnd_test_m1std');
%
save('stdev.mat');
%%%
%%%
f = figure('Position',[200 240 350 300]);
stdev = {stdev_shr_test;...
    %
        stdev_ten_test;...
    %
        stdev_tor_test/((pin_dia/2)*pin_area*1e6);...
    %
        stdev_lap_test;...
    %
        stdev_bnd_test};
    %
cnames = {'Test Standard Deviation'};
rnames = {'Shear','Tension','Torsion',...
    'Lap Shear','Bending'};
t = uitable('Parent',f,'Data',stdev,'ColumnName',cnames,...
            'RowName',rnames,'Position',[20 20 300 280]);
        saveas(gcf,'stdev_test','png');
```

Appendix D

Matlab code for Drucker-Prager calculations

Listing D.1: Matlab code for Drucker-Prager calculations

```
clear all
close all
clc
%%  SHEAR STUFF
%   NOTE: there is no tru strain and stress in this case
load('db_bulk_test.mat')
nom_strain_shr = db.sw.shr(:,1);
nom_stress_shr = db.sw.shr(:,2);
figure(1);
axes('FontSize',10);
nom_modulus_shr = polyfitZero(nom_strain_shr(1:15),nom_stress_shr...
    (1:15)*1e6,1);
func_shr = @(x) nom_modulus_shr(1)*x + 0;
[maximus_shr,id_shr] = max(nom_stress_shr*1e6);
x_new_shr = nom_strain_shr(1:id_shr);
y_new_shr = nom_stress_shr(1:id_shr)*1e6;
plot(nom_strain_shr(1:id_shr),nom_stress_shr(1:id_shr)*1e6,'+-b')
title('Shear test data')
xlabel('Strain');
ylabel('Stress (Pa)');
hold on
fplot(func_shr,[x_new_shr(1) x_new_shr(end)],2e-3,'r');
axis([0 0.2 0 3.5e7])
hold on
c_shr = -nom_modulus_shr(1)*0.002;
func_yield_shr = @(x) nom_modulus_shr(1)*x + c_shr;
fplot(func_yield_shr,[x_new_shr(1) x_new_shr(end)],2e-3,'c');
hold on
%
offset_shr = [nom_modulus_shr(1) c_shr];
fn_pts_shr = polyval(offset_shr,x_new_shr);
yield_idx_shr = find(flipud(fn_pts_shr) - flipud(y_new_shr) < 0.1e7, ...
    1);
plot(x_new_shr(length(x_new_shr)-yield_idx_shr),y_new_shr(length(...
    y_new_shr)-yield_idx_shr),'pk');
saveas(gcf,'shear_data','png');
hold off;
yield_shr = y_new_shr(length(y_new_shr)-yield_idx_shr);
nom_plastic_strain_shr = [0; x_new_shr(21:end)] - [0;y_new_shr(21:end...
    )/nom_modulus_shr(1)];
nom_plastic_stress_shr = y_new_shr(20:end);
%%  TENSILE STUFF
nom_strain_ten = db.sw.ten(:,1);
```

```
nom_stress_ten = db.sw.ten(:,2);
nom_poisson_ten = -0.429;
tru_strain_ten = log(1+nom_strain_ten);
tru_stress_ten = nom_stress_ten./(1-(nom_poisson_ten*nom_strain_ten)).^2;
figure(2);
axes('FontSize',10);
tru_modulus_ten = polyfitZero(tru_strain_ten(1:15),tru_stress_ten(1:15)*1e6,1);
func_ten = @(x) tru_modulus_ten(1)*x + 0;
[maximus_ten,id_ten] = max(tru_stress_ten*1e6);
x_new_ten = tru_strain_ten(1:id_ten);
y_new_ten = tru_stress_ten(1:id_ten)*1e6;
plot(tru_strain_ten(1:id_ten),tru_stress_ten(1:id_ten)*1e6,'+-b')
title('Tensile test data')
xlabel('Strain');
ylabel('Stress (Pa)');
hold on
fplot(func_ten,[x_new_ten(1) x_new_ten(end)],2e-3,'r');
axis([0 0.025 0 5e7])
hold on
c_ten = -tru_modulus_ten(1)*0.002;
func_yield_ten = @(x) tru_modulus_ten(1)*x + c_ten;
fplot(func_yield_ten,[x_new_ten(1) x_new_ten(end)],100,'c');
hold on
%
offset_ten = [tru_modulus_ten(1) c_ten];
fn_pts_ten = polyval(offset_ten,x_new_ten);
yield_idx_ten = find(flipud(fn_pts_ten) - flipud(y_new_ten) < 0.5e6, ...
    1);
plot(x_new_ten(length(x_new_ten)-yield_idx_ten),y_new_ten(length(...
    y_new_ten)-yield_idx_ten),'pk');
saveas(gcf,'tensile_data','png');
hold off;
yield_ten = y_new_ten(length(y_new_ten)-yield_idx_ten);
tru_plastic_strain_ten = [0; x_new_ten(29:end)] - [0;y_new_ten(29:end...
    )/tru_modulus_ten(1)];
tru_plastic_stress_ten = y_new_ten(28:end);
figure(3);
axes('FontSize',10);
shr_pts = (nom_plastic_stress_shr).*nom_plastic_strain_shr;
ten_pts = (tru_plastic_stress_ten).*tru_plastic_strain_ten;
plot(shr_pts,shr_pts,'+b')
hold on;
plot(ten_pts,ten_pts,'.r')
title('Data analysis (stress v/s plastic strain)')
xlabel('Plastic strain');
ylabel('Stress (Pa)');
saveas(gcf,'eqv_points','png');
%%  Plotting of the points on the graph
figure(4);
axes('FontSize',10);
plot(nom_plastic_strain_shr,nom_plastic_stress_shr,'b');
hold on
plot(tru_plastic_strain_ten,tru_plastic_stress_ten,'r');
hold on
%
% plot(nom_plastic_strain_shr(3),nom_plastic_stress_shr(3),'dr');
% hold on;
```

```
% plot(nom_plastic_strain_shr(6),nom_plastic_stress_shr(6),'dr');
% hold on;
% plot(nom_plastic_strain_shr(8),nom_plastic_stress_shr(8),'dr');
% hold on;
% plot(nom_plastic_strain_shr(9),nom_plastic_stress_shr(9),'dr');
% hold on;
% plot(nom_plastic_strain_shr(12),nom_plastic_stress_shr(12),'dr');
% hold on;
% plot(nom_plastic_strain_shr(14),nom_plastic_stress_shr(14),'dr');
% hold on;
% plot(nom_plastic_strain_shr(17),nom_plastic_stress_shr(17),'dr');
% hold on;
% plot(nom_plastic_strain_shr(21),nom_plastic_stress_shr(21),'dr');
% hold on;
% plot(nom_plastic_strain_shr(22),nom_plastic_stress_shr(22),'dr');
% hold on;
% %
% plot(tru_plastic_strain_ten(23),tru_plastic_stress_ten(23),'sr');
% hold on;
% plot(tru_plastic_strain_ten(25),tru_plastic_stress_ten(25),'sr');
% hold on;
% plot(tru_plastic_strain_ten(26),tru_plastic_stress_ten(26),'sr');
% hold on;
% plot(tru_plastic_strain_ten(28),tru_plastic_stress_ten(28),'sr');
% hold on;
% plot(tru_plastic_strain_ten(32),tru_plastic_stress_ten(32),'sr');
% hold on;
% plot(tru_plastic_strain_ten(35),tru_plastic_stress_ten(35),'sr');
% hold on;
% plot(tru_plastic_strain_ten(38),tru_plastic_stress_ten(38),'sr');
% hold on;
% plot(tru_plastic_strain_ten(47),tru_plastic_stress_ten(47),'sr');
% hold on;
% plot(tru_plastic_strain_ten(50),tru_plastic_stress_ten(50),'sr');
% hold on;
%%
tru_plastic_stress_eff = sqrt(3)*nom_plastic_stress_shr;
tru_plastic_strain_eff = (1/sqrt(3))*nom_plastic_strain_shr;
plot(tru_plastic_strain_eff,tru_plastic_stress_eff,'c');
legend('Shear','Tensile','Effective','location','best');
title('Effective plastic stress strain diagram')
xlabel('Plastic Strain');
ylabel('Stress (Pa)');
saveas(gcf,'eff_stress_plasticstrain','png');
%% PRODUCE TABLE
set_tensile = [8;14;18;25];
set_shear = [2;3;4;5];
table_stress_ten = [];
table_stress_shr = [];
for ii = 1:4
table_stress_ten = [table_stress_ten;tru_plastic_stress_ten(...
    set_tensile(ii))];
table_stress_shr = [table_stress_shr;nom_plastic_stress_shr(set_shear...
    (ii))];
end
ratio = table_stress_ten./table_stress_shr;
alpha = 3*((sqrt(3)*(1./ratio))-1);
alpha = alpha(:);
lambda = 3*(1./ratio).^2;
```

```
151 a = 1./(3*table_stress_ten.*(lambda-1));
152 %%
153 E = 2.45e9;
154 ansys_x = [0;tru_plastic_stress_eff(1)/E];
155 for jj = 2:6
156     ansys_x = [ansys_x; (tru_plastic_stress_eff(jj)/E)+...
            tru_plastic_strain_eff(jj)];
157 end
158 ansys_y = [0; tru_plastic_stress_eff];
159 figure(5)
160 axes('FontSize',10);
161 plot(ansys_x,ansys_y)
162 title('Effective stress strain curve fed into Ansys')
163 xlabel('Strain');
164 ylabel('Stress (Pa)');
165 saveas(gcf,'eff_stress_strain_ansys','png');
```

To formulate the equivalent stress-strain curve for extended Drucker-Prager we need to combine the data from shear and tensile tests. The shear test data for bulk specimen is plotted in Fig. D.1.

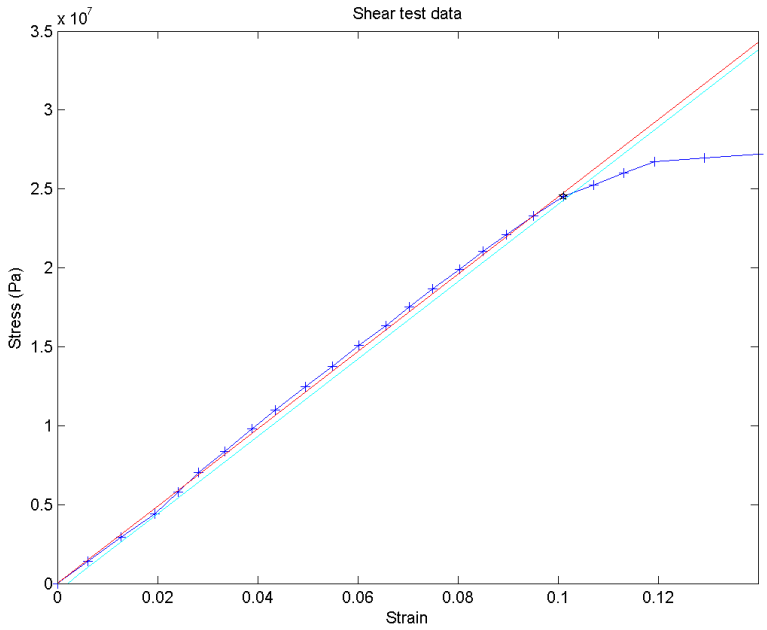

Figure D.1: Shear test data.

The tensile test data for bulk sample tested at same strain rate as the shear test is plotted in Fig. D.2.

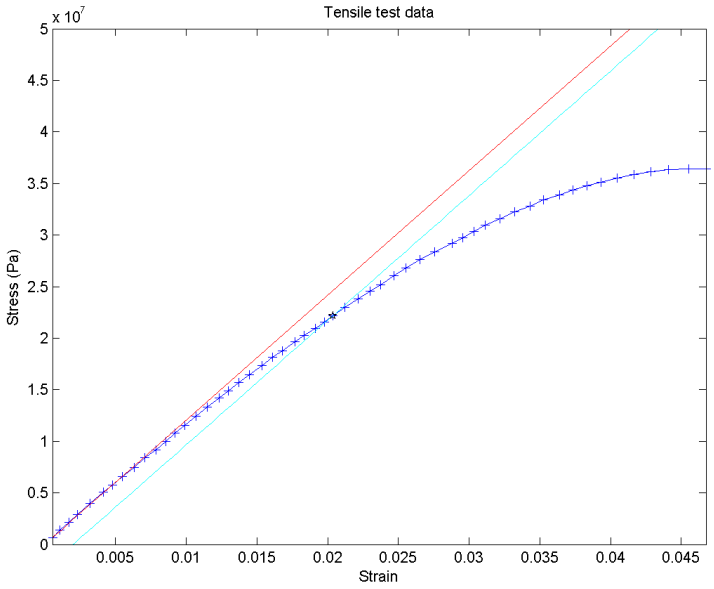

Figure D.2: Tensile test data.

Equivalent data points marked by blue crosses in Fig. D.3 are identified to be used in further calculations. The yield stress values used in the calculations must correspond to the same effective plastic strain.

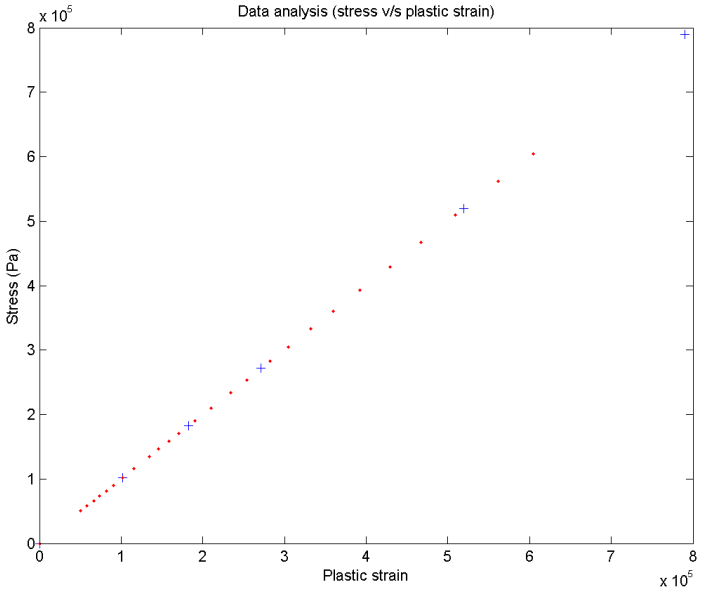

Figure D.3: Equivalent data points marked by blue crosses.

The equivalent stress curve is plotted for corresponding plastic strain.

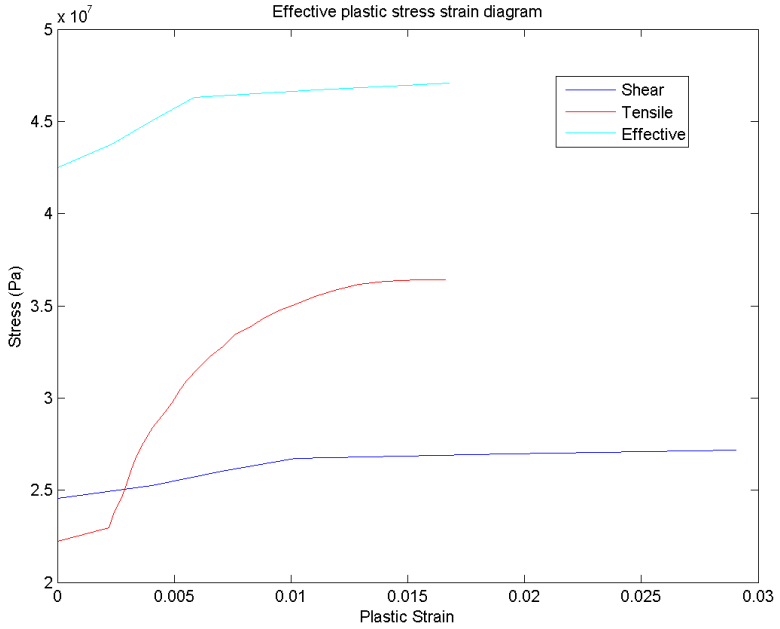

Figure D.4: Tensile, shear & equivalent stress v/s plastic strain.

The entire effective stress-strain curved to be used as the Extended Drucker-Prager material model is shown in Fig. D.5.

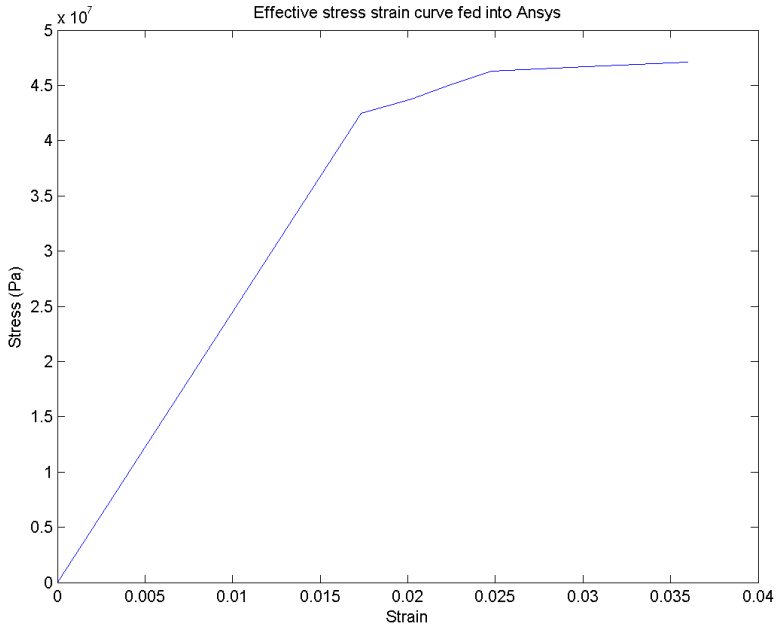

Figure D.5: Equivalent stress v/s strain to be into Ansys.

Appendix E

Sample Matlab code for reading of stresses from Ansys to Matlab

Listing E.1: Sample Matlab code for reading of stresses from Ansys to Matlab

```
%%Change the path names before running the file
clear all
close all
clc
%
fid=fopen('b2_comp.txt');
lap_b2_s=[];
lap_b2_sx=[];
lap_b2_sy=[];
lap_b2_sz=[];
lap_b2_sxy=[];
lap_b2_syz=[];
lap_b2_sxz=[];
while ¬feof(fid),
  line=deblank(fgetl(fid));
  if ¬isempty(line),
    [data,count,errmsg,nextindex]=sscanf(line,'%f %f %f %f %f %f %f'...
       ,7);
    if isempty(errmsg),
      lap_b2_s=[lap_b2_s;data(1)];
      lap_b2_sx=[lap_b2_sx;data(2)];
      lap_b2_sy=[lap_b2_sy;data(3)];
      lap_b2_sz=[lap_b2_sz;data(4)];
      lap_b2_sxy=[lap_b2_sxy;data(5)];
      lap_b2_syz=[lap_b2_syz;data(6)];
      lap_b2_sxz=[lap_b2_sxz;data(7)];
    end
  end
end
status=fclose(fid);
%
fid=fopen('b2_prin.txt');
lap_b2_s=[];
lap_b2_s1=[];
lap_b2_s2=[];
lap_b2_s3=[];
lap_b2_sint=[];
lap_b2_seqv=[];
while ¬feof(fid),
  line=deblank(fgetl(fid));
  if ¬isempty(line),
    [data,count,errmsg,nextindex]=sscanf(line,'%f %f %f %f %f %f',6);
    if isempty(errmsg),
```

```
43        lap_b2_s=[lap_b2_s;data(1)];
44        lap_b2_s1=[lap_b2_s1;data(2)];
45        lap_b2_s2=[lap_b2_s2;data(3)];
46        lap_b2_s3=[lap_b2_s3;data(4)];
47        lap_b2_sint=[lap_b2_sint;data(5)];
48        lap_b2_seqv=[lap_b2_seqv;data(6)];
49      end
50    end
51  end
52  status=fclose(fid);
53  %
54  save('lap_b2.mat','lap_b2_s','lap_b2_sx','lap_b2_sy','lap_b2_sz',...
55      'lap_b2_sxy','lap_b2_syz','lap_b2_sxz','lap_b2_s1','lap_b2_s2',...
            ...
56      'lap_b2_s3','lap_b2_sint','lap_b2_seqv');
```

Appendix F

Sample Matlab code for finding maximum value

Listing F.1: Sample Matlab code for finding maximum value

```
clear all
close all
clc
%% Peak calculations from ANSYS
load('lap_t.mat');
lap_t_s1_pk = max(abs(lap_t_s1(4005:5997)));
lap_t_mxshr_pk = max(abs(lap_t_mxshr(4005:5997)));
lap_t_seqv_pk = max(abs(lap_t_seqv(4005:5997)));
lap_t_peel_pk = max(abs(lap_t_peel(4005:5997)));
lap_t_ipmxshr_pk = max(lap_t_ipmxshr(4005:5997));
lap_t_mnstr_pk = max(lap_t_mnstr(4005:5997));
lap_t_lee_pk = max(lap_t_lee(4005:5997));
lap_t_frac_pk = max(lap_t_frac(4005:5997));
lap_t_mc_pk = max(lap_t_mc(4005:5997));
lap_t_dp_pk = max(lap_t_dp(4005:5997));
save('lap_pk.mat','lap_t_s1_pk','lap_t_mxshr_pk','lap_t_seqv_pk',...
    'lap_t_peel_pk','lap_t_ipmxshr_pk','lap_t_mnstr_pk','lap_t_lee_pk...
        ',...
    'lap_t_frac_pk','lap_t_mc_pk','lap_t_dp_pk');
%
clear all
close all
clc
%
load('lap_mid.mat');
lap_mid_s1_pk = max(abs(lap_mid_s1));
lap_mid_mxshr_pk = max(abs(lap_mid_mxshr));
lap_mid_seqv_pk = max(abs(lap_mid_seqv));
lap_mid_peel_pk = max(abs(lap_mid_peel));
lap_mid_ipmxshr_pk = max(lap_mid_ipmxshr);
lap_mid_mnstr_pk = max(lap_mid_mnstr);
lap_mid_lee_pk = max(lap_mid_lee);
lap_mid_frac_pk = max(lap_mid_frac);
lap_mid_mc_pk = max(lap_mid_mc);
lap_mid_dp_pk = max(lap_mid_dp);
save('lap_pk.mat','lap_mid_s1_pk','lap_mid_mxshr_pk','lap_mid_seqv_pk...
    ',...
    'lap_mid_peel_pk','lap_mid_ipmxshr_pk','lap_mid_mnstr_pk',...
    'lap_mid_lee_pk','lap_mid_frac_pk','lap_mid_mc_pk','lap_mid_dp_pk...
        ','-append');
%
clear all
close all
```

```
clc
%
load('lap_b.mat');
lap_b_s1_pk = max(abs(lap_b_s1(5:1997)));
lap_b_mxshr_pk = max(abs(lap_b_mxshr(5:1997)));
lap_b_seqv_pk = max(abs(lap_b_seqv(5:1997)));
lap_b_peel_pk = max(abs(lap_b_peel(5:1997)));
lap_b_ipmxshr_pk = max(lap_b_ipmxshr(5:1997));
lap_b_mnstr_pk = max(lap_b_mnstr(5:1997));
lap_b_lee_pk = max(lap_b_lee(5:1997));
lap_b_frac_pk = max(lap_b_frac(5:1997));
lap_b_mc_pk = max(lap_b_mc(5:1997));
lap_b_dp_pk = max(lap_b_dp(5:1997));
save('lap_pk.mat','lap_b_s1_pk','lap_b_mxshr_pk','lap_b_seqv_pk',...
    'lap_b_peel_pk','lap_b_ipmxshr_pk','lap_b_mnstr_pk',...
    'lap_b_lee_pk','lap_b_frac_pk','lap_b_mc_pk','lap_b_dp_pk','-...
       append');
%%
clear all
close all
clc
%
load('lap_pk.mat');
load('../../print_table/test_results_analysis_outlies/lap_test_m3std'...
    );
load('../../print_table/test_results_analysis_outlies/...
    lap_pl_test_m3std');
%% Ultimate failure
ansys_force = 1000;
lap_fact = lap_test_m3std/ansys_force;
lap_t_s1_array = lap_t_s1_pk * lap_fact;
lap_t_mxshr_array = lap_t_mxshr_pk * lap_fact;
lap_t_seqv_array = lap_t_seqv_pk * lap_fact;
lap_t_peel_array = lap_t_peel_pk * lap_fact;
lap_t_ipmxshr_array = lap_t_ipmxshr_pk * lap_fact;
lap_t_mnstr_array = lap_t_mnstr_pk * lap_fact;
lap_t_lee_array = lap_t_lee_pk * lap_fact;
lap_t_frac_array = lap_t_frac_pk * lap_fact;
lap_t_mc_array = lap_t_mc_pk * lap_fact;
lap_t_dp_array = lap_t_dp_pk * lap_fact;
lap_mid_s1_array = lap_mid_s1_pk * lap_fact;
lap_mid_mxshr_array = lap_mid_mxshr_pk * lap_fact;
lap_mid_seqv_array = lap_mid_seqv_pk * lap_fact;
lap_mid_peel_array = lap_mid_peel_pk * lap_fact;
lap_mid_ipmxshr_array = lap_mid_ipmxshr_pk * lap_fact;
lap_mid_mnstr_array = lap_mid_mnstr_pk * lap_fact;
lap_mid_lee_array = lap_mid_lee_pk * lap_fact;
lap_mid_frac_array = lap_mid_frac_pk * lap_fact;
lap_mid_mc_array = lap_mid_mc_pk * lap_fact;
lap_mid_dp_array = lap_mid_dp_pk * lap_fact;
lap_b_s1_array = lap_b_s1_pk * lap_fact;
lap_b_mxshr_array = lap_b_mxshr_pk * lap_fact;
lap_b_seqv_array = lap_b_seqv_pk * lap_fact;
lap_b_peel_array = lap_b_peel_pk * lap_fact;
lap_b_ipmxshr_array = lap_b_ipmxshr_pk * lap_fact;
lap_b_mnstr_array = lap_b_mnstr_pk * lap_fact;
lap_b_lee_array = lap_b_lee_pk * lap_fact;
lap_b_frac_array = lap_b_frac_pk * lap_fact;
lap_b_mc_array = lap_b_mc_pk * lap_fact;
```

```
97  lap_b_dp_array = lap_b_dp_pk * lap_fact;
98  %% Yield failure
99  lap_pl_fact = lap_pl_test_m3std/ansys_force;
100 lap_t_s1_pl_array = lap_t_s1_pk * lap_pl_fact;
101 lap_t_mxshr_pl_array = lap_t_mxshr_pk * lap_pl_fact;
102 lap_t_seqv_pl_array = lap_t_seqv_pk * lap_pl_fact;
103 lap_t_peel_pl_array = lap_t_peel_pk * lap_pl_fact;
104 lap_t_ipmxshr_pl_array = lap_t_ipmxshr_pk * lap_pl_fact;
105 lap_t_mnstr_pl_array = lap_t_mnstr_pk * lap_pl_fact;
106 lap_t_lee_pl_array = lap_t_lee_pk * lap_pl_fact;
107 lap_t_frac_pl_array = lap_t_frac_pk * lap_pl_fact;
108 lap_t_mc_pl_array = lap_t_mc_pk * lap_pl_fact;
109 lap_t_dp_pl_array = lap_t_dp_pk * lap_pl_fact;
110 lap_mid_s1_pl_array = lap_mid_s1_pk * lap_pl_fact;
111 lap_mid_mxshr_pl_array = lap_mid_mxshr_pk * lap_pl_fact;
112 lap_mid_seqv_pl_array = lap_mid_seqv_pk * lap_pl_fact;
113 lap_mid_peel_pl_array = lap_mid_peel_pk * lap_pl_fact;
114 lap_mid_ipmxshr_pl_array = lap_mid_ipmxshr_pk * lap_pl_fact;
115 lap_mid_mnstr_pl_array = lap_mid_mnstr_pk * lap_pl_fact;
116 lap_mid_lee_pl_array = lap_mid_lee_pk * lap_pl_fact;
117 lap_mid_frac_pl_array = lap_mid_frac_pk * lap_pl_fact;
118 lap_mid_mc_pl_array = lap_mid_mc_pk * lap_pl_fact;
119 lap_mid_dp_pl_array = lap_mid_dp_pk * lap_pl_fact;
120 lap_b_s1_pl_array = lap_b_s1_pk * lap_pl_fact;
121 lap_b_mxshr_pl_array = lap_b_mxshr_pk * lap_pl_fact;
122 lap_b_seqv_pl_array = lap_b_seqv_pk * lap_pl_fact;
123 lap_b_peel_pl_array = lap_b_peel_pk * lap_pl_fact;
124 lap_b_ipmxshr_pl_array = lap_b_ipmxshr_pk * lap_pl_fact;
125 lap_b_mnstr_pl_array = lap_b_mnstr_pk * lap_pl_fact;
126 lap_b_lee_pl_array = lap_b_lee_pk * lap_pl_fact;
127 lap_b_frac_pl_array = lap_b_frac_pk * lap_pl_fact;
128 lap_b_mc_pl_array = lap_b_mc_pk * lap_pl_fact;
129 lap_b_dp_pl_array = lap_b_dp_pk * lap_pl_fact;
130 %%
131 save('../../print_table\lap_array.mat','lap_t_s1_array','...
        lap_t_peel_array',...
132      'lap_t_mxshr_array','lap_t_seqv_array','lap_t_ipmxshr_array',...
133      'lap_t_mnstr_array','lap_t_lee_array','lap_t_frac_array','...
            lap_t_mc_array','lap_t_dp_array',...
134      'lap_mid_s1_array','lap_mid_peel_array','lap_mid_mxshr_array',...
135      'lap_mid_seqv_array','lap_mid_ipmxshr_array','lap_mid_mnstr_array...
            ','lap_mid_lee_array',...
136      'lap_mid_frac_array','lap_mid_mc_array','lap_mid_dp_array',...
137      'lap_b_s1_array','lap_b_peel_array','lap_b_mxshr_array','...
            lap_b_seqv_array',...
138      'lap_b_ipmxshr_array','lap_b_mnstr_array','lap_b_lee_array',...
139      'lap_b_frac_array','lap_b_mc_array','lap_b_dp_array',...
140      'lap_t_s1_pl_array','lap_t_peel_pl_array',...
141      'lap_t_mxshr_pl_array','lap_t_seqv_pl_array','...
            lap_t_ipmxshr_pl_array',...
142      'lap_t_mnstr_pl_array','lap_t_lee_pl_array','lap_t_frac_pl_array'...
            ,'lap_t_mc_pl_array','lap_t_dp_pl_array',...
143      'lap_mid_s1_pl_array','lap_mid_peel_pl_array','...
            lap_mid_mxshr_pl_array',...
144      'lap_mid_seqv_pl_array','lap_mid_ipmxshr_pl_array','...
            lap_mid_mnstr_pl_array',...
145      'lap_mid_lee_pl_array','lap_mid_frac_pl_array','...
            lap_mid_mc_pl_array','lap_mid_dp_pl_array',...
```

```
146     'lap_b_s1_pl_array','lap_b_peel_pl_array','lap_b_mxshr_pl_array',...
            'lap_b_seqv_pl_array',...
147     'lap_b_ipmxshr_pl_array','lap_b_mnstr_pl_array','...
            lap_b_lee_pl_array','lap_b_frac_pl_array',...
148     'lap_b_mc_pl_array','lap_b_dp_pl_array');
```

Appendix G

Sample Matlab code for calculating stress for criteria

Listing G.1: Sample Matlab code for calculating stress for criteria

```
clear all
close all
clc
%
load('lap_t1.mat');
load('lap_t2.mat');
load('lap_top.mat');
%
%lapshear total top distance
lap_t_s = [lap_t1_s ; lap_t1_s(end)+lap_t2_s(2:end)] ;
lap_t_s = [lap_t_s ; lap_t_s(end)+lap_top_s(2:end)] ;
%lapshear total top peel
lap_t_peel = [lap_t1_sy ; lap_t2_sx(2:end) ; ...
   lap_top_sy(2:end)] ;
%lapshear total top maximum principal
lap_t_s1 = [lap_t1_s1 ; lap_t2_s1(2:end) ; ...
   lap_top_s1(2:end)] ;
lap_t_s2 = [lap_t1_s2 ; lap_t2_s2(2:end) ; ...
   lap_top_s2(2:end)] ;
lap_t_s3 = [lap_t1_s3 ; lap_t2_s3(2:end) ; ...
   lap_top_s3(2:end)] ;
%lapshear total top von Mises equivalent
lap_t_seqv = [lap_t1_seqv ; lap_t2_seqv(2:end) ; ...
   lap_top_seqv(2:end)] ;
%
lap_t_sint = [lap_t1_sint ; lap_t2_sint(2:end) ; ...
   lap_top_sint(2:end) ];
%
lap_t_mxshr = lap_t_sint/2;
%LEE CRITERIA
lap_t_mnstr = (lap_t_s1 + lap_t_s2 + lap_t_s3)/3;
lap_t_lee = lap_t_mnstr./lap_t_seqv;
%-----------------------------------
%lapshear total top in-plane maximum shear
%-----------------------------------
lap_t1_ipmxshr = sqrt(lap_t1_sxy.^2+lap_t1_syz.^2);
lap_t2_ipmxshr = sqrt(lap_t2_sxy.^2+lap_t2_sxz.^2);
lap_top_ipmxshr = sqrt(lap_top_sxy.^2+lap_top_syz.^2);
%
lap_t_ipmxshr = [lap_t1_ipmxshr ; lap_t2_ipmxshr(2:end) ; ...
   lap_top_ipmxshr(2:end)] ;
%-----------------------------------
%lapshear total top Fracture stress criteria
```

```
%-------------------------------------
lap_t_frac = sqrt(lap_t_peel.^2+lap_t_ipmxshr.^2);
%-------------------------------------
%lapshear total top Mohr-Coulomb stress criteria
%-------------------------------------
m = 1.5; %Syc/Syt assumed from literature
K = (m-1)/(m+1);
maxi1 = max(abs(lap_t_s1-lap_t_s2)+K*(lap_t_s1+lap_t_s2),...
    abs(lap_t_s1-lap_t_s3)+K*(lap_t_s1+lap_t_s3));
maxi = max(maxi1,abs(lap_t_s2-lap_t_s3)+K*(lap_t_s2+lap_t_s3));
lap_t_mc = ((m+1)/(2*m))*maxi;
%-------------------------------------
%lapshear total top Drucker-Prager stress criteria
%-------------------------------------
lap_t_dp = ((m-1)/(2*m))*(3*lap_t_mnstr) + ((m+1)/(2*m))*lap_t_seqv;
%saving total top
save('lap_t.mat');
%%%%%%%%%%%%%%%%%%%%%%%%
%PLOTS
%%%%%%%%%%%%%%%%%%%%%%%%
load('lap_t.mat');
%plot lapshear total top Peel stress
figure(1);
axes('FontSize',10);
plot(lap_t_s(1:2001),lap_t_peel(1:2001),'-b','linewidth',1),
hold on
plot(lap_t_s(2001:4001),lap_t_peel(2001:4001),'-r','linewidth',1),
hold on
plot(lap_t_s(4001:6001),lap_t_peel(4001:6001),'-m','linewidth',1),
hold off
%
legend('vertical','radius','flat','location','best');
title('Peel stress distribution along top bond line for lapshear');
xlabel('Distance');
ylabel('Peel stress (Pa)');
xlim([lap_t_s(1) lap_t_s(end)]);
saveas(gcf,'lap_t_peel','png');
%
%plot lapshear total top Maximum shear stress
figure(2);
axes('FontSize',10);
plot(lap_t_s(1:2001),lap_t_mxshr(1:2001),'-b','linewidth',1),
hold on
plot(lap_t_s(2001:4001),lap_t_mxshr(2001:4001),'-r','linewidth',1),
hold on
plot(lap_t_s(4001:6001),lap_t_mxshr(4001:6001),'-m','linewidth',1),
hold off
%
legend('vertical','radius','flat','location','best');
title('Maximum shear stress distribution along top bond line for ...
    lapshear');
xlabel('Distance');
ylabel('Maximum shear stress (Pa)');
xlim([lap_t_s(1) lap_t_s(end)]);
saveas(gcf,'lap_t_mxshr','png');
%
%plot lapshear total top Maximum principal stress
figure(3);
axes('FontSize',10);
```

```
plot(lap_t_s(1:2001),lap_t_s1(1:2001),'-b','linewidth',1),
hold on
plot(lap_t_s(2001:4001),lap_t_s1(2001:4001),'-r','linewidth',1),
hold on
plot(lap_t_s(4001:6001),lap_t_s1(4001:6001),'-m','linewidth',1),
hold off
%
legend('vertical','radius','flat','location','best');
title('Maximum principal stress distribution along top bond line for ...
    lapshear');
xlabel('Distance');
ylabel('Maximum principal stress (Pa)');
xlim([lap_t_s(1) lap_t_s(end)]);
saveas(gcf,'lap_t_s1','png');
%
%plot lapshear total top von Mises equivalent stress
figure(4);
axes('FontSize',10);
plot(lap_t_s(1:2001),lap_t_seqv(1:2001),'-b','linewidth',1),
hold on
plot(lap_t_s(2001:4001),lap_t_seqv(2001:4001),'-r','linewidth',1),
hold on
plot(lap_t_s(4001:6001),lap_t_seqv(4001:6001),'-m','linewidth',1),
hold off
%
legend('vertical','radius','flat','location','best');
title('von Mises equivalent stress distribution along top bond line ...
    for lapshear');
xlabel('Distance');
ylabel('von Mises equivalent stress (Pa)');
xlim([lap_t_s(1) lap_t_s(end)]);
saveas(gcf,'lap_t_seqv','png');
%
%plot lapshear total top In-plane maximum shear stress
figure(5);
axes('FontSize',10);
plot(lap_t_s(1:2001),lap_t_ipmxshr(1:2001),'-b','linewidth',1),
hold on
plot(lap_t_s(2001:4001),lap_t_ipmxshr(2001:4001),'-r','linewidth',1),
hold on
plot(lap_t_s(4001:6001),lap_t_ipmxshr(4001:6001),'-m','linewidth',1),
hold off
%
legend('vertical','radius','flat','location','best');
title('In-plane maximum shear stress distribution along top bond line...
     for lapshear');
xlabel('Distance');
ylabel('In-plane maximum shear stress (Pa)');
xlim([lap_t_s(1) lap_t_s(end)]);
saveas(gcf,'lap_t_ipmxshr','png');
%
%plot lapshear Maximum shear and In-plane maximum shear stress ...
    together
figure(6);
axes('FontSize',10);
plot(lap_t_s,lap_t_ipmxshr,'-b','linewidth',1),
hold on
plot(lap_t_s,lap_t_mxshr,'-m','linewidth',1),
hold off
```

```
157 %
158 legend('in-plane mx shear','max shear','location','best');
159 title('In-plane max shear stress v/s max shear along top bond line ...
       for lapshear');
160 xlabel('Distance');
161 ylabel('Maximum shear stress (Pa)');
162 xlim([lap_t_s(1) lap_t_s(end)]);
163 saveas(gcf,'lap_t_ipmxshr_mxshr','png');
164 %
165 %plot lapshear total top Mean stress
166 figure(7);
167 axes('FontSize',10);
168 plot(lap_t_s(1:2001),lap_t_mnstr(1:2001),'-b','linewidth',1),
169 hold on
170 plot(lap_t_s(2001:4001),lap_t_mnstr(2001:4001),'-r','linewidth',1),
171 hold on
172 plot(lap_t_s(4001:6001),lap_t_mnstr(4001:6001),'-m','linewidth',1),
173 hold off
174 %
175 legend('vertical','radius','flat','location','best');
176 title('Mean stress distribution along top bond line for lapshear');
177 xlabel('Distance');
178 ylabel('Mean stress (Pa)');
179 xlim([lap_t_s(1) lap_t_s(end)]);
180 saveas(gcf,'lap_t_mnstr','png');
181 %
182 %plot lapshear total top Lee number
183 figure(8);
184 axes('FontSize',10);
185 plot(lap_t_s(1:2001),lap_t_lee(1:2001),'-b','linewidth',1),
186 hold on
187 plot(lap_t_s(2001:4001),lap_t_lee(2001:4001),'-r','linewidth',1),
188 hold on
189 plot(lap_t_s(4001:6001),lap_t_lee(4001:6001),'-m','linewidth',1),
190 hold off
191 %
192 legend('vertical','radius','flat','location','best');
193 title('Lee number distribution along top bond line for lapshear');
194 xlabel('Distance');
195 ylabel('Lee number');
196 xlim([lap_t_s(1) lap_t_s(end)]);
197 saveas(gcf,'lap_t_lee','png');
198 %
199 %plot lapshear total top fracture stress
200 figure(9);
201 axes('FontSize',10);
202 plot(lap_t_s(1:2001),lap_t_frac(1:2001),'-b','linewidth',1),
203 hold on
204 plot(lap_t_s(2001:4001),lap_t_frac(2001:4001),'-r','linewidth',1),
205 hold on
206 plot(lap_t_s(4001:6001),lap_t_frac(4001:6001),'-m','linewidth',1),
207 hold off
208 %
209 legend('vertical','radius','flat','location','best');
210 title('Fracture stress distribution along top bond line for lapshear'...
       );
211 xlabel('Distance');
212 ylabel('Fracture stress');
213 xlim([lap_t_s(1) lap_t_s(end)]);
```

```
saveas(gcf,'lap_t_frac','png');
%
%plot lapshear total top Mohr-Coulomb stress
figure(10);
axes('FontSize',10);
plot(lap_t_s(1:2001),lap_t_mc(1:2001),'-b','linewidth',1),
hold on
plot(lap_t_s(2001:4001),lap_t_mc(2001:4001),'-r','linewidth',1),
hold on
plot(lap_t_s(4001:6001),lap_t_mc(4001:6001),'-m','linewidth',1),
hold off
%
legend('vertical','radius','flat','location','best');
title('Mohr-Coulomb stress distribution along top bond line for ...
    lapshear');
xlabel('Distance');
ylabel('Mohr-Coulomb stress');
xlim([lap_t_s(1) lap_t_s(end)]);
saveas(gcf,'lap_t_mc','png');
%
%plot lapshear total top Drucker-Prager stress
figure(11);
axes('FontSize',10);
plot(lap_t_s(1:2001),lap_t_dp(1:2001),'-b','linewidth',1),
hold on
plot(lap_t_s(2001:4001),lap_t_dp(2001:4001),'-r','linewidth',1),
hold on
plot(lap_t_s(4001:6001),lap_t_dp(4001:6001),'-m','linewidth',1),
hold off
%
legend('vertical','radius','flat','location','best');
title('Drucker-Prager stress distribution along top bond line for ...
    lapshear');
xlabel('Distance');
ylabel('Drucker-Prager stress');
xlim([lap_t_s(1) lap_t_s(end)]);
saveas(gcf,'lap_t_dp','png');
%
figure(12);
axes('FontSize',10);
hold on;
grid on;
plot(lap_t_s,lap_t_peel,'-r','linewidth',1), %figure 1
plot(lap_t_s,lap_t_mxshr,'-g','linewidth',1),   %figure 2
plot(lap_t_s,lap_t_s1,'-c','linewidth',1),  %figure 3
plot(lap_t_s,lap_t_seqv,'-y','linewidth',1),    %figure 4
plot(lap_t_s,lap_t_mnstr,'-b','linewidth',1),   %figure 7
plot(lap_t_s,lap_t_frac,'--b','linewidth',1),    %figure 9
plot(lap_t_s,lap_t_mc,'-k','linewidth',1),  %figure 10
plot(lap_t_s,lap_t_dp,'-m','linewidth',1),  %figure 11
%
legend('normal','mx shear','mx prin','von Mises',...
    'mean stress','frac stress','mohr-coulomb','drucker-prager',...
    'location','best');
title('Stress distributions along top bond line for lapshear');
xlabel('Distance (m)');
ylabel('Stress (Pa)');
xlim([lap_t_s(1) lap_t_s(end)]);
saveas(gcf,'lap_t_all','png');
```

```
271 %
272 clear all
273 close all
274 clc
```

Appendix H

Matlab code for printing standard deviation table

Listing H.1: Matlab code for printing standard deviation table

```
%%%%%%%%%%%%%%%%%%%%%%%%
%%printing table
%%%%%%%%%%%%%%%%%%%%%%%%
clear all
close all
clc
%
f = figure('Position',[200 240 750 300]);
load('tor_array.mat');
load('ten_array.mat');
load('shr_array.mat');
load('lap_array.mat');
load('bnd_array.mat');
load('stdev.mat');
%
ovr_t_s1_array = [tor_t_s1_array;ten_t_s1_array;shr_t_s1_array;...
    lap_t_s1_array; bnd_t_s1_array];
ovr_t_mxshr_array = [tor_t_mxshr_array;ten_t_mxshr_array;...
    shr_t_mxshr_array;...
    lap_t_mxshr_array; bnd_t_mxshr_array];
ovr_t_seqv_array = [tor_t_seqv_array;ten_t_seqv_array;...
    shr_t_seqv_array;...
    lap_t_seqv_array; bnd_t_seqv_array];
ovr_t_peel_array = [tor_t_peel_array;ten_t_peel_array;...
    shr_t_peel_array;...
    lap_t_peel_array; bnd_t_peel_array];
%
ovr_mid_s1_array = [tor_mid_s1_array;ten_mid_s1_array;...
    shr_mid_s1_array;...
    lap_mid_s1_array; bnd_mid_s1_array];
ovr_mid_mxshr_array = [tor_mid_mxshr_array;ten_mid_mxshr_array;...
    shr_mid_mxshr_array;...
    lap_mid_mxshr_array; bnd_mid_mxshr_array];
ovr_mid_seqv_array = [tor_mid_seqv_array;ten_mid_seqv_array;...
    shr_mid_seqv_array;...
    lap_mid_seqv_array; bnd_mid_seqv_array];
ovr_mid_peel_array = [tor_mid_peel_array;ten_mid_peel_array;...
    shr_mid_peel_array;...
    lap_mid_peel_array; bnd_mid_peel_array];
%
ovr_bot_s1_array = [tor_bot_s1_array;ten_bot_s1_array;...
    shr_bot_s1_array;...
    lap_b_s1_array; bnd_bot_s1_array];
```

```
36 ovr_bot_mxshr_array = [tor_bot_mxshr_array;ten_bot_mxshr_array;...
       shr_bot_mxshr_array;...
37     lap_b_mxshr_array; bnd_bot_mxshr_array];
38 ovr_bot_seqv_array = [tor_bot_seqv_array;ten_bot_seqv_array;...
       shr_bot_seqv_array;...
39     lap_b_seqv_array; bnd_bot_seqv_array];
40 ovr_bot_peel_array = [tor_bot_peel_array;ten_bot_peel_array;...
       shr_bot_peel_array;...
41     lap_b_peel_array; bnd_bot_peel_array];
42 %
43 ovr_pk = {mean(tor_t_s1_array)/1e6,mean(ten_t_s1_array)/1e6,mean(...
       shr_t_s1_array)/1e6,...
44     mean(lap_t_s1_array)/1e6,mean(bnd_t_s1_array)/1e6,std(...
           ovr_t_s1_array,1)/1e6;...
45     %
46     mean(tor_t_mxshr_array)/1e6,mean(ten_t_mxshr_array)/1e6,mean(...
           shr_t_mxshr_array)/1e6,...
47     mean(lap_t_mxshr_array)/1e6,mean(bnd_t_mxshr_array)/1e6,std(...
           ovr_t_mxshr_array,1)/1e6;...
48     %
49     mean(tor_t_seqv_array)/1e6,mean(ten_t_seqv_array)/1e6,mean(...
           shr_t_seqv_array)/1e6,...
50     mean(lap_t_seqv_array)/1e6,mean(bnd_t_seqv_array)/1e6,std(...
           ovr_t_seqv_array,1)/1e6;...
51     %
52     mean(tor_t_peel_array)/1e6,mean(ten_t_peel_array)/1e6,mean(...
           shr_t_peel_array)/1e6,...
53     mean(lap_t_peel_array)/1e6,mean(bnd_t_peel_array)/1e6,std(...
           ovr_t_peel_array,1)/1e6;...
54     %
55     %
56     %
57     mean(tor_mid_s1_array)/1e6,mean(ten_mid_s1_array)/1e6,mean(...
           shr_mid_s1_array)/1e6,...
58     mean(lap_mid_s1_array)/1e6,mean(bnd_mid_s1_array)/1e6,std(...
           ovr_mid_s1_array,1)/1e6;...
59     %
60     mean(tor_mid_mxshr_array)/1e6,mean(ten_mid_mxshr_array)/1e6,mean(...
           shr_mid_mxshr_array)/1e6,...
61     mean(lap_mid_mxshr_array)/1e6,mean(bnd_mid_mxshr_array)/1e6,std(...
           ovr_mid_mxshr_array,1)/1e6;...
62     %
63     mean(tor_mid_seqv_array)/1e6,mean(ten_mid_seqv_array)/1e6,mean(...
           shr_mid_seqv_array)/1e6,...
64     mean(lap_mid_seqv_array)/1e6,mean(bnd_mid_seqv_array)/1e6,std(...
           ovr_mid_seqv_array,1)/1e6;...
65     %
66     mean(tor_mid_peel_array)/1e6,mean(ten_mid_peel_array)/1e6,mean(...
           shr_mid_peel_array)/1e6,...
67     mean(lap_mid_peel_array)/1e6,mean(bnd_mid_peel_array)/1e6,std(...
           ovr_mid_peel_array,1)/1e6;...
68     %
69     %
70     %
71     mean(tor_bot_s1_array)/1e6,mean(ten_bot_s1_array)/1e6,mean(...
           shr_bot_s1_array)/1e6,...
72     mean(lap_b_s1_array)/1e6,mean(bnd_bot_s1_array)/1e6,std(...
           ovr_bot_s1_array,1)/1e6;...
73     %
```

```
74      mean(tor_bot_mxshr_array)/1e6,mean(ten_bot_mxshr_array)/1e6,mean(...
            shr_bot_mxshr_array)/1e6,...
75      mean(lap_b_mxshr_array)/1e6,mean(bnd_bot_mxshr_array)/1e6,std(...
            ovr_bot_mxshr_array,1)/1e6;...
76      %
77      mean(tor_bot_seqv_array)/1e6,mean(ten_bot_seqv_array)/1e6,mean(...
            shr_bot_seqv_array)/1e6,...
78      mean(lap_b_seqv_array)/1e6,mean(bnd_bot_seqv_array)/1e6,std(...
            ovr_bot_seqv_array,1)/1e6;...
79      %
80      mean(tor_bot_peel_array)/1e6,mean(ten_bot_peel_array)/1e6,mean(...
            shr_bot_peel_array)/1e6,...
81      mean(lap_b_peel_array)/1e6,mean(bnd_bot_peel_array)/1e6,std(...
            ovr_bot_peel_array,1)/1e6;...
82      %
83      stdev_tor_test/((pin_dia/2)*pin_area*1e6),stdev_ten_test,...
            stdev_shr_test,...
84      stdev_lap_test,stdev_bnd_test,''};
85      %
86      %
87  cnames = {'Torsion','Tensile','Shear','Lap shear','Bending','Standard...
        Deviation'};
88  rnames = {'Max Principal - Top','Max Shear - Top','Equivalent - Top',...
        ...
89      'Peel - Top','Max Principal - Mid','Max Shear - Mid','Equivalent ...
            - Mid',...
90      'Peel - Mid','Max Principal - Bot','Max Shear - Bot','Equivalent ...
            - Bot',...
91      'Peel - Bot','Measurement Std Dev'};
92  t = uitable('Parent',f,'Data',ovr_pk,'ColumnName',cnames,...
93              'RowName',rnames,'Position',[20 20 700 280]);
94          saveas(gcf,'std_dev_table','png');
```

Appendix I

Ansys code

I.1 Sample Pre-processing code

```
/filn,ibs1_100um
/title,ibs1_100um
resume
!
/filn,ibs1_100um_shear_sw
/titl,ibs1_100um_shear_sw
/prep7
shpp,off
!
mat,2
*use,sw.mac
save,ibs1_100um_shear_sw,db
!
/solu
csys,0
allsel
ddele,all,all
nsel,s,loc,y,-10e-3
d,all,all
!
allsel
csys,0
nsel,s,loc,y,bot_forc_ht+adh_thk/2
nsel,r,loc,z,
nsel,r,loc,x,pin_rad
*get,num_shear_bot,node,,count
shear_force_bot=(shear_force**2/(shear_force-(shear_force*bot_forc_ht/top_forc_ht)
f,all,fx,-shear_force_bot
!
nsel,s,loc,y,top_forc_ht+adh_thk/2
nsel,r,loc,z,
nsel,r,loc,x,-pin_rad
*get,num_shear_top,node,,count
shear_force_top=(shear_force_bot-shear_force)/num_shear_top
f,all,fx,shear_force_top
!
```

```
allsel
antype,static
eqslv,sparse
solve
/eof
```

I.2 Sample Post-processing code

```
fini
/clear
/cwd,Z:\ibs1_100um\shear
/filname,ibs1_100um_bending_sw
/title,ibs1_100um_bending_sw
resume,ibs1_100um_bending_sw,db
!
/post1
set,last
/gra,full
/dscale,,off
/plopts,info,on
!
esel,s,mat,,2
nsle
csys,0
nsel,r,loc,z,0
nsel,r,ext
!
wpcsys,,0
wpoffs,-pin_rad+pin_fill,adh_thk+pin_fill
wprota,,,180
cswpla,11,1
!
wpcsys,,0
wprota,-90
cswpla,12,0
!
wpcsys,,0
wpoffs,pin_rad-pin_fill,adh_thk+pin_fill
cswpla,13,1
!
csys,0
allsel
padele,all
!
path,mid,2,30,2000
ppath,1,1643
ppath,2,8561
!
path,bot,2,30,2000
```

```
ppath,1,1675
ppath,2,7246
!
path,top,2,30,2000
ppath,1,1700
ppath,2,3825
!
path,t_1,2,30,2000
ppath,1,1647
ppath,2,1627
!
path,t_2,2,30,2000
ppath,1,,-pin_rad,adh_thk+pin_fill,,0
ppath,2,,-pin_rad+pin_fill,adh_thk,,11
!
path,t_3,2,30,2000
ppath,1,,pin_rad-pin_fill,adh_thk,,0
ppath,2,,pin_rad,adh_thk+pin_fill,,13
!
path,t_4,2,30,2000
ppath,1,9550
ppath,2,8614
!
allsel
rsys,13
pdef,s_x,s,x
pdef,s_y,s,y
pdef,s_z,s,z
pdef,s_xy,s,xy
pdef,s_yz,s,yz
pdef,s_xz,s,xz
pdef,s_1,s,1
pdef,s_2,s,2
pdef,s_3,s,3
pdef,s_int,s,int
pdef,s_eqv,s,eqv
!!!
*use,stress_out.mac,'mid',1
*use,stress_out.mac,'mid',2
*use,stress_out.mac,'bot',1
*use,stress_out.mac,'bot',2
*use,stress_out.mac,'top',1
*use,stress_out.mac,'top',2
*use,stress_out.mac,'t_1',1
*use,stress_out.mac,'t_1',2
*use,stress_out.mac,'t_2',1
*use,stress_out.mac,'t_2',2
*use,stress_out.mac,'t_3',1
*use,stress_out.mac,'t_3',2
```

```
*use,stress_out.mac,'t_4',1
*use,stress_out.mac,'t_4',2
!!!!!!!!!!!!!!!!!!!!
!PLOTS
!!!!!!!!!!!!!!!!!!!!
/out
/PAGE,100000,,100000
/out,bending_lin,txt
path,mid
rsys,0
*get,mid_s_x,section,membrane,inside,s,x
*get,mid_s_y,section,membrane,inside,s,y
*get,mid_s_z,section,membrane,inside,s,z
*get,mid_s_xy,section,membrane,inside,s,xy
*get,mid_s_yz,section,membrane,inside,s,yz
*get,mid_s_xz,section,membrane,inside,s,xz
*get,mid_s_1,section,membrane,inside,s,1
*get,mid_s_2,section,membrane,inside,s,2
*get,mid_s_3,section,membrane,inside,s,3
*get,mid_s_int,section,membrane,inside,s,int
*get,mid_s_eqv,section,membrane,inside,s,eqv
!
path,mid
rsys,0
*get,mid_s_x,section,membrane,inside,s,x
*get,mid_s_y,section,membrane,inside,s,y
*get,mid_s_z,section,membrane,inside,s,z
*get,mid_s_xy,section,membrane,inside,s,xy
*get,mid_s_yz,section,membrane,inside,s,yz
*get,mid_s_xz,section,membrane,inside,s,xz
*get,mid_s_1,section,membrane,inside,s,1
*get,mid_s_2,section,membrane,inside,s,2
*get,mid_s_3,section,membrane,inside,s,3
*get,mid_s_int,section,membrane,inside,s,int
*get,mid_s_eqv,section,membrane,inside,s,eqv
!
path,bot
rsys,0
*get,bot_s_x,section,membrane,inside,s,x
*get,bot_s_y,section,membrane,inside,s,y
*get,bot_s_z,section,membrane,inside,s,z
*get,bot_s_xy,section,membrane,inside,s,xy
*get,bot_s_yz,section,membrane,inside,s,yz
*get,bot_s_xz,section,membrane,inside,s,xz
*get,bot_s_1,section,membrane,inside,s,1
*get,bot_s_2,section,membrane,inside,s,2
*get,bot_s_3,section,membrane,inside,s,3
*get,bot_s_int,section,membrane,inside,s,int
*get,bot_s_eqv,section,membrane,inside,s,eqv
```

```
!
path,t_1
rsys,12
*get,t1_s_x,section,membrane,inside,s,x
*get,t1_s_y,section,membrane,inside,s,y
*get,t1_s_z,section,membrane,inside,s,z
*get,t1_s_xy,section,membrane,inside,s,xy
*get,t1_s_yz,section,membrane,inside,s,yz
*get,t1_s_xz,section,membrane,inside,s,xz
*get,t1_s_1,section,membrane,inside,s,1
*get,t1_s_2,section,membrane,inside,s,2
*get,t1_s_3,section,membrane,inside,s,3
*get,t1_s_int,section,membrane,inside,s,int
*get,t1_s_eqv,section,membrane,inside,s,eqv
!
path,t_2
rsys,11
*get,t2_s_x,section,membrane,inside,s,x
*get,t2_s_y,section,membrane,inside,s,y
*get,t2_s_z,section,membrane,inside,s,z
*get,t2_s_xy,section,membrane,inside,s,xy
*get,t2_s_yz,section,membrane,inside,s,yz
*get,t2_s_xz,section,membrane,inside,s,xz
*get,t2_s_1,section,membrane,inside,s,1
*get,t2_s_2,section,membrane,inside,s,2
*get,t2_s_3,section,membrane,inside,s,3
*get,t2_s_int,section,membrane,inside,s,int
*get,t2_s_eqv,section,membrane,inside,s,eqv
!
path,top
rsys,0
*get,top_s_x,section,membrane,inside,s,x
*get,top_s_y,section,membrane,inside,s,y
*get,top_s_z,section,membrane,inside,s,z
*get,top_s_xy,section,membrane,inside,s,xy
*get,top_s_yz,section,membrane,inside,s,yz
*get,top_s_xz,section,membrane,inside,s,xz
*get,top_s_1,section,membrane,inside,s,1
*get,top_s_2,section,membrane,inside,s,2
*get,top_s_3,section,membrane,inside,s,3
*get,top_s_int,section,membrane,inside,s,int
*get,top_s_eqv,section,membrane,inside,s,eqv
!
path,t_3
rsys,13
*get,t3_s_x,section,membrane,inside,s,x
*get,t3_s_y,section,membrane,inside,s,y
*get,t3_s_z,section,membrane,inside,s,z
*get,t3_s_xy,section,membrane,inside,s,xy
```

```
*get,t3_s_yz,section,membrane,inside,s,yz
*get,t3_s_xz,section,membrane,inside,s,xz
*get,t3_s_1,section,membrane,inside,s,1
*get,t3_s_2,section,membrane,inside,s,2
*get,t3_s_3,section,membrane,inside,s,3
*get,t3_s_int,section,membrane,inside,s,int
*get,t3_s_eqv,section,membrane,inside,s,eqv
!
path,t_4
rsys,12
*get,t4_s_x,section,membrane,inside,s,x
*get,t4_s_y,section,membrane,inside,s,y
*get,t4_s_z,section,membrane,inside,s,z
*get,t4_s_xy,section,membrane,inside,s,xy
*get,t4_s_yz,section,membrane,inside,s,yz
*get,t4_s_xz,section,membrane,inside,s,xz
*get,t4_s_1,section,membrane,inside,s,1
*get,t4_s_2,section,membrane,inside,s,2
*get,t4_s_3,section,membrane,inside,s,3
*get,t4_s_int,section,membrane,inside,s,int
*get,t4_s_eqv,section,membrane,inside,s,eqv
/out
```

I.3 Sample code for Stress output from Ansys

```
/out
/PAGE,100000,,100000
*if,%arg2%,eq,1,then
stress = 'comp'
*elseif,%arg2%,eq,2
stress = 'prin'
*endif
/out,%arg1%_%stress%,txt
path,%arg1%
*if,%arg2%,eq,1,then
prpath,s_x,s_y,s_z,s_xy,s_yz,s_xz
/out
*elseif,%arg2%,eq,2,then
prpath,s_1,s_2,s_3,s_int,s_eqv
/out
*endif
```